Status and Prospects of Higgs CP Properties with CMS and ATLAS

Andrew Whitbeck – Fermilab

The CP Nature of the Higgs Boson Workshop
@ U. Mass. Amherst

May 1, 2015

What we know about the Higgs...

- 125 GeV narrow width resonance
  - driven by the two high-resolution decay channels, $ZZ \rightarrow 4\ell$ & $\gamma\gamma$
  - mass has now been determined to be **~.2 GeV!**
- constraints from off-shell production suggest that the width is consistent with the SM prediction
- Branching ratios consistent with SM Higgs boson
  - Only moderate sensitivity, yet, in the fermionic decay channels
- Various production modes seen
  - overall rates are consistent with SM expectation
  - still not sensitive to SM strength ttH production
- In general, couplings to various SM fields *(constrained by yields)* are consistent with SM predictions

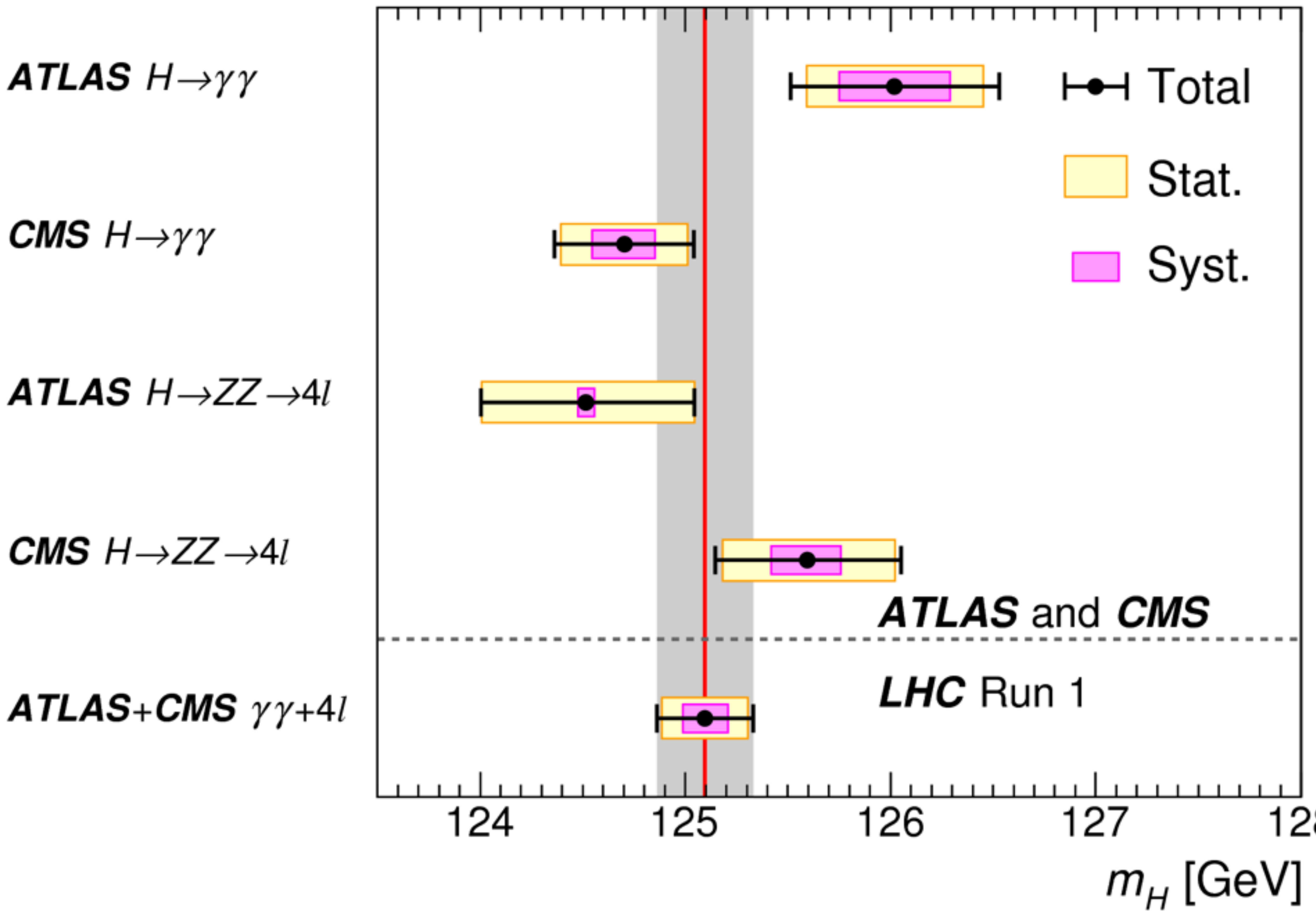

Fermilab

What we know about the Higgs...

- 125 GeV narrow width resonance
  - driven by the two high-resolution decay channels, $ZZ \to 4\ell$ & $\gamma\gamma$
  - mass has now been determined to be **~.2 GeV!**
- constraints from events off-shell suggest that the width is consistent with the SM prediction
- Branching ratios consistent with SM Higgs boson
  - Only moderate sensitivity, yet, in the fermionic decay channels
- Various production modes seen
  - overall rates are consistent with SM expectation
  - still not sensitive to SM strength ttH production
- In general, couplings to various SM fields *(constrained by yields)* are consistent with SM predictions

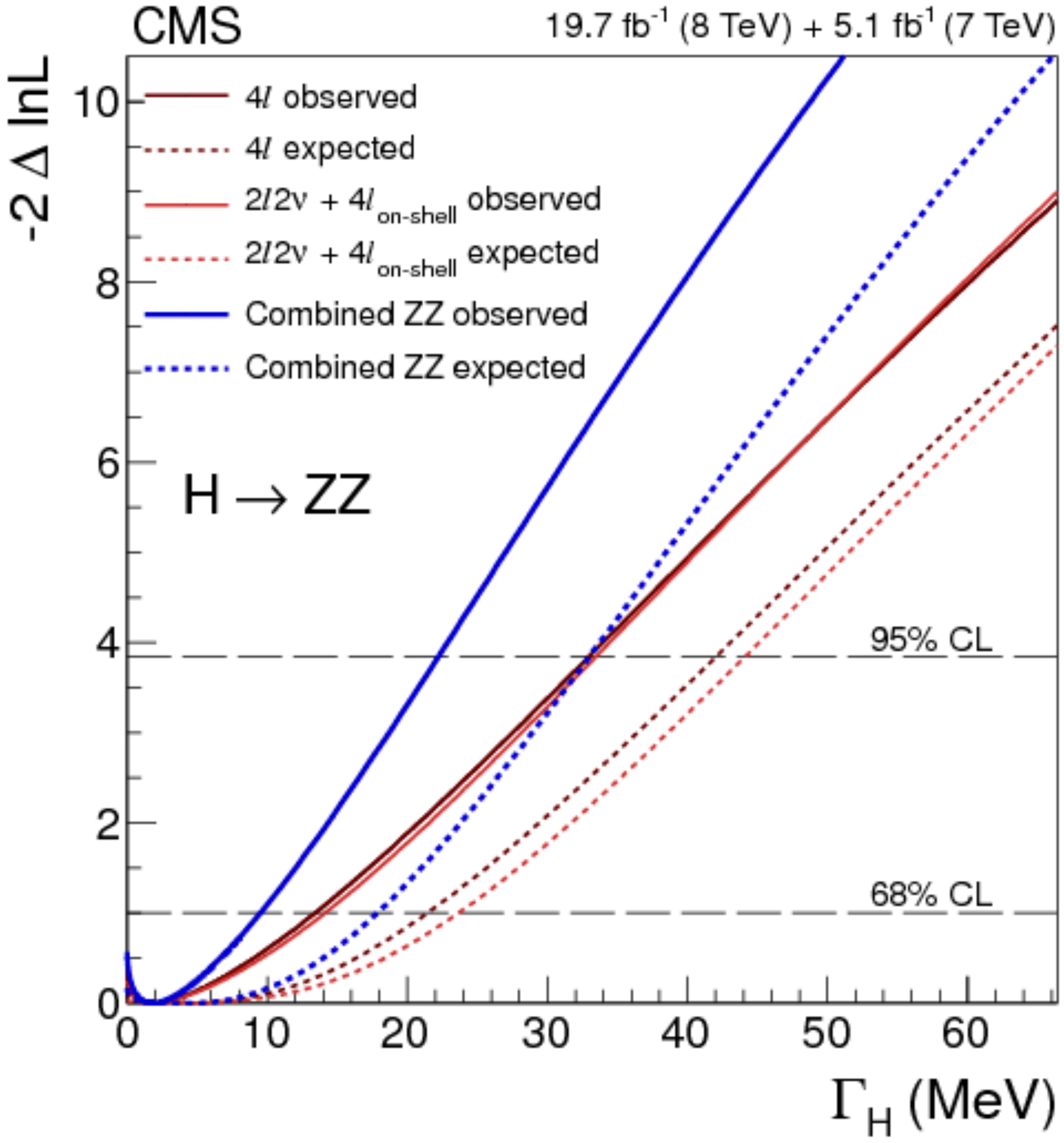

Fermilab

What we know about the Higgs...

- 125 GeV narrow width resonance
  - driven by the two high-resolution decay channels, $ZZ \to 4\ell$ & $\gamma\gamma$
  - mass has now been determined to be **~.2 GeV!**
- constraints from off-shell production suggest that the width is consistent with the SM prediction
- Branching ratios consistent with SM Higgs boson
  - Only moderate sensitivity, yet, in the fermionic decay channels
- Various production modes seen
  - overall rates are consistent with SM expectation
  - still not sensitive to SM strength ttH production
- In general, couplings to various SM fields *(constrained by yields)* are consistent with SM predictions

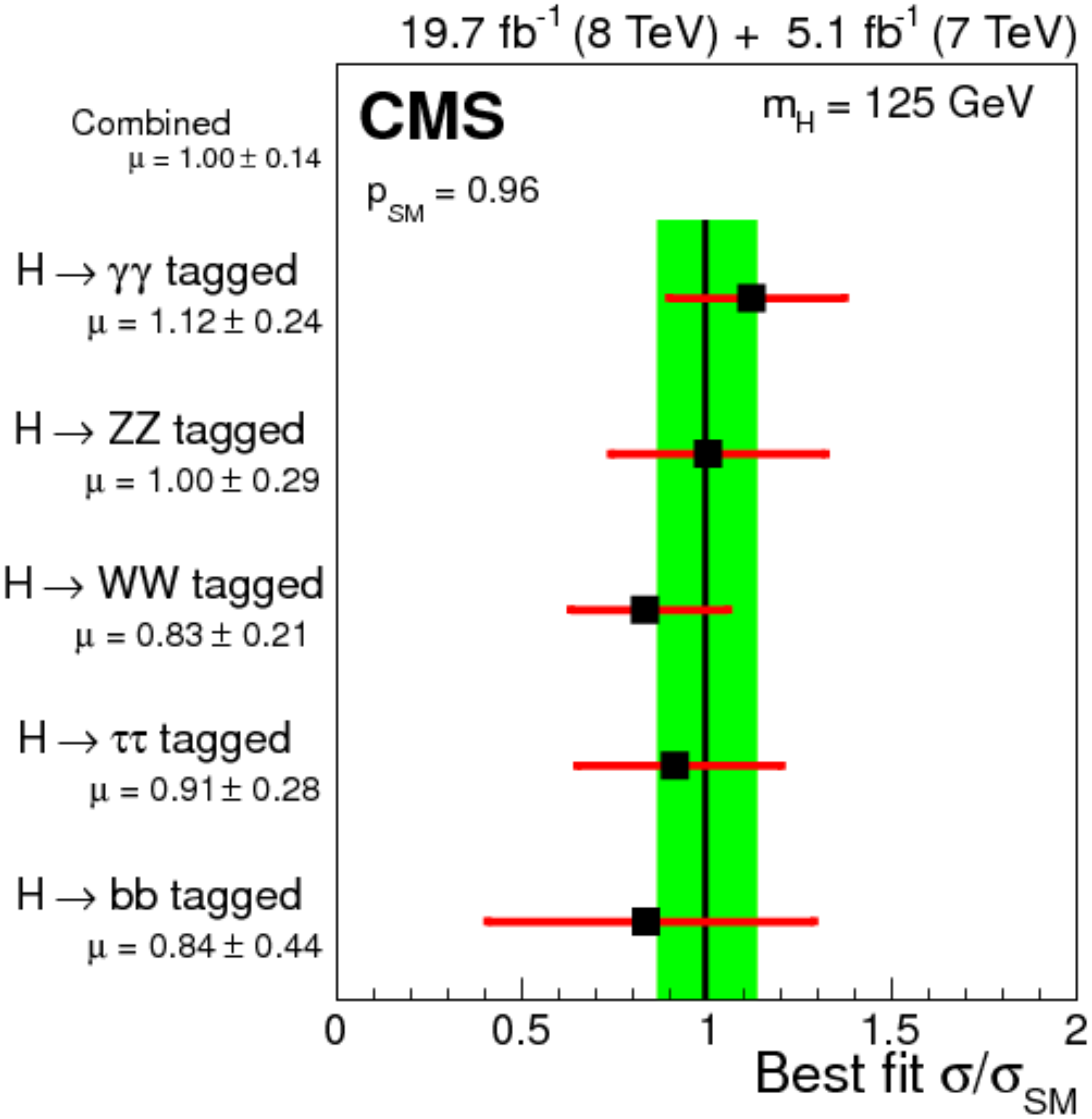

Fermilab

What we know about the Higgs...

- 125 GeV narrow width resonance
  - driven by the two high-resolution decay channels, $ZZ \rightarrow 4\ell$ & $\gamma\gamma$
  - mass has now been determined to be **~.2 GeV!**
- constraints from off-shell production suggest that the width is consistent with the SM prediction
- Branching ratios consistent with SM Higgs boson
  - Only moderate sensitivity, yet, in the fermionic decay channels
- Various production modes seen
  - overall rates are consistent with SM expectation
  - still not sensitive to SM strength ttH production
- In general, couplings to various SM fields ***(constrained by yields)*** are consistent with SM predictions

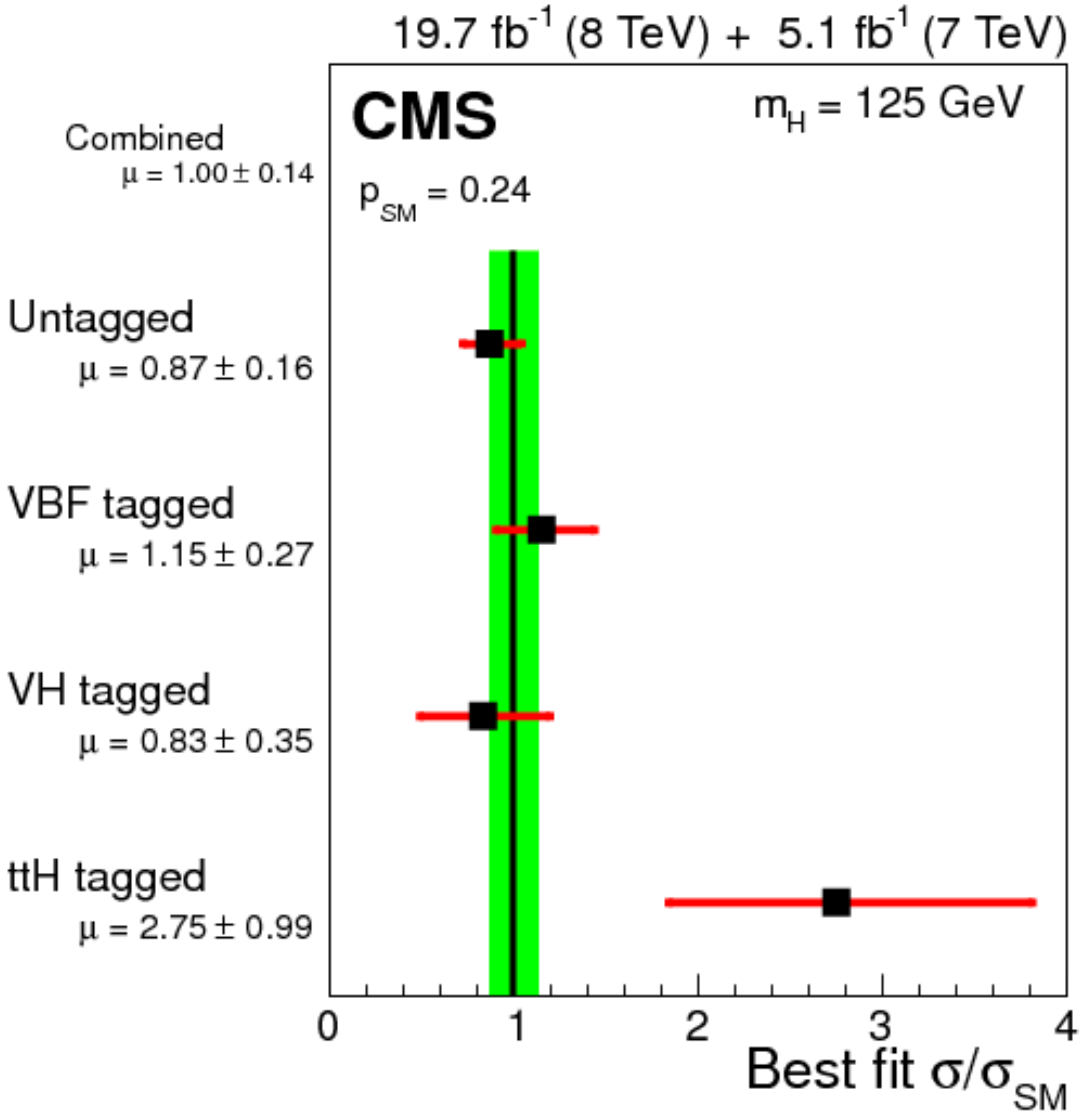

Fermilab

What we know about the Higgs...

- Kinematic used to test various J^P signal hypotheses
  - these measurements use ***distributions*** for characterizing signal models making them ***complementary*** to coupling fit based on rates
  - early analyses focused on hypothesis separation, but now we are starting to constrain the tensor structure of a generic spin-0 resonance decaying to a pair of vector bosons
- Anomalous HVV couplings are currently the primary focus since these are the channels that have the most sensitivity to signal events

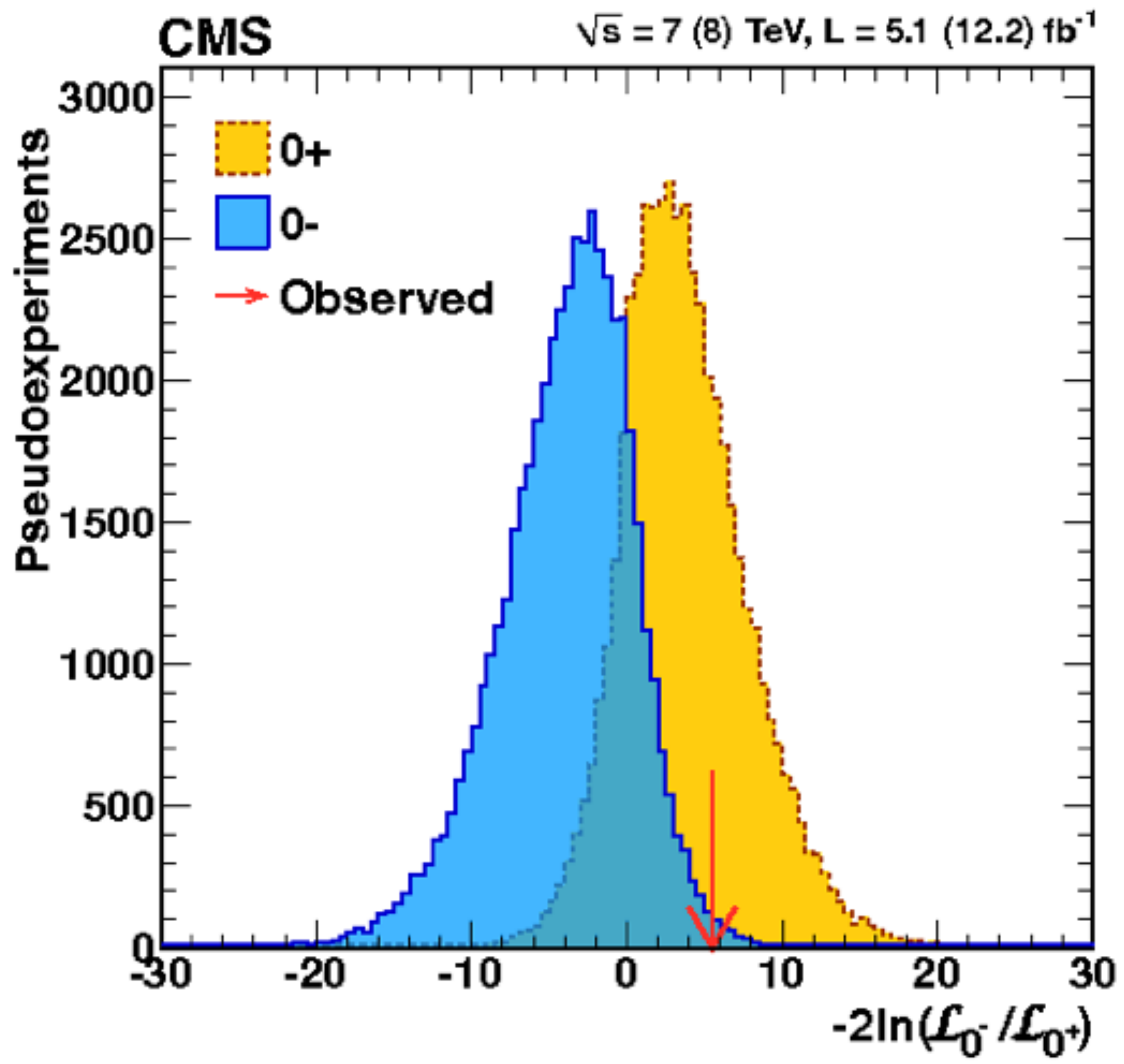

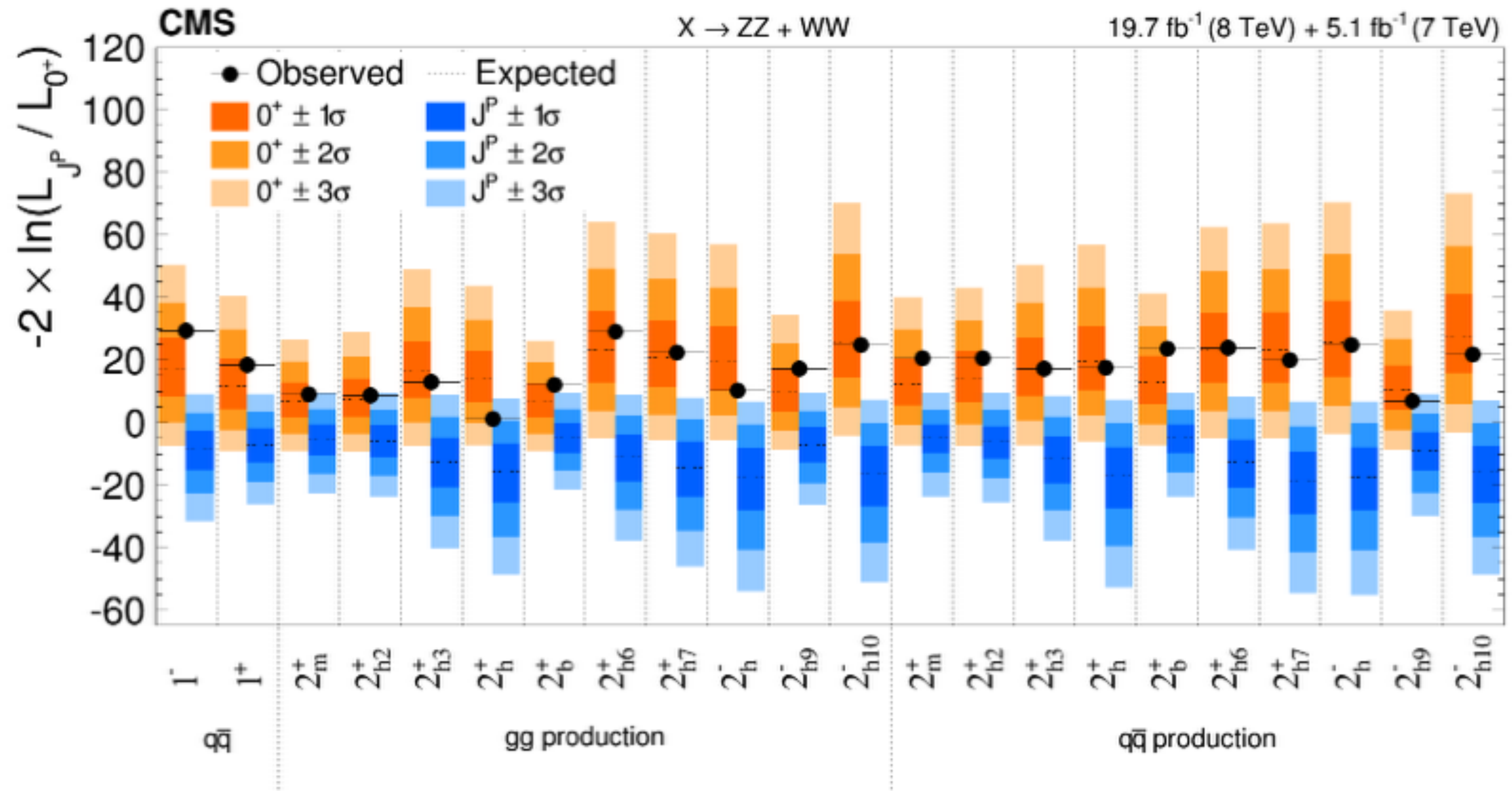

Outline

- CMS & ATLAS 4ℓ analyses
  - detailed explanation of observables, model parameters, and methods
- $W(\ell\nu)W(\ell\nu)$ analyses & ZZ-WW combination
- γγ & Zγ couplings
- Prospects for the future

Model Parameters

$$A(X_{J=0} \to V_1V_2) \sim v^{-1}\left(\left[a_1 - e^{i\phi_{\Lambda_1}}\frac{q_{Z_1}^2 + q_{Z_2}^2}{(\Lambda_1)^2}\right] m_Z^2 \epsilon_{Z_1}^* \epsilon_{Z_2}^* + a_2 f_{\mu\nu}^{*(Z_1)} f^{*(Z_2),\mu\nu} + a_3 f_{\mu\nu}^{*(Z_1)} \tilde{f}^{*(Z_2),\mu\nu} + a_2^{Z\gamma} f_{\mu\nu}^{*(Z)} f^{*(\gamma),\mu\nu} + a_3^{Z\gamma} f_{\mu\nu}^{*(Z)} \tilde{f}^{*(\gamma),\mu\nu} + a_2^{\gamma\gamma} f_{\mu\nu}^{*(\gamma_1)} f^{*(\gamma_2),\mu\nu} + a_3^{\gamma\gamma} f_{\mu\nu}^{*(\gamma_1)} \tilde{f}^{*(\gamma_2),\mu\nu}\right)$$

- Starting from a more generic set of couplings →
- More convenient notation defines parameters which are functions of couplings squared & cross sections
  - anomalous couplings are redefined onto a unit interval:

$$f_{a3} = \frac{|a_3|^2\sigma_3}{|a_1|^2\sigma_1 + |a_2|^2\sigma_2 + |a_3|^2\sigma_3 + \tilde{\sigma}_{\Lambda_1}/(\Lambda_1)^4} \qquad \phi_{a3} = \arg\left(\frac{a_3}{a_1}\right)$$

$$f_{a2} = \frac{|a_2|^2\sigma_2}{|a_1|^2\sigma_1 + |a_2|^2\sigma_2 + |a_3|^2\sigma_3 + \tilde{\sigma}_{\Lambda_1}/(\Lambda_1)^4} \qquad \phi_{a2} = \arg\left(\frac{a_2}{a_1}\right)$$

$$f_{\Lambda 1} = \frac{\tilde{\sigma}_{\Lambda_1}/(\Lambda_1)^4}{|a_1|^2\sigma_1 + |a_2|^2\sigma_2 + |a_3|^2\sigma_3 + \tilde{\sigma}_{\Lambda_1}/(\Lambda_1)^4} \qquad \phi_{\Lambda 1},$$

where σ_i is the cross section of the process corresponding to $a_i = 1, a_{j\neq i} = 0$, while $\tilde{\sigma}_{\Lambda_1}$ is the effective cross section of the process corresponding to $\Lambda_1 > 0, a_{j\neq\Lambda_1} = 0$, given in units fb · GeV^4.

a_1: SM HZZ couplings
a_2: higher dim. 0^+ ZZ coupling
a_3: 0^+ ZZ coupling
$a_2^{Z\gamma}$: 0^+ Zγ coupling
$a_3^{Z\gamma}$: 0^+ Zγ coupling
$a_2^{\gamma\gamma}$: 0^+ γγ coupling
$a_3^{\gamma\gamma}$: 0^+ γγ coupling

e.g. *f_{a3} = 1, f_{a2} = 0 for pure pseudoscalar*
f_{a3} = f_{a2} = 0 for SM Higgs (up to higher order corrections)

Fermilab

Generic Amplitudes vs. Effective Field Theories

$$
\begin{aligned}
L(\mathrm{HVV}) \sim\ & a_1 \frac{m_Z^2}{2} \mathrm{H} Z^\mu Z_\mu + \frac{1}{(\Lambda_1)^2} m_Z^2 \mathrm{H} Z_\mu \Box Z^\mu - \frac{1}{2} a_2 \mathrm{H} Z^{\mu\nu} Z_{\mu\nu} - \frac{1}{2} a_3 \mathrm{H} Z^{\mu\nu} \tilde{Z}_{\mu\nu} \\
& + a_1^{WW} \frac{m_W^2}{2} \mathrm{H} W^\mu W_\mu + \frac{1}{(\Lambda_1^{WW})^2} m_W^2 \mathrm{H} W_\mu \Box W^\mu - \frac{1}{2} a_2^{WW} \mathrm{H} W^{\mu\nu} W_{\mu\nu} - \frac{1}{2} a_3^{WW} \mathrm{H} W^{\mu\nu} \tilde{W}_{\mu\nu} \\
& + \frac{1}{\left(\Lambda_1^{Z\gamma}\right)^2} m_Z^2 \mathrm{H} Z_\mu \partial_\nu F^{\mu\nu} - a_2^{Z\gamma} \mathrm{H} F^{\mu\nu} Z_{\mu\nu} - a_3^{Z\gamma} \mathrm{H} F^{\mu\nu} \tilde{Z}_{\mu\nu} - \frac{1}{2} a_2^{\gamma\gamma} \mathrm{H} F^{\mu\nu} F_{\mu\nu} - \frac{1}{2} a_3^{\gamma\gamma} \mathrm{H} F^{\mu\nu} \tilde{F}_{\mu\nu},
\end{aligned}
$$

$$
\begin{aligned}
\mathcal{L}_0^V = \ & \Big\{ c_\alpha \kappa_{\mathrm{SM}} \left[\tfrac{1}{2} g_{HZZ} Z_\mu Z^\mu + g_{HWW} W_\mu^+ W^{-\mu} \right] \\
& - \frac{1}{4} \frac{1}{\Lambda} \left[c_\alpha \kappa_{HZZ} Z_{\mu\nu} Z^{\mu\nu} + s_\alpha \kappa_{AZZ} Z_{\mu\nu} \tilde{Z}^{\mu\nu} \right] \\
& - \frac{1}{2} \frac{1}{\Lambda} \left[c_\alpha \kappa_{HWW} W_{\mu\nu}^+ W^{-\mu\nu} + s_\alpha \kappa_{AWW} W_{\mu\nu}^+ \tilde{W}^{-\mu\nu} \right] \Big\} X_0
\end{aligned}
$$

Conversion:

$$
f_{g_i} = \frac{r_{i1}^2}{1 + r_{i1}^2}; \quad (i = 2, 4),
$$

$\sigma_{HVV} / \sigma_{SM} = 0.349$

$\sigma_{AVV} / \sigma_{SM} = 0.143$

$$
r_{21}^2 = \frac{\sigma_{HVV}}{\sigma_{\mathrm{SM}}} \left(\frac{\tilde{k}_{HVV}}{k_{\mathrm{SM}}} \right)^2, \quad \text{and} \quad r_{41}^2 = \frac{\sigma_{AVV}}{\sigma_{\mathrm{SM}}} \left(\frac{\tilde{k}_{AVV}}{k_{\mathrm{SM}}} \right)^2 \tan^2 \alpha .
$$

4ℓ analyses

- two pairs of opposite-sign same flavor leptons (e,μ only)
- SM ZZ contributions taken from NLO MC simulation
- Z+X backgrounds estimated from a loose ID control region
- similar strategy employed by CMS
  (see backup for details)

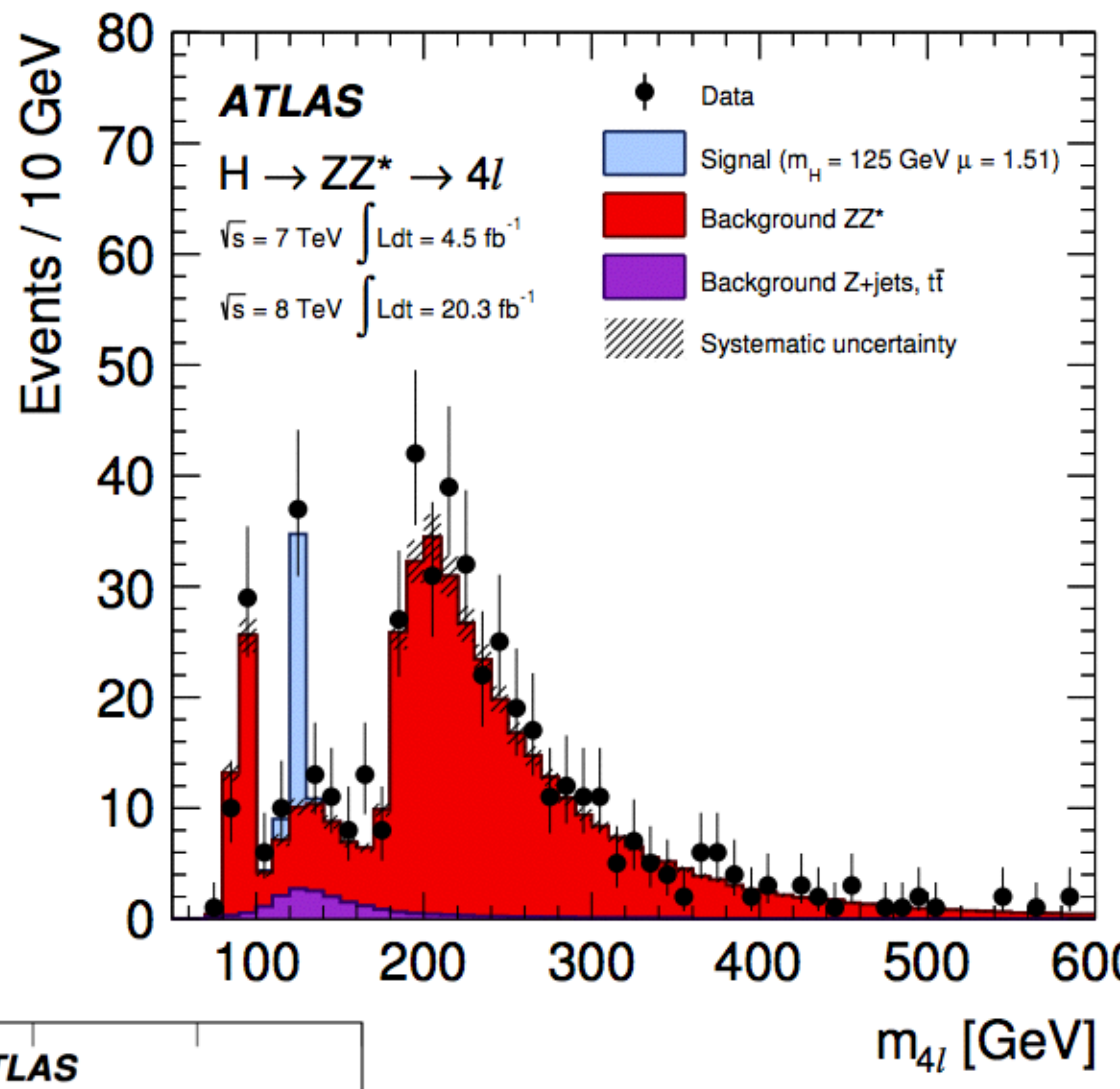

arXiv:1408.5191v3

$115 < m_{4\ell} < 130$ GeV

	Signal	ZZ^*	$t\bar{t}$, Z + jets	Observed
		$\sqrt{s}$ = 7 TeV		
4μ	1.02±0.10	0.65±0.03	0.14±0.06	3
$2\mu 2e$	0.47±0.05	0.29±0.02	0.53±0.12	1
$2e2\mu$	0.64±0.06	0.45±0.02	0.13±0.05	2
$4e$	0.45±0.04	0.26±0.02	0.59±0.12	2
Total	2.58±0.25	1.65±0.09	1.39±0.26	8
		$\sqrt{s}$ = 8 TeV		
4μ	5.81±0.58	3.36±0.17	0.97±0.18	13
$2\mu 2e$	3.00±0.30	1.59±0.10	0.52±0.12	8
$2e2\mu$	3.72±0.37	2.33±0.11	0.84±0.14	9
$4e$	2.91±0.29	1.44±0.09	0.52±0.11	7
Total	15.4 ±1.5	8.72±0.47	2.85±0.39	37

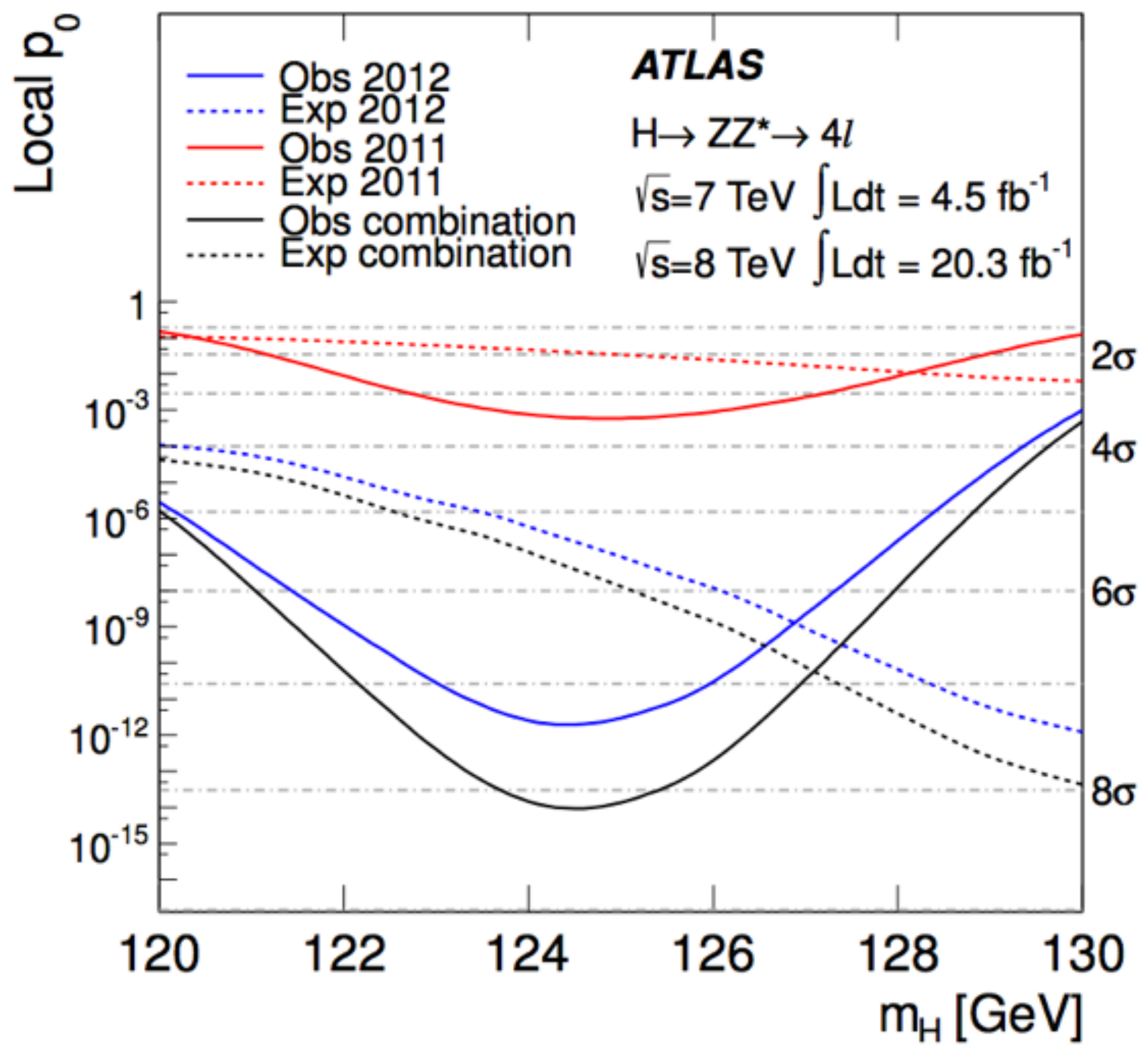

Fermilab

Observables

- An example of a complete set of observables describing the higgs decay kinematics

invariant masses: $m_{4\ell}, m_1, m_2$

powerful background discrimination, incensitive to CP properties

production angles: $\cos(\theta^*)$, Φ_1

sensitive to the spin and polarization of the X resonance

decay angles: $\cos(\theta_{1,2})$, Φ

sensitive to the CP properties of X

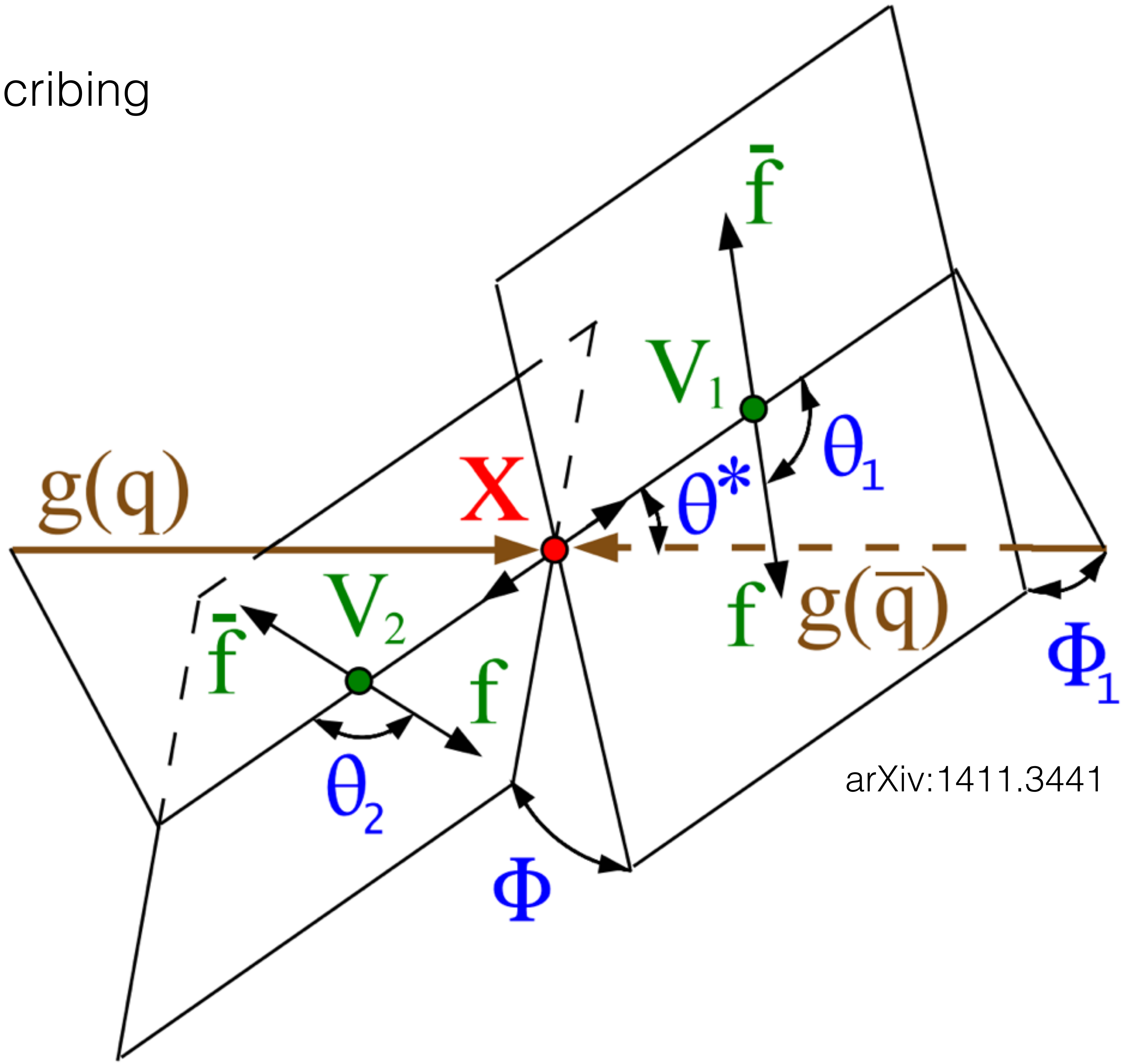

arXiv:1411.3441

- other variables, pT & η, are sensitive to NLO effects & insensitive to CP

Fermilab

Distributions masses

- In some sense, the power of the 4ℓ channel stems from the ability to reconstruct masses with very good resolution
  - both CMS and ATLAS exploit the masses to discriminate signal from background
  - not much sensitivity different CP quantum numbers
  - sensitive to form factors

arXiv:1411.3441

Distributions production angles

- Angles describing Z's with respect to incoming partons
- Sensitive to the spin and polarization of X resonance, but aren't sensitive to various CP quantum numbers
  - some help in distinguishing signal from backgrounds

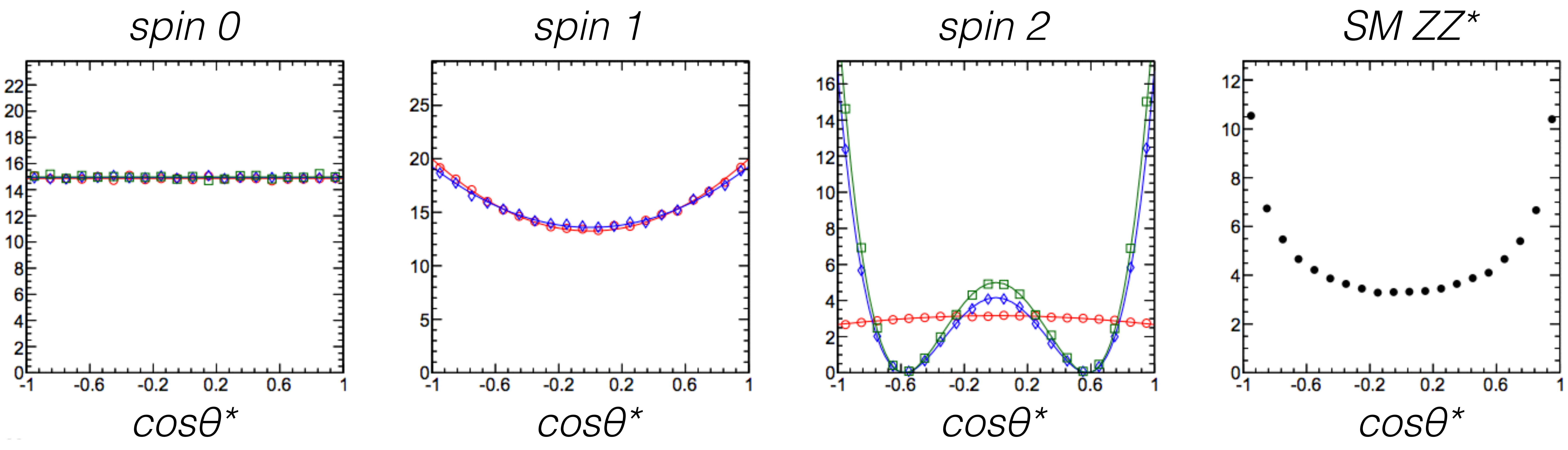

arXiv1208.4018v3

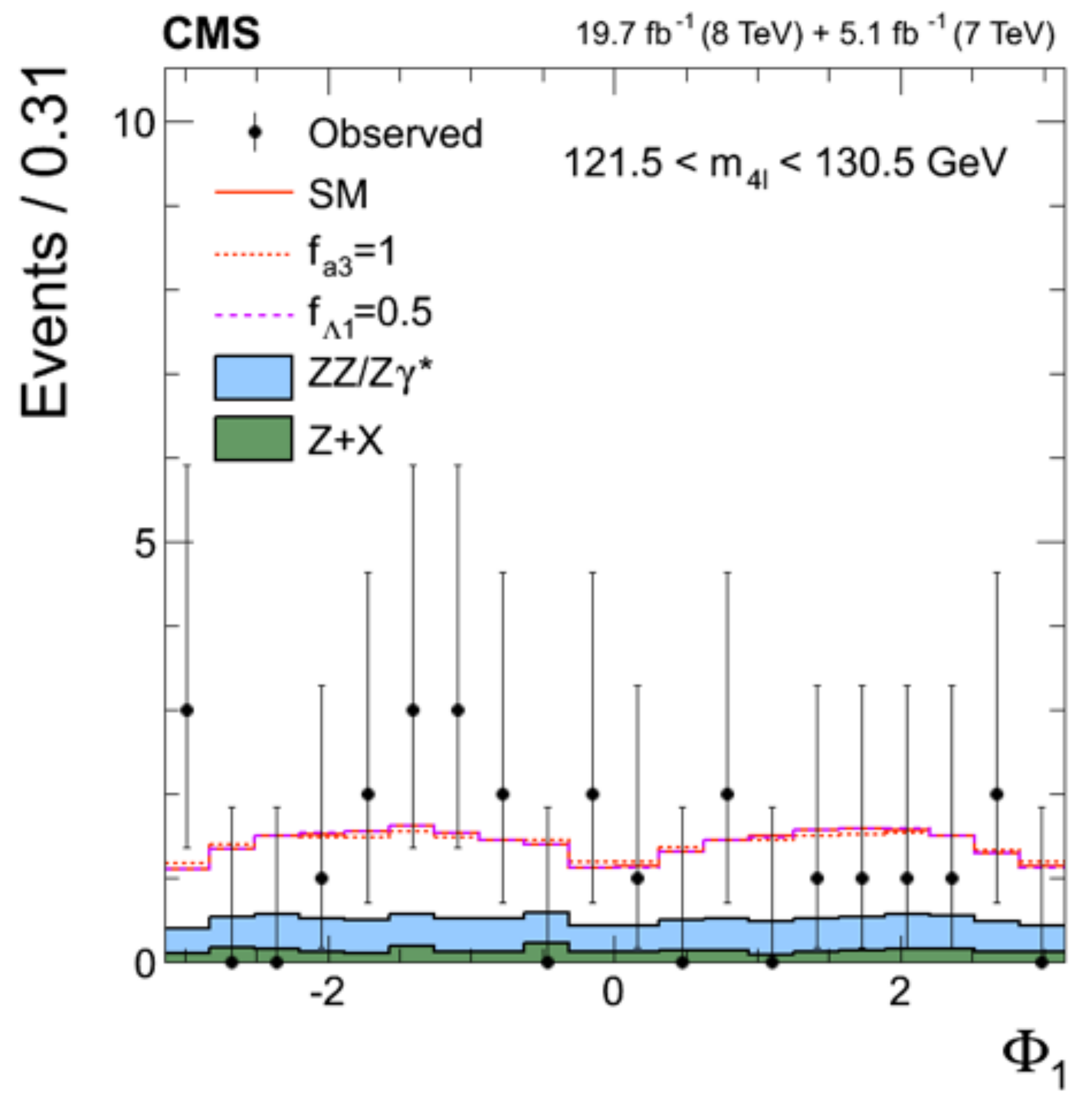

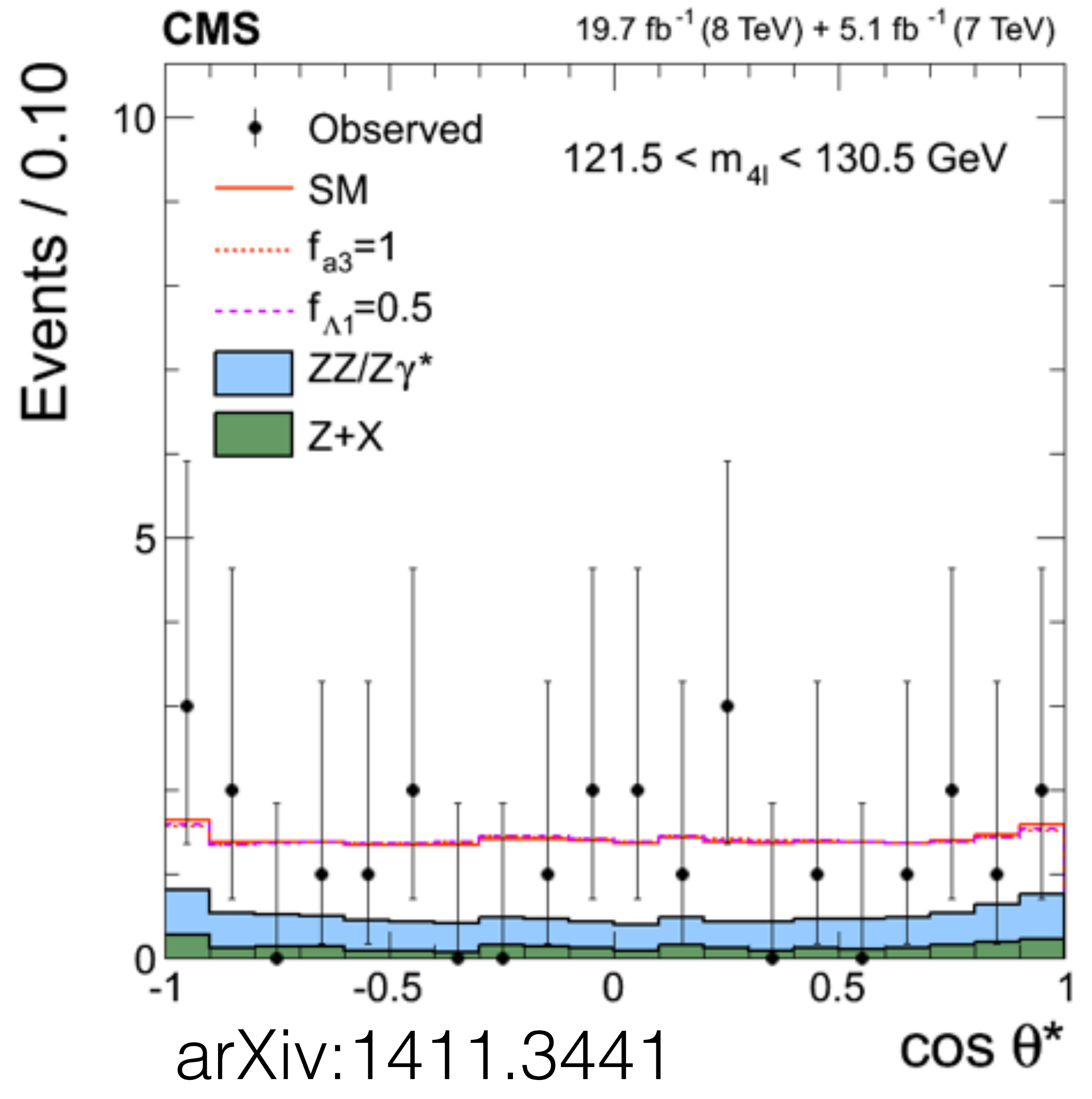

arXiv:1411.3441

Fermilab

arXiv:1411.3441

Distributions decay angles

- Angles describing directions of leptons with respect to Z's
- These ***are*** sensitive to the CP properties!

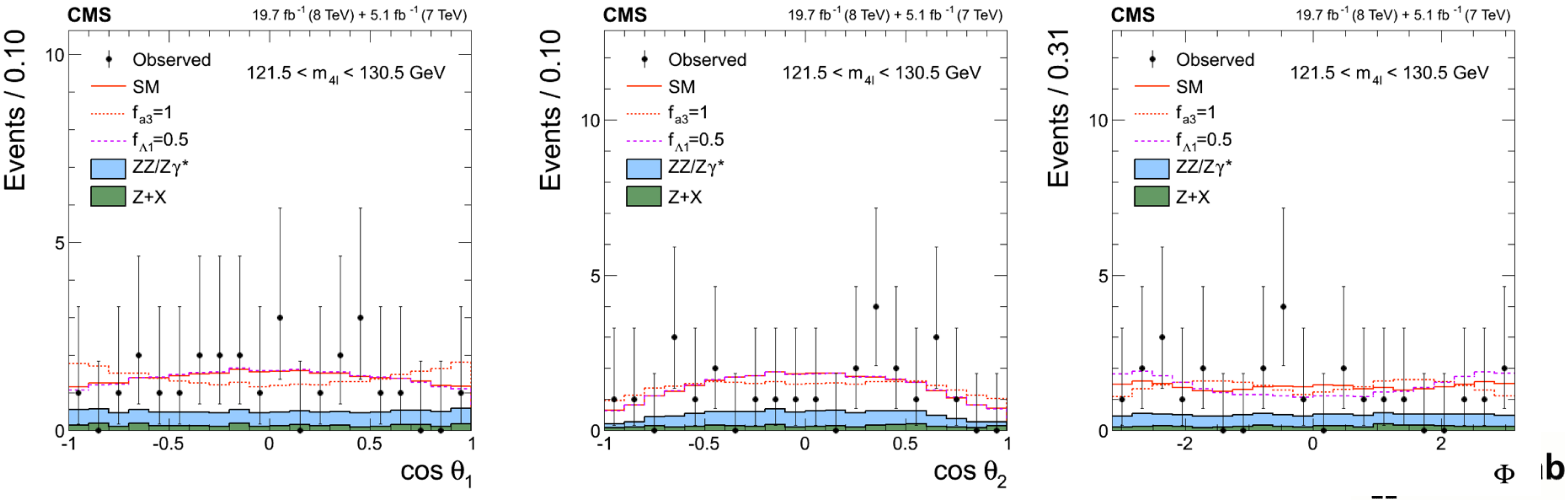

ATLAS distributions

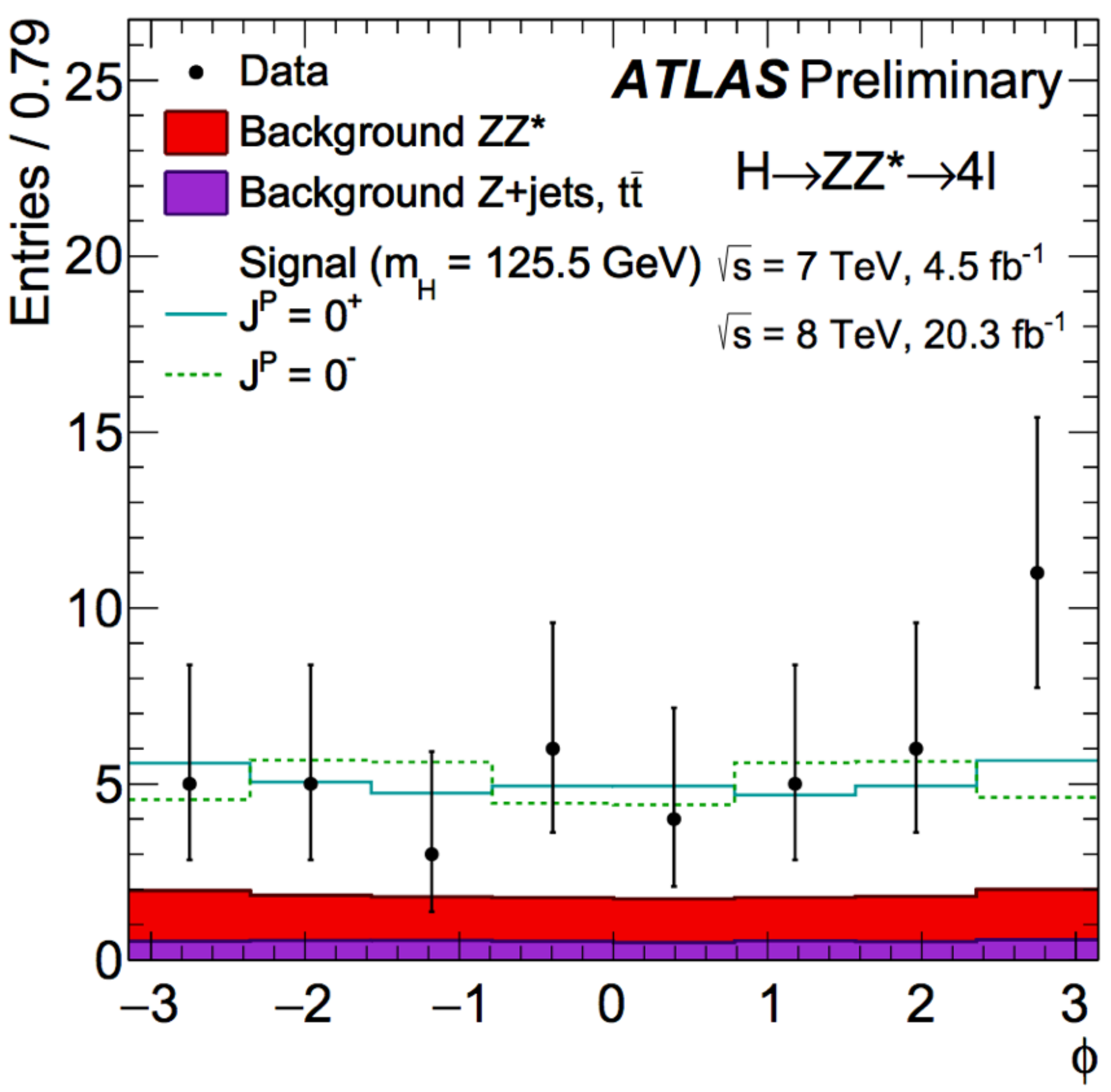

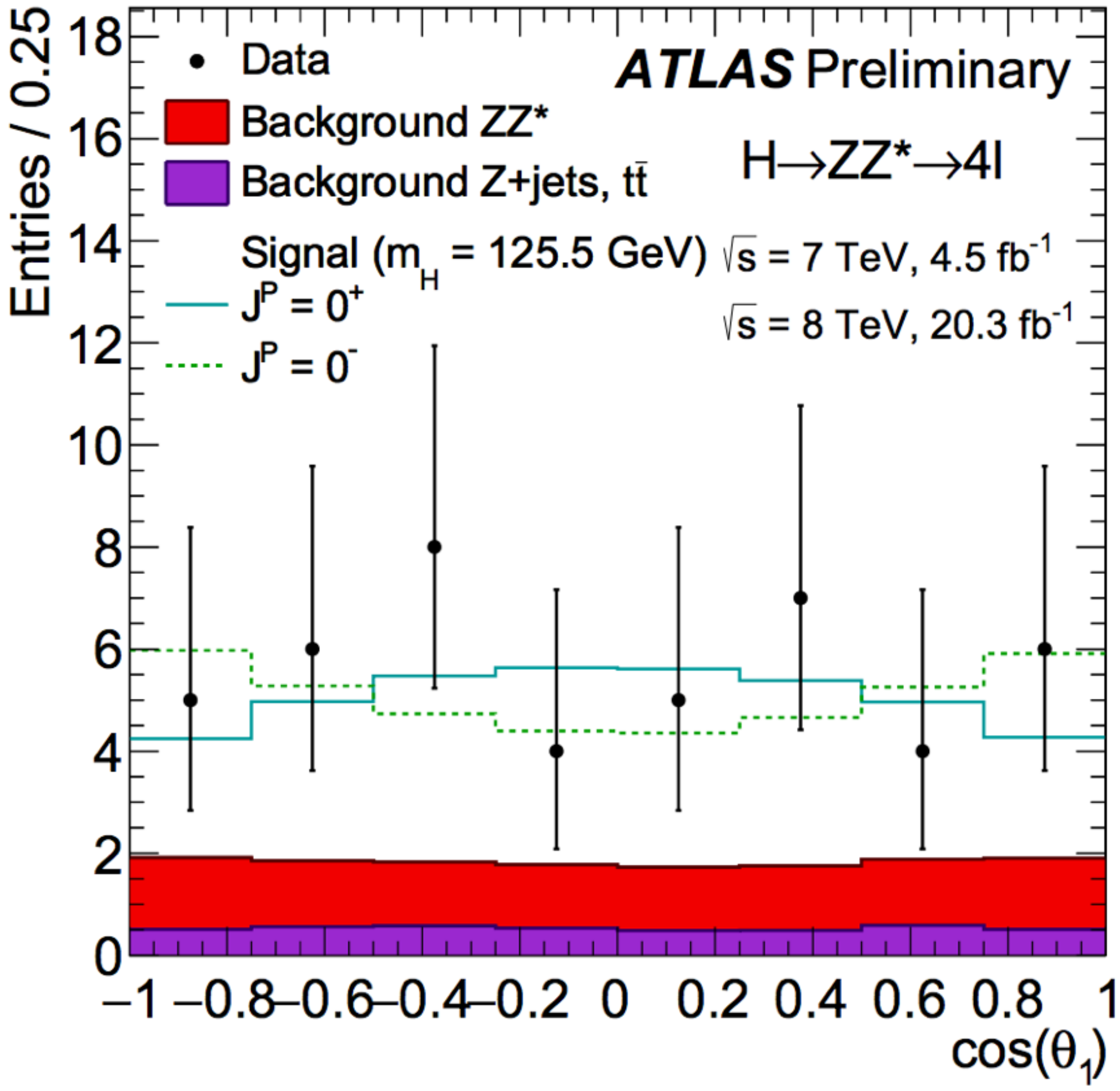

see backup for more plots

Fermilab

Multidimensional fits & modeling data

- modeling data with either
  - templates based on kinematic discriminants
    - discriminants based on LO ME or BDT
    - 3D templates describing various event categories
      (one sensitive to signal/background,
      one sensitive to CP eigenstates,
      one sensitive to interference)
  - fully correlated multi-dim likelihood
    (including approx. detector effects)
    - CMS: 8D
      ($m_{4\ell}$, $m_{1,2}$, $\cos\theta_{1,2}$, ϕ, $\cos\theta^*$, ϕ_1)
      ATLAS: 9D
      ($p_T^{4\ell}$, $\eta_{4\ell}$, $m_{4\ell}$, $m_{1,2}$, $\cos\theta_{1,2}$, ϕ, $\cos\theta^*$)
    - used to validate discriminant fits

e.g.:

$$|\mathcal{ME}|^2 = |\mathcal{ME}_{0+}|^2 + |\mathcal{ME}_{0-}|^2 + 2\mathcal{R}e(\mathcal{ME}^*_{0+}\mathcal{ME}_{0-})$$

$$\mathcal{D}_{0-} = |\mathcal{ME}_{0-}|^2 / [|\mathcal{ME}_{0+}|^2 + |\mathcal{ME}_{0-}|^2]$$

$$\mathcal{D}_{\mathrm{int}} = 2\mathcal{R}e(\mathcal{ME}^*_{0+}\mathcal{ME}_{0-}) / [|\mathcal{ME}_{0+}|^2 + |\mathcal{ME}_{0-}|^2]$$

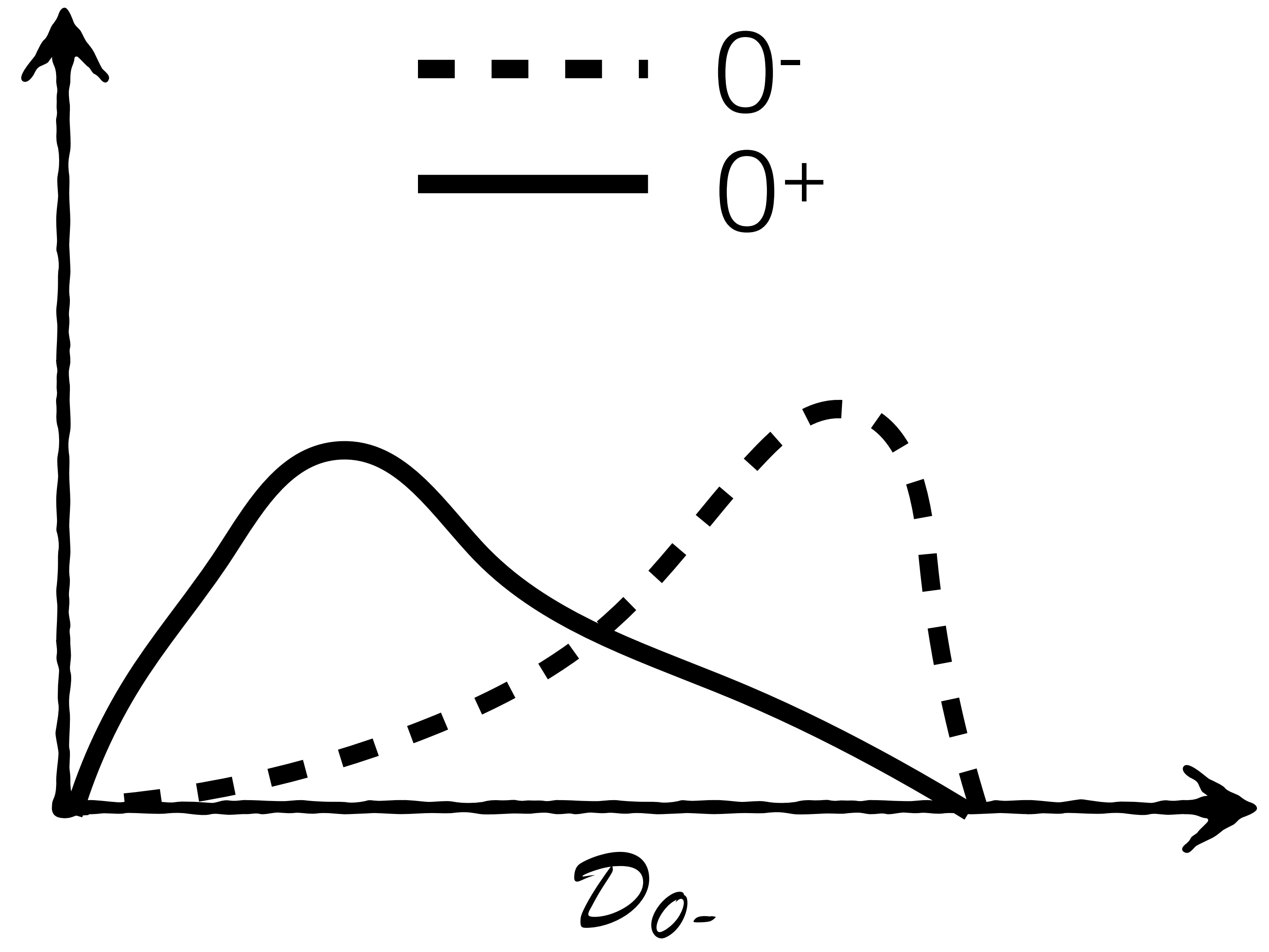

Distributions discriminants

- ***D_{bkg}*** used to distinguish signal from background, dominant contribution from masses
- ***D_{0-}*** used to distinguish 0+ from 0- neglecting kinematics from interference
- ***D_{CP}*** used to enhance interference effects, become important at small values of fa3

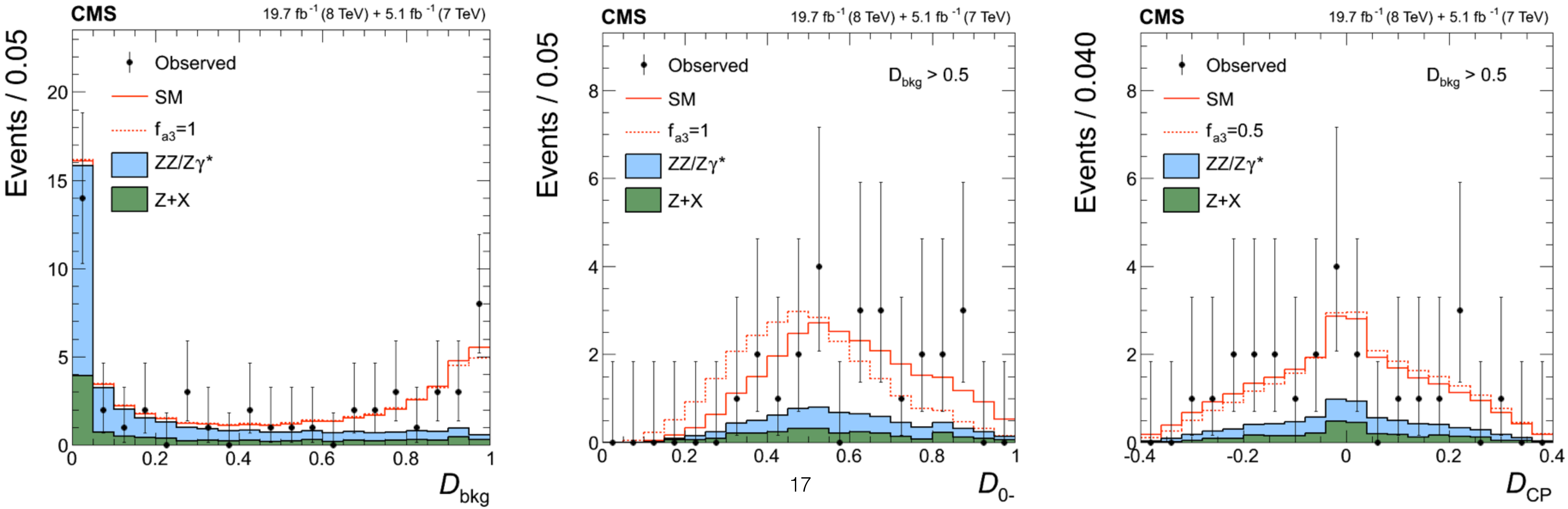

ATLAS discriminants

- Three discriminants are qualitatively similar to those used for the CMS analysis

- BDT_{ZZ} trained for signal versus backgrounds (*inputs:* $\eta_{4\ell}$, $p_T^{4\ell}$, $m_{4\ell}$, $\cos(\theta^*)$, ϕ_1)

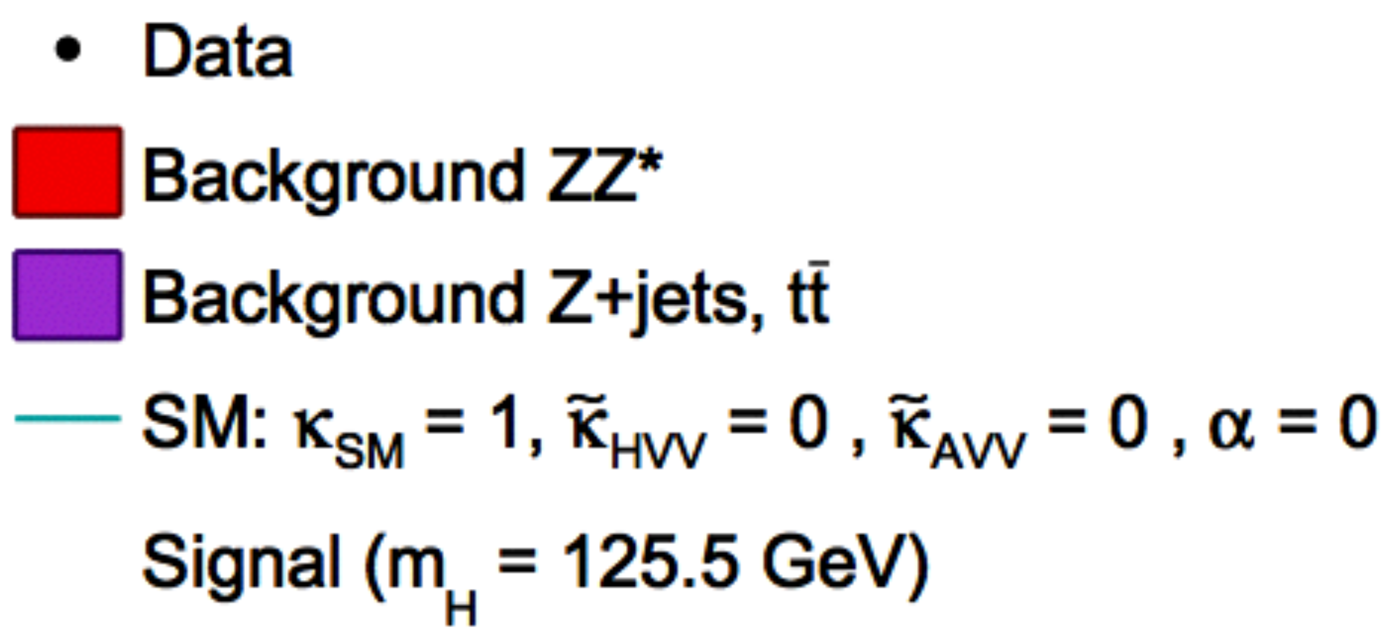

1D likelihood scans CMS

- log-likelihood scans for f_{a3} show consistency with the SM
- f_{a3} is a direct probe of CP-violating interactions - 95% C.L. upper limits set as low as f_{a3}<0.2 (depending on the assumptions made)

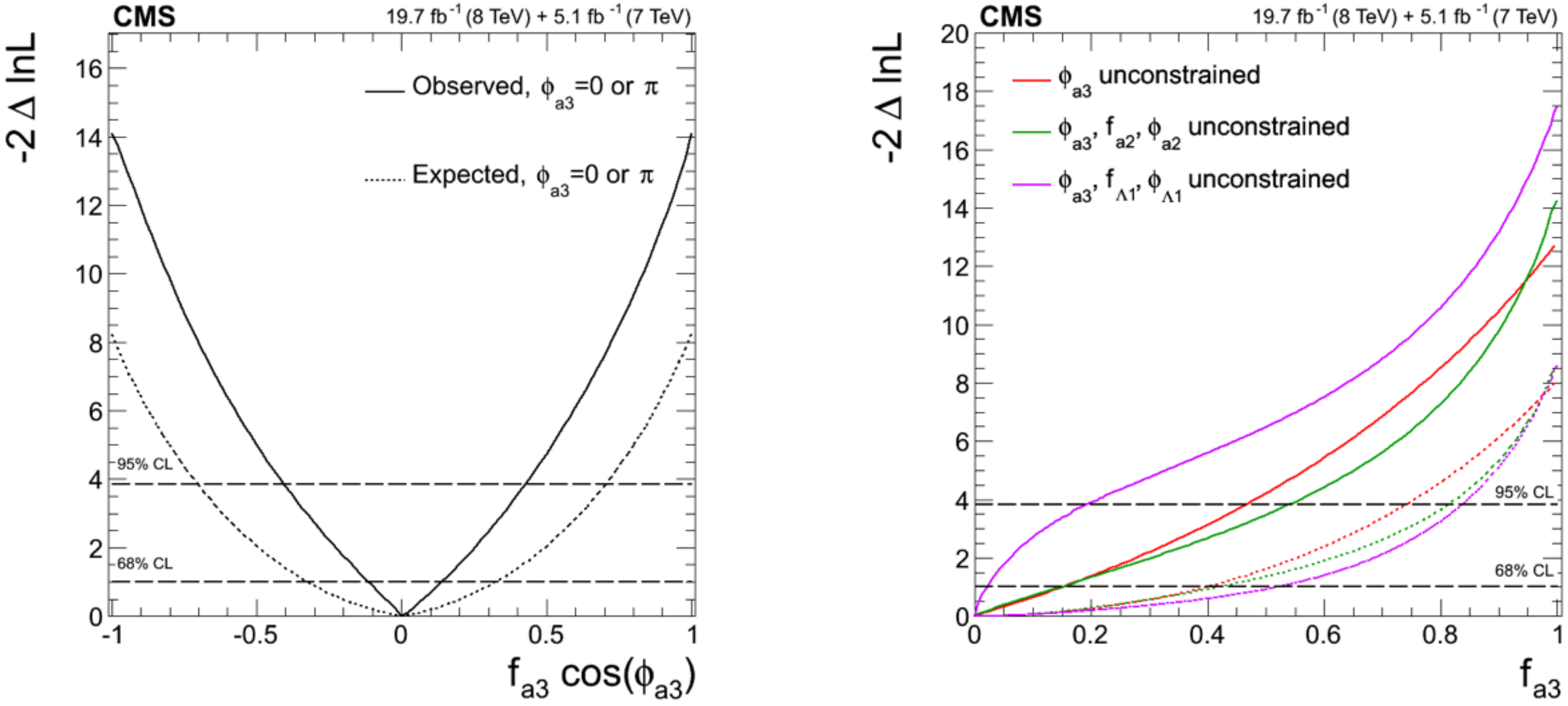

Parameter	Observed	Expected
$f_{a3}\cos(\phi_{a3})$	$0.00^{+0.14}_{-0.11}$ $[-0.40, 0.43]$	$0.00^{+0.33}_{-0.33}$ $[-0.70, 0.70]$
a_3/a_1	$[-2.05, 2.19]$	$[-3.85, 3.85]$

1D likelihood scans ATLAS

- Results consistent with SM expectations (κ_{AVV}/κ_{SM}=0)
  - small deviation from zero observed, only 1σ effect
- Results similar to CMS

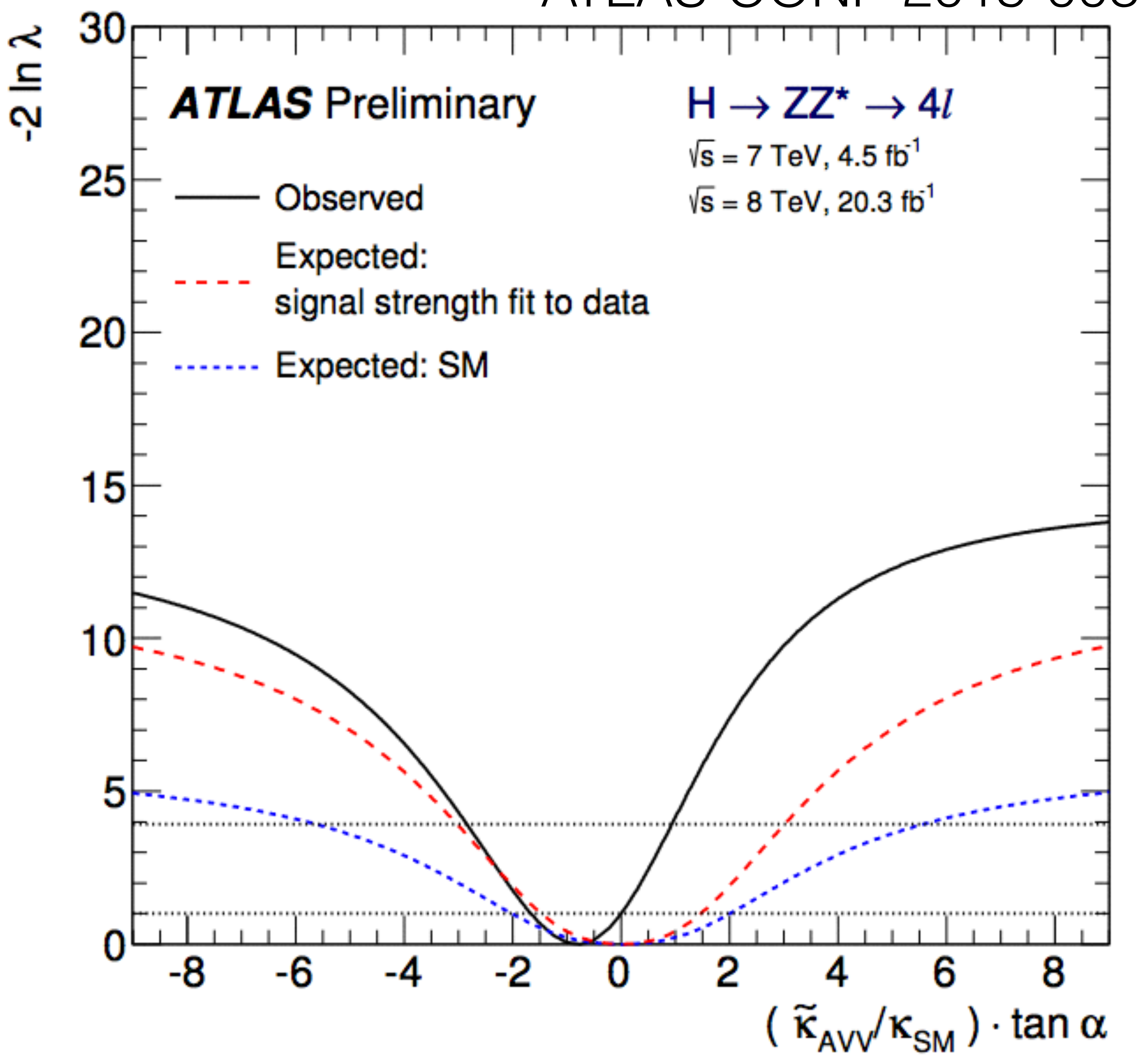

Coupling ratio $H \to ZZ^* \to 4\ell$	Best fit value Expected	Observed	95% CL Exclusion Regions Expected	Observed
$\tilde{\kappa}_{HVV}/\kappa_{SM}$	0.0	−0.2	$(-\infty, -0.75] \bigcup [6.95, \infty)$	$(-\infty, -0.75] \bigcup [2.45, \infty)$
$(\tilde{\kappa}_{AVV}/\kappa_{SM}) \cdot \tan\alpha$	0.0	−0.8	$(-\infty, -2.95] \bigcup [2.95, \infty)$	$(-\infty, -2.85] \bigcup [0.95, \infty)$

Fermilab

2D likelihood scans CMS

- For completeness: 2D scan of f_{a2}, $f_{\Lambda 1}$ versus f_{a3} are shown

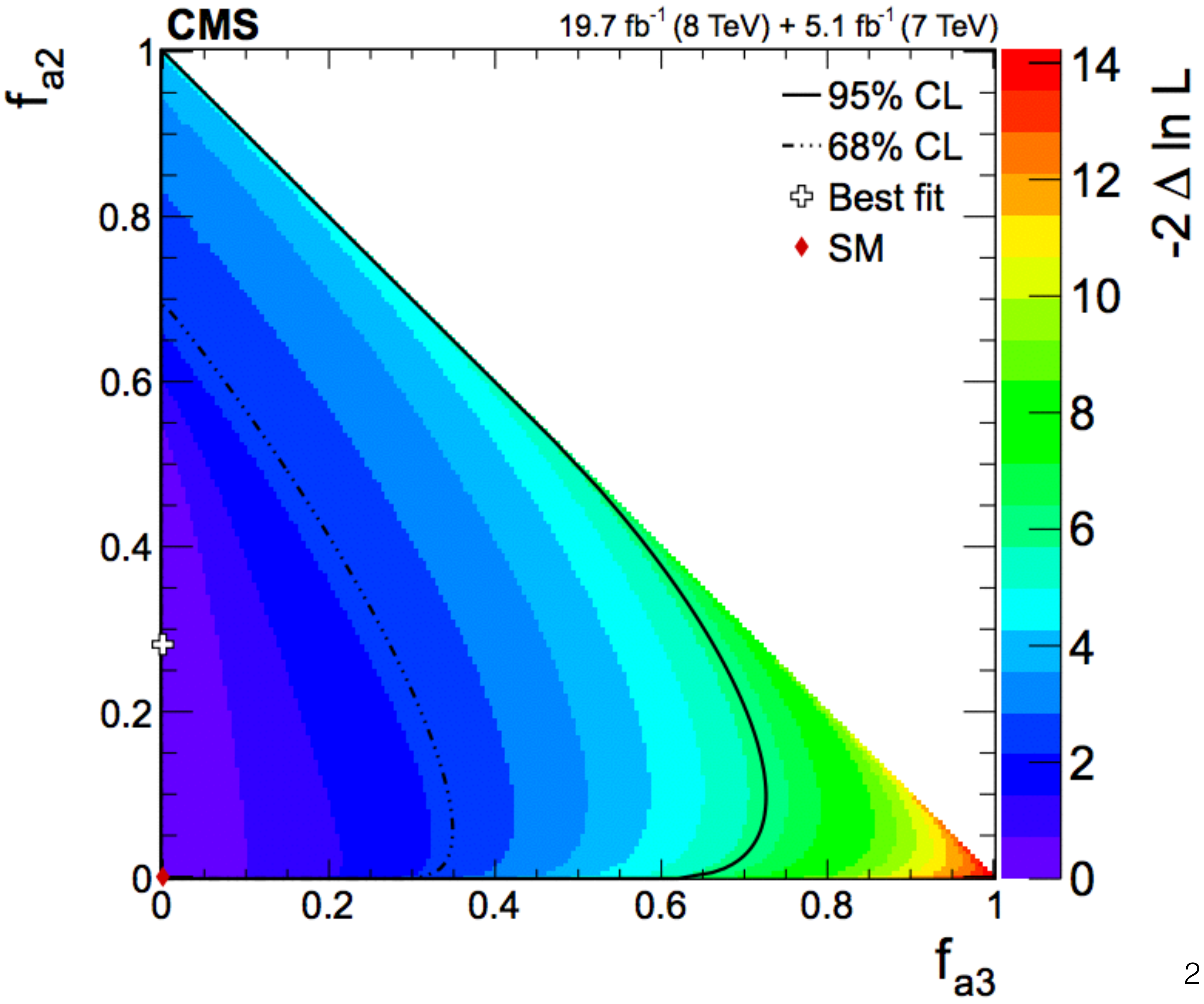

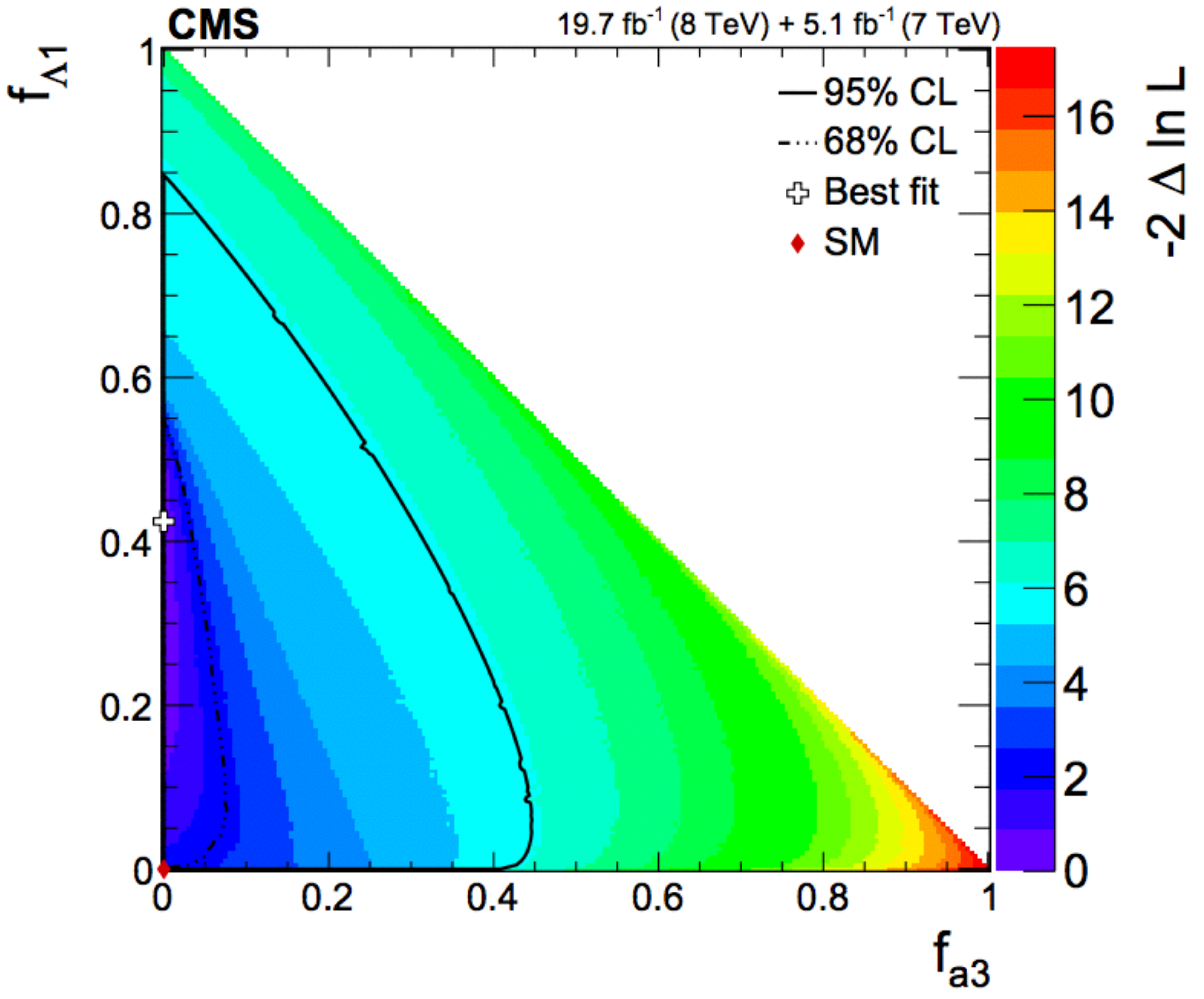

WW analysis

- opposite sign e-μ events selected
- Events classified based on the exclusive numbers of jets (0 or 1 jet)
- Main backgrounds, WW, ttbar/tW, and Z/W+jets are extrapolated from data control regions
- CMS: 2D distribution of mll and mT distributions are used to describe events
  ATLAS: 2D distributions of BDT discriminants are used

Channel	0-jet		1-jet	
Energy	7 TeV	8 TeV	7 TeV	8 TeV
WW	861 ± 12	4185 ± 63	249.9 ± 4.0	1268 ± 21
$WZ + ZZ + Z/\gamma^*$	22.7 ± 1.2	178.3 ± 9.5	26.4 ± 1.4	193 ± 11
$t\bar{t} + tW$	91 ± 20	500 ± 96	226 ± 14	1443 ± 46
W+jets	150 ± 39	620 ± 160	60 ± 16	283 ± 72
$W\gamma^{(*)}$	68 ± 20	282 ± 76	10.1 ± 2.8	55 ± 14
Background	1193 ± 50	5760 ± 210	573 ± 22	3242 ± 90
Signal $gg \to H$	50 ± 10	227 ± 46	17.1 ± 5.5	88 ± 28
Signal VBF+VH	0.44 ± 0.03	10.27 ± 0.41	2.09 ± 0.12	19.83 ± 0.81
Observed	1207	5747	589	3281

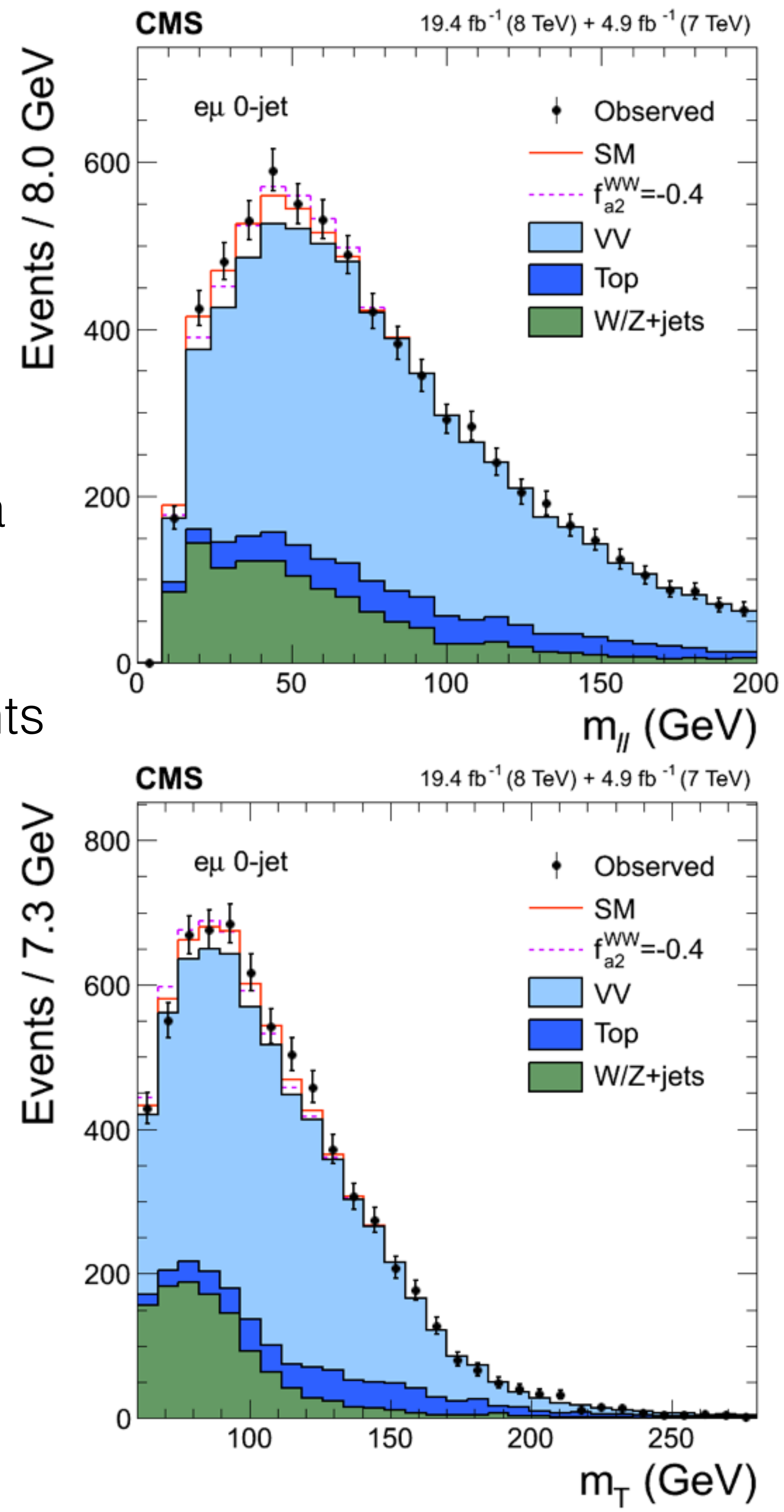

arXiv:1411.3441

1D likelihood scans WW

CMS

Parameter	Observed	Expected
$f_{\Lambda1}^{WW}\cos(\phi_{\Lambda1}^{WW})$	$0.21^{+0.18}_{-1.21}$ $[-1.00, 1.00]$	$0.00^{+0.34}_{-1.00}$ $[-1.00, 0.41] \cup [0.49, 1.00]$
$f_{a2}^{WW}\cos(\phi_{a2}^{WW})$	$-0.02^{+1.02}_{-0.16}$ $[-1.00, -0.54] \cup [-0.29, 1.00]$	$0.00^{+1.00}_{-0.12}$ $[-1.00, -0.58] \cup [-0.22, 1.00]$
$f_{a3}^{WW}\cos(\phi_{a3}^{WW})$	$-0.03^{+1.03}_{-0.97}$ $[-1.00, 1.00]$	$0.00^{+1.00}_{-1.00}$ $[-1.00, 1.00]$

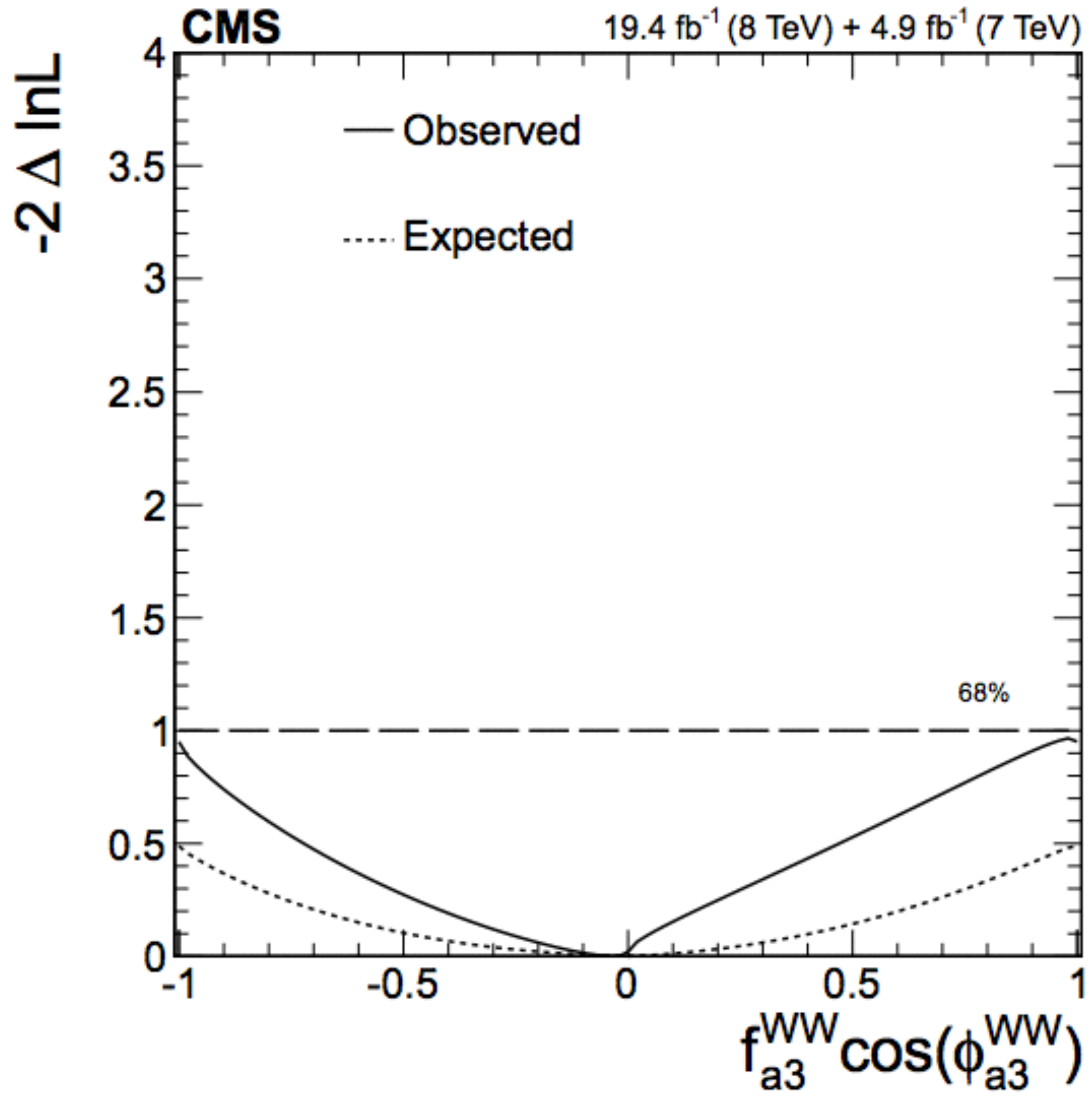

arXiv:1411.3441

ATLAS

Coupling ratio	Best fit value		95% CL Exclusion Regions	
$H \to WW^* \to e\nu\mu\nu$	Expected	Observed	Expected	Observed
$\tilde{\kappa}_{HVV}/\kappa_{SM}$	0.0	−1.3	$[-1.2, -0.7]$	$(-\infty, -2.2] \cup [-1, -0.85] \cup [0.4, \infty)$
$(\tilde{\kappa}_{AVV}/\kappa_{SM}) \cdot \tan\alpha$	0.0	−0.2	–	$(-\infty, -6] \cup [5, \infty)$

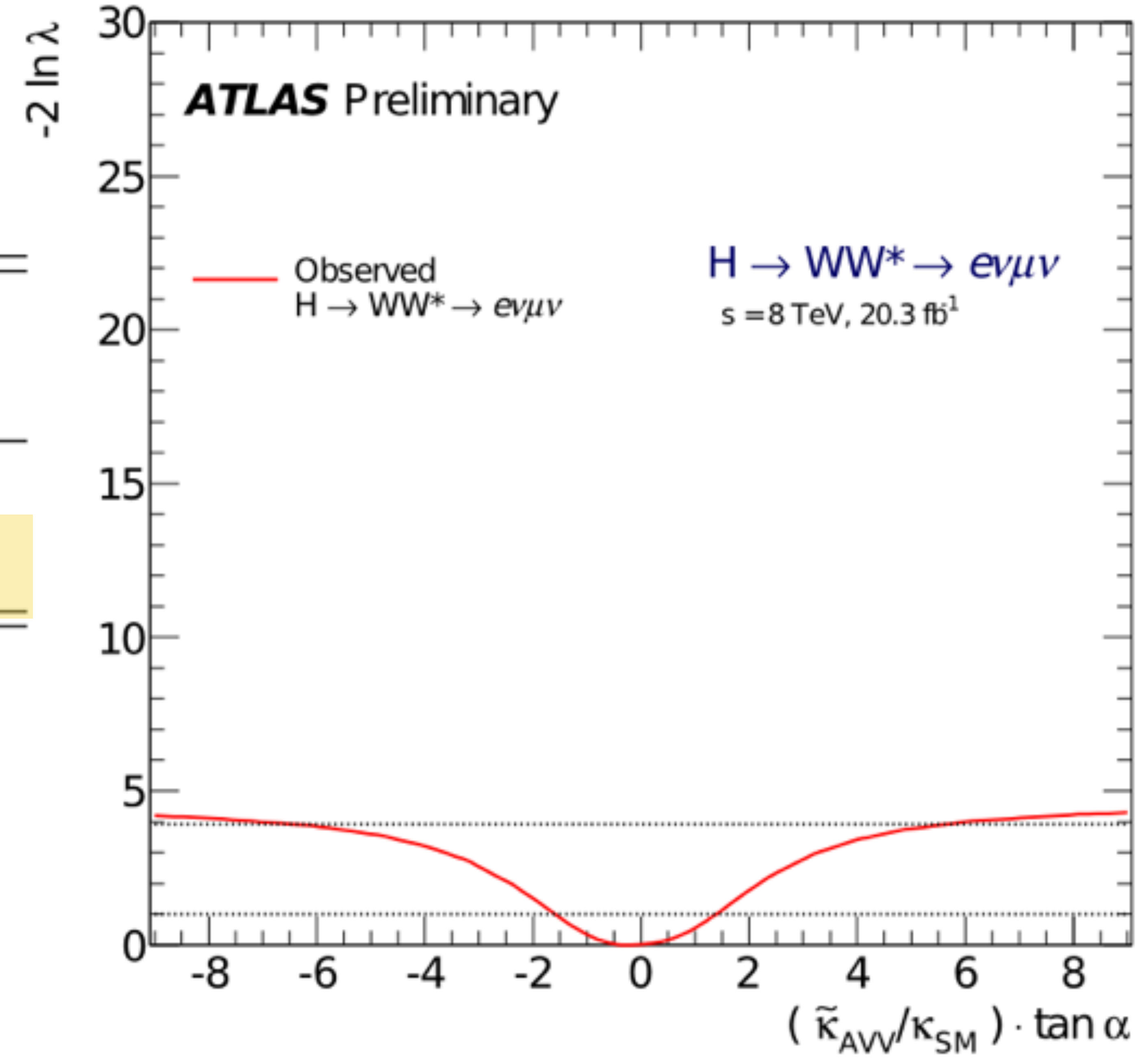

ATLAS-CONF-2015-008

b

Combined fits (ZZ&WW) CMS

- The combination of ZZ & WW channels involves twice as many degrees of freedom
  - We can constrain the size of the SM couplings (a_1) to be the same — custodial symmetry
    - fits are done both **with** and **without** this assumption
  - The relative strange of a_3/a_1 can also be fixed

$$r_{ai} = \frac{a_i^{WW}/a_1^{WW}}{a_i/a_1}, \text{ or } R_{ai} = \frac{r_{ai}|r_{ai}|}{1+r_{ai}^2}.$$

  - custodial symmetry & $R_{a3} = 0.5$ implies that $a_1^{WW} = a_1$ & $a_3^{WW} = a_3$

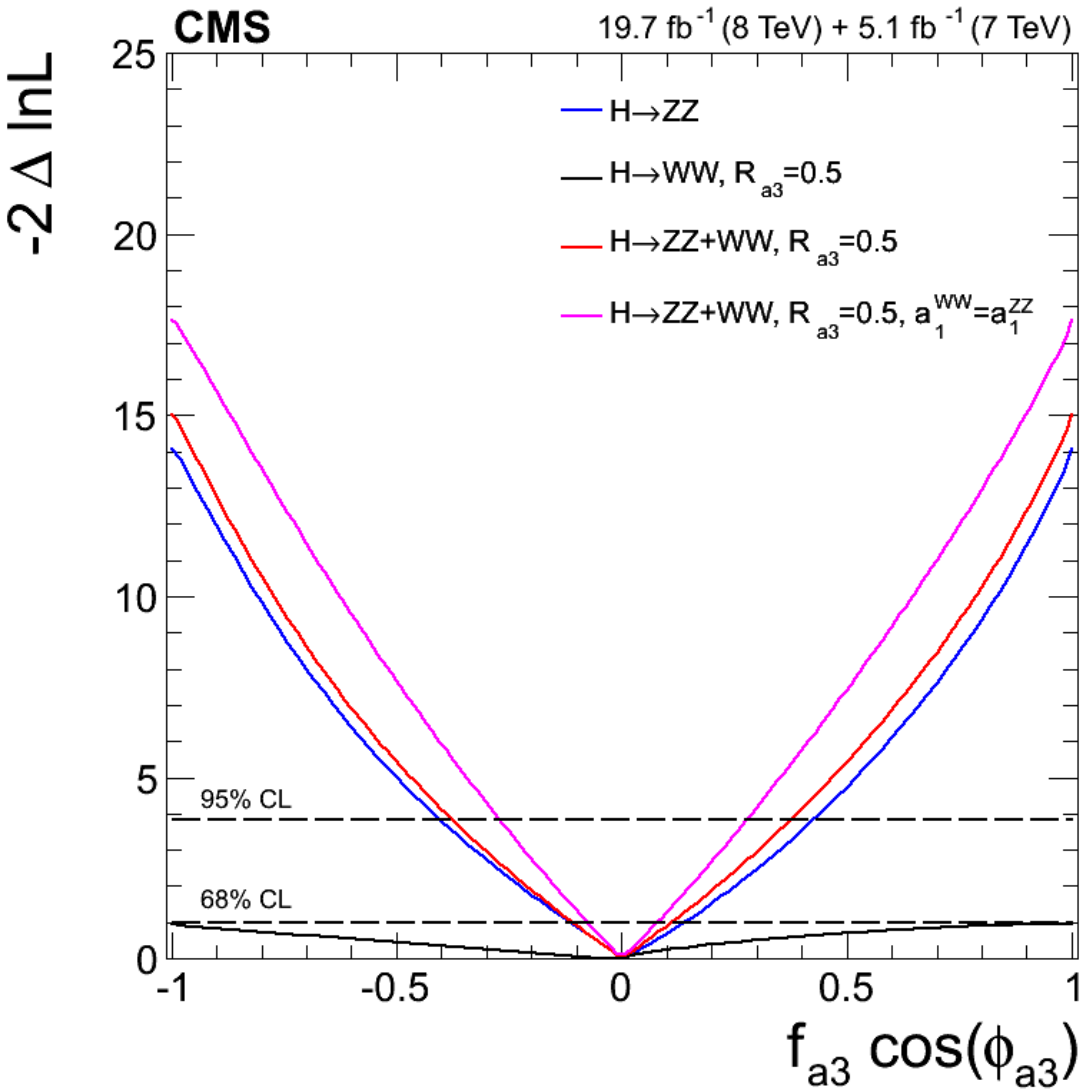

Parameter	Observed	Expected
$f_{\Lambda 1}\cos(\phi_{\Lambda 1})$	$0.21^{+0.11}_{-0.17}$ $[-0.42, 0.38]$	$0.00^{+0.15}_{-0.80}$ $[-1, 0.27] \cup [0.95, 1]$
$f_{a2}\cos(\phi_{a2})$	$-0.01^{+0.02}_{-0.05}$ $[-0.11, 0.17]$	$0.00^{+0.08}_{-0.03}$ $[-0.07, 0.51]$
$f_{a3}\cos(\phi_{a3})$	$0.00^{+0.08}_{-0.08}$ $[-0.27, 0.28]$	$0.00^{+0.23}_{-0.23}$ $[-0.53, 0.53]$

arXiv:1411.3441

Combined fits (ZZ & WW) ATLAS

- Assuming $a_1/a_3 = a_1^{WW}/ a_3^{WW}$ ($R_{a3} = 0.5$)
- Deviation slightly reduced when combining ZZ & WW

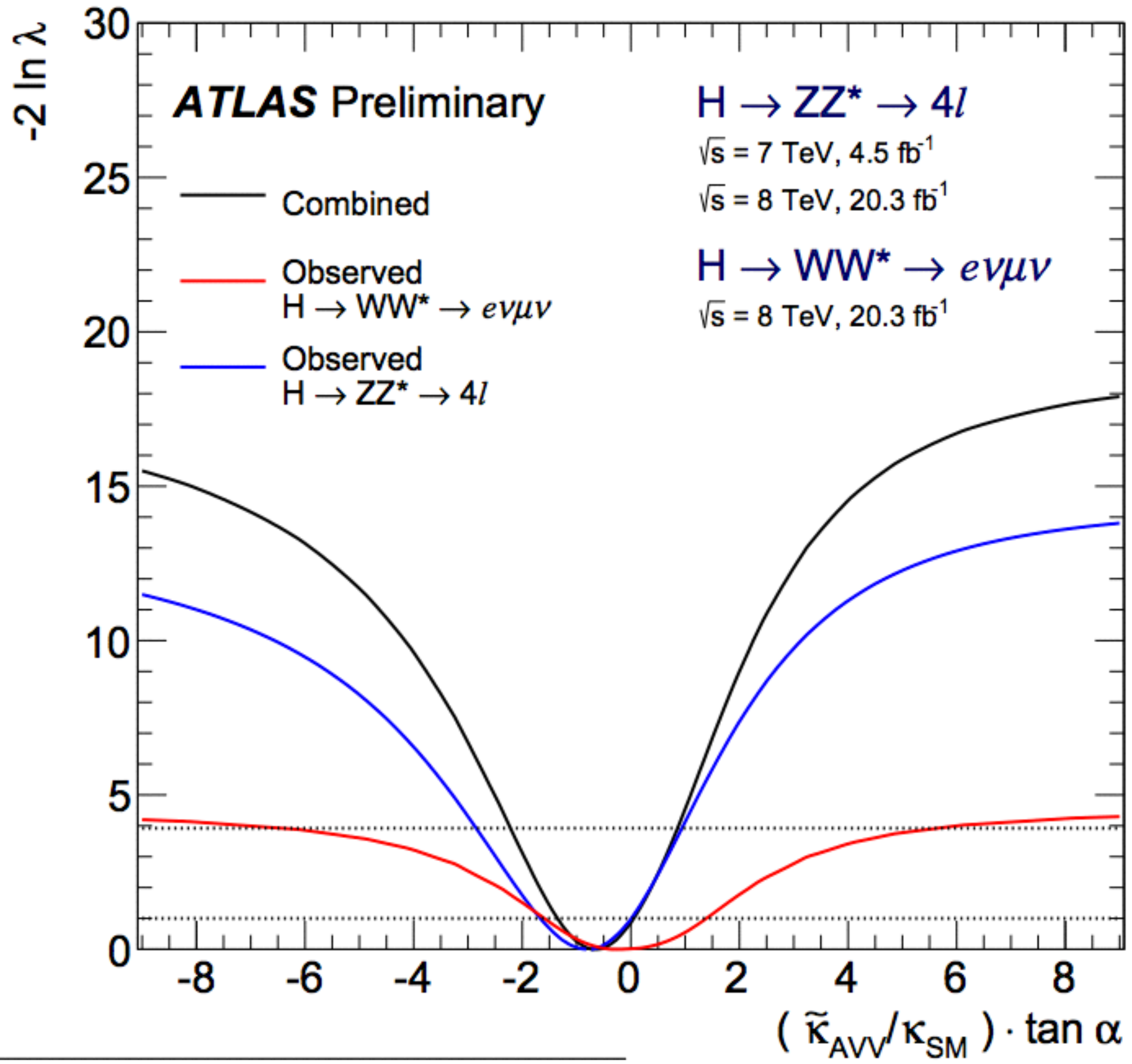

Coupling ratio	Best fit value		95% CL Exclusion Regions	
Combined	Expected	Observed	Expected	Observed
$\tilde{\kappa}_{HVV}/\kappa_{SM}$	0.0	−0.48	$(-\infty, -0.55] \bigcup [4.80, \infty)$	$(-\infty, -0.73] \bigcup [0.63, \infty)$
$(\tilde{\kappa}_{AVV}/\kappa_{SM}) \cdot \tan\alpha$	0.0	−0.68	$(-\infty, -2.33] \bigcup [2.30, \infty)$	$(-\infty, -2.18] \bigcup [0.83, \infty)$

Fermilab

Combined fits (ZZ&WW) CMS

- This combination takes advantage of the relationship between the expected yields in the two channels, significantly enhancing the overall sensitivity.

assuming $a_1^{WW} = a_1$

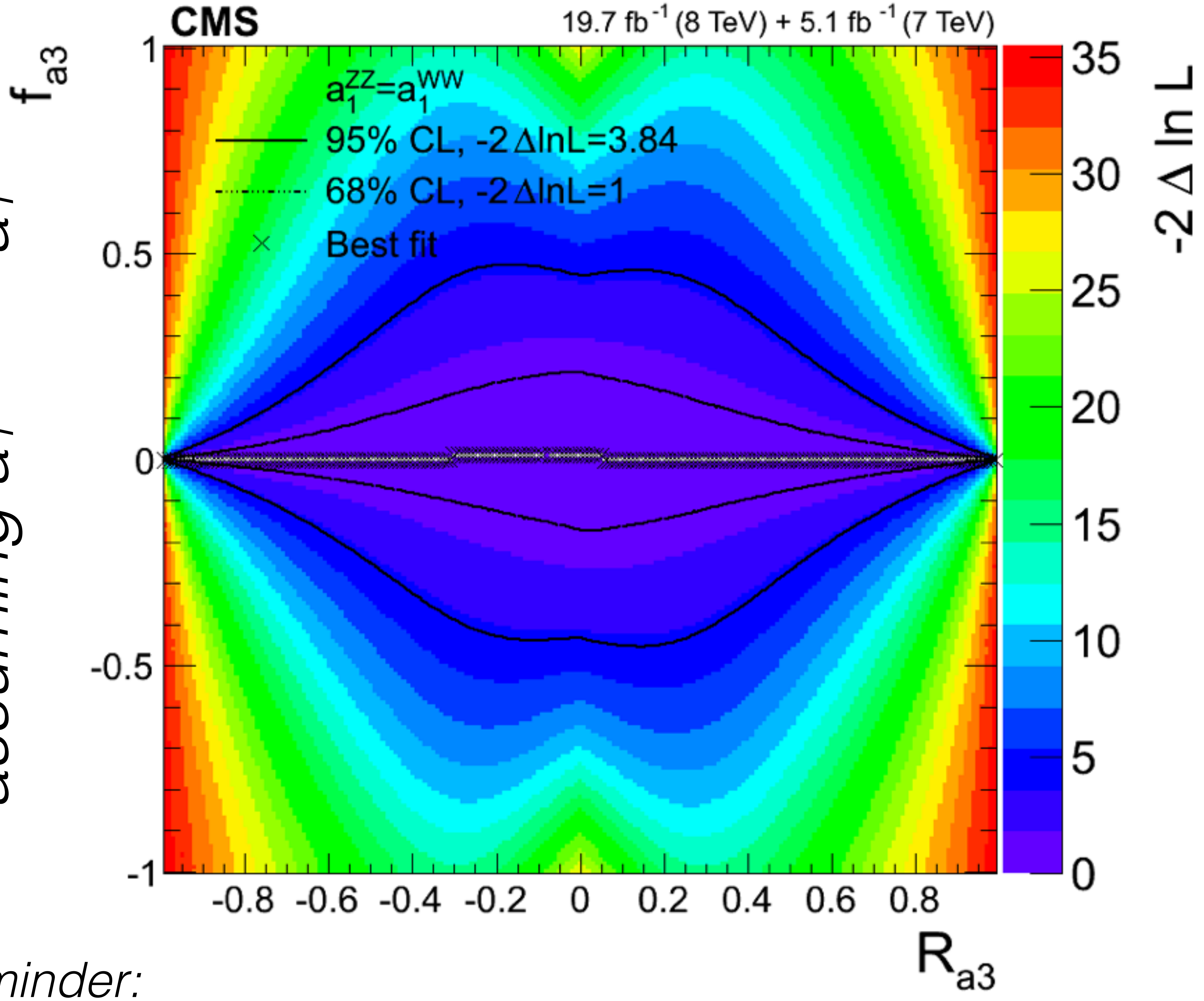

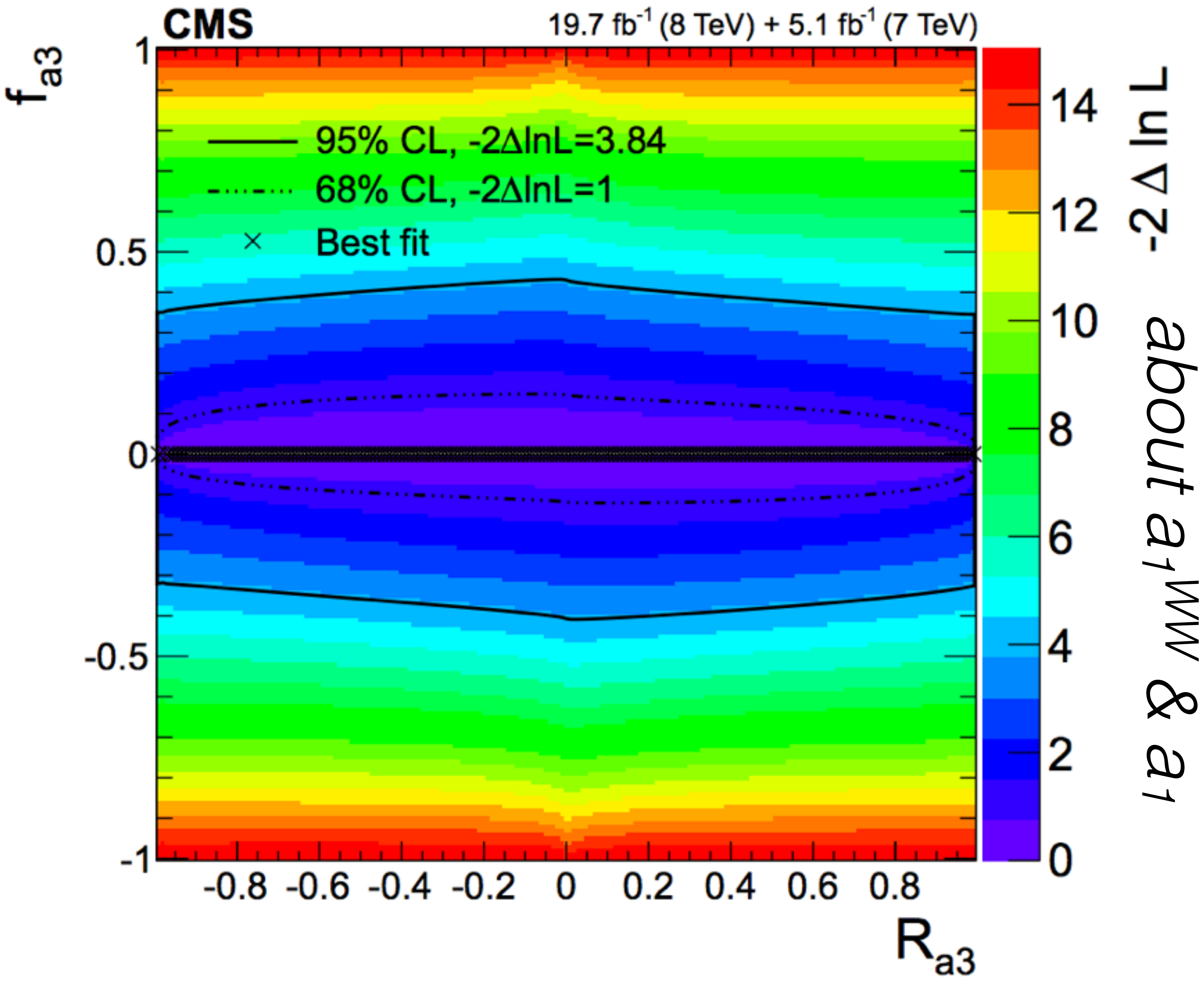

no assumption about a_1^{WW} & a_1

reminder:

$$r_{ai} = \frac{a_i^{WW}/a_1^{WW}}{a_i/a_1}, \text{ or } R_{ai} = \frac{r_{ai}|r_{ai}|}{1+r_{ai}^2}.$$

Fermilab

γγ & Zγ couplings

- Can even start to probe Zγ and γγ couplings with 4ℓ events

- Different discriminants used in order to be sensitive to these couplings

Measurement	Observables $\vec{x}$		
$f_{a3}^{\gamma\gamma}$	$\mathcal{D}_{bkg}$	$\mathcal{D}_{a3}^{\gamma\gamma}$	$\mathcal{D}_{CP}^{\gamma\gamma}$
$f_{a3}^{Z\gamma}$	$\mathcal{D}_{bkg}$	$\mathcal{D}_{a3}^{Z\gamma}$	$\mathcal{D}_{CP}^{Z\gamma}$

- note, sensitivity to these events is much weaker with 4ℓ events than search with on-shell photons
    - direct searches with on-shell photons are not sensitive to different CP states (only to the total cross section)

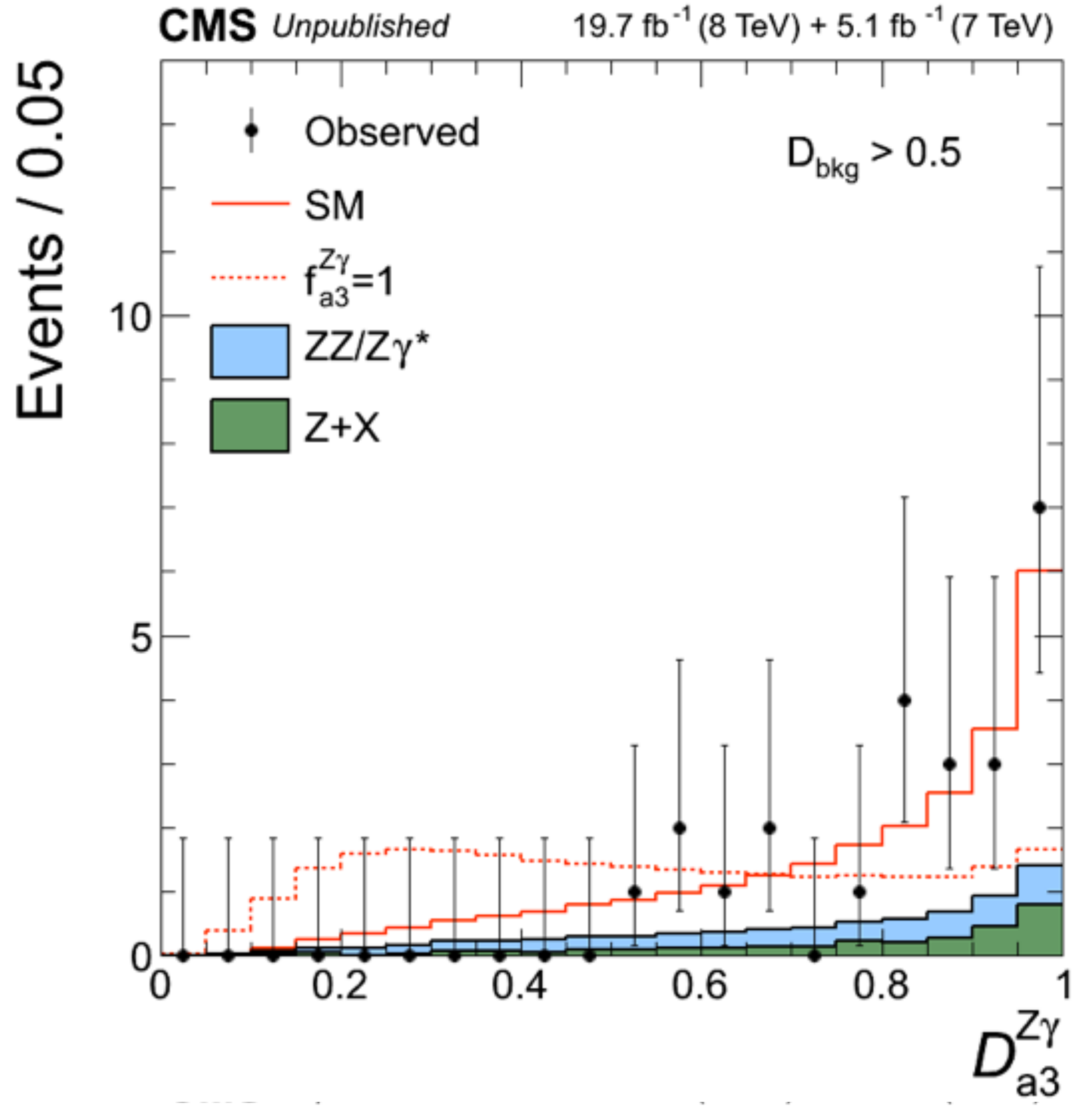

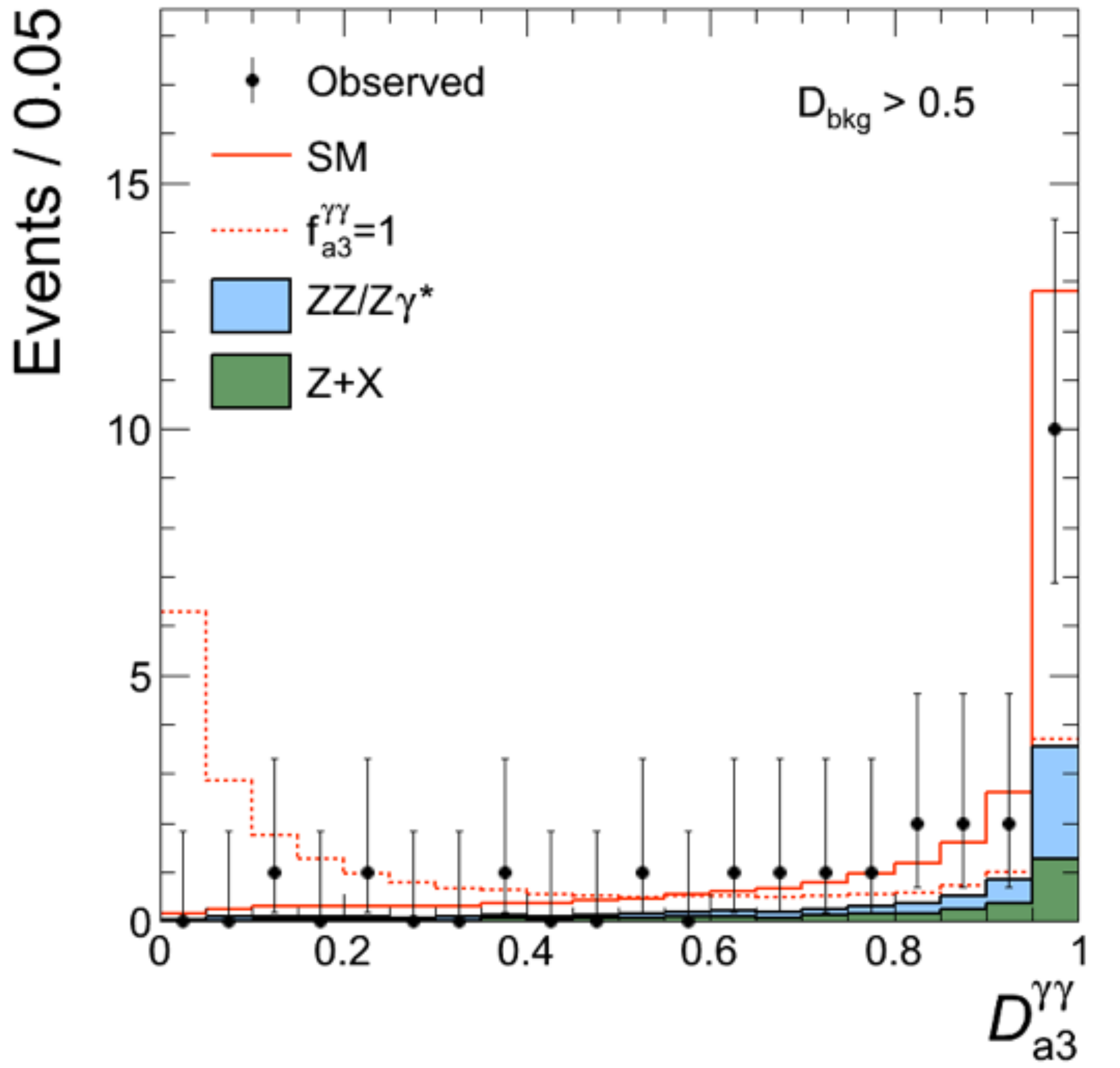

arXiv:1411.3441

γγ & Zγ couplings

- Overall sensitivity still far from SM expectation
  - orders of magnitude small than searches with on-shell photons
    - 95% C.L. upper limit on $\mu^{Z\gamma}$ ($\mu^{\gamma\gamma}$) ~ 170 (730) with 4ℓ events
    - 95% (68%) C.L upper limit on $\mu^{Z\gamma}$ = 9.5 with 2ℓ+γ events

Parameter	Observed	Expected	$f_{ai}^{VV}=1$
$f_{\Lambda1}^{Z\gamma}\cos(\phi_{\Lambda1}^{Z\gamma})$	$-0.27^{+0.34}_{-0.49}$ $[-1.00, 1.00]$	$0.00^{+0.83}_{-0.53}$ $[-1.00, 1.00]$	26% (16%)
$f_{a2}^{Z\gamma}\cos(\phi_{a2}^{Z\gamma})$	$0.00^{+0.14}_{-0.20}$ $[-0.49, 0.46]$	$0.00^{+0.51}_{-0.51}$ $[-0.78, 0.79]$	<0.01% (0.01%)
$f_{a3}^{Z\gamma}\cos(\phi_{a3}^{Z\gamma})$	$0.02^{+0.21}_{-0.13}$ $[-0.40, 0.51]$	$0.00^{+0.51}_{-0.51}$ $[-0.75, 0.75]$	<0.01% (<0.01%)
$f_{a2}^{\gamma\gamma}\cos(\phi_{a2}^{\gamma\gamma})$	$0.12^{+0.20}_{-0.11}$ $[-0.04, +0.51]$	$0.00^{+0.11}_{-0.09}$ $[-0.32, 0.34]$	<0.01% (<0.01%)
$f_{a3}^{\gamma\gamma}\cos(\phi_{a3}^{\gamma\gamma})$	$-0.02^{+0.06}_{-0.13}$ $[-0.35, 0.32]$	$0.00^{+0.15}_{-0.11}$ $[-0.37, 0.40]$	<0.01% (<0.01%)

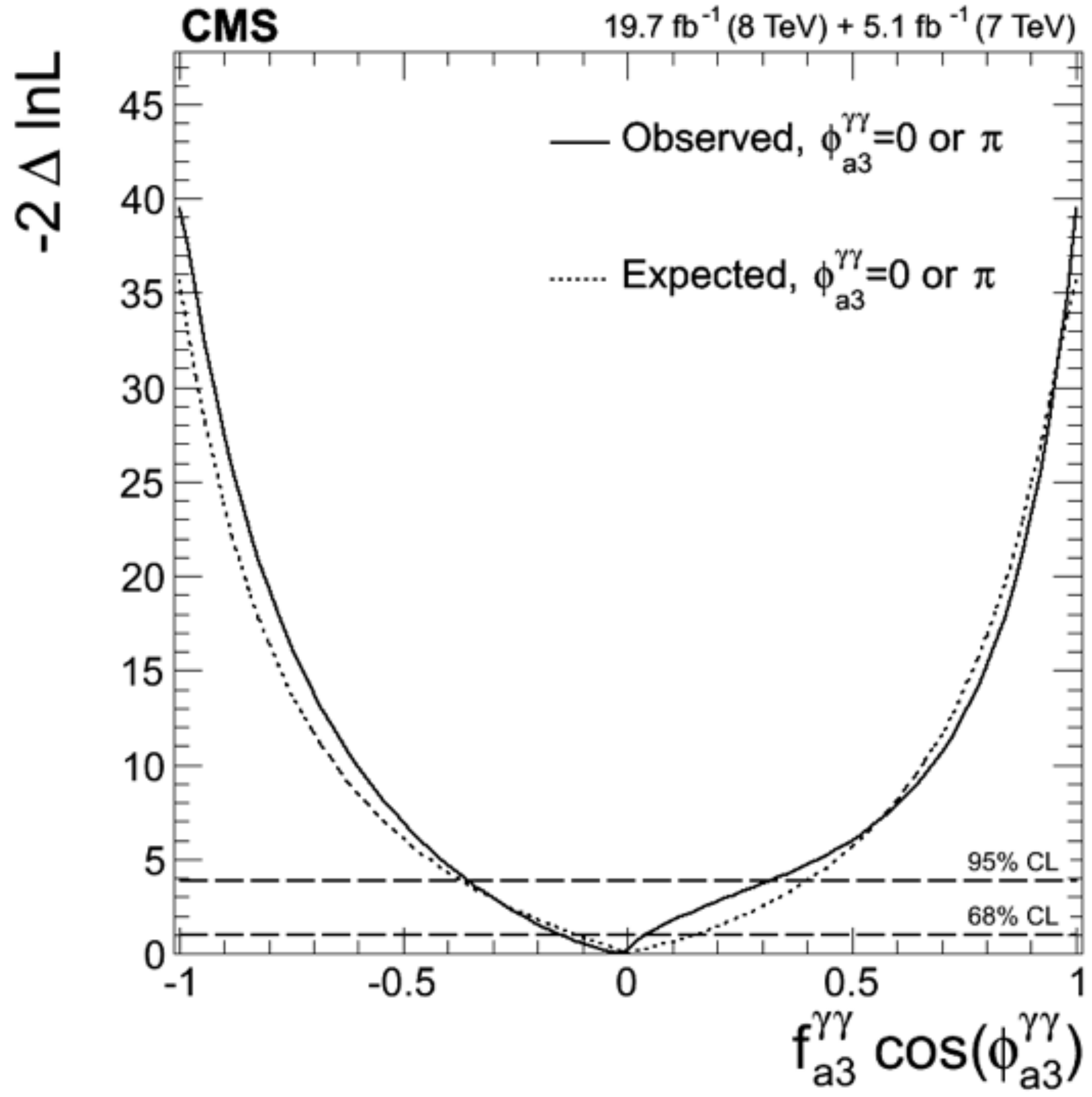

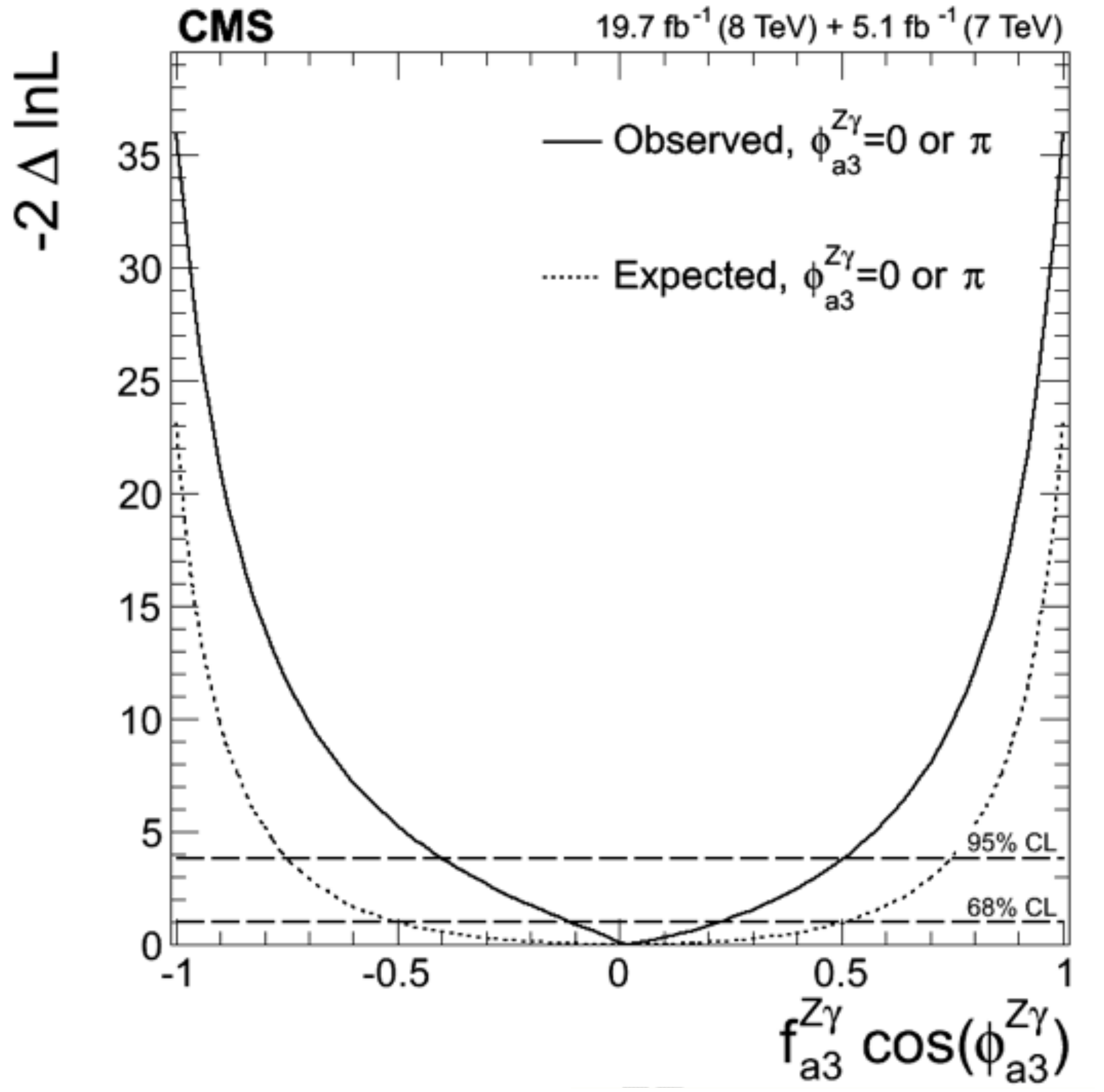

arXiv:1411.3441

Prospects for the LHC CMS

- Projections out to 300/fb & 3000/fb
  - fits are performed with templates in which events are described by 2D distributions of kinematic discriminants:
  - $$\mathcal{D}_{\rm bkg} = \left[1 + \frac{\mathcal{P}^{\rm kin}_{\rm bkg}(m_{Z_1}, m_{Z_2}, \vec{\Omega}|m_{4\ell}) \times \mathcal{P}^{\rm mass}_{\rm bkg}(m_{4\ell})}{\mathcal{P}^{\rm kin}_{0^+}(m_{Z_1}, m_{Z_2}, \vec{\Omega}|m_{4\ell}) \times \mathcal{P}^{\rm mass}_{\rm sig}(m_{4\ell}|m_{0^+})}\right]^{-1}$$
    $$\mathcal{D}_{J^P} = \left[1 + \frac{\mathcal{P}^{\rm kin}_{J^P}(m_{Z_1}, m_{Z_2}, \vec{\Omega}|m_{4\ell})}{\mathcal{P}^{\rm kin}_{0^+}(m_{Z_1}, m_{Z_2}, \vec{\Omega}|m_{4\ell})}\right]^{-1}$$
  - signals model with LO MC
  - scaling up all background predictions
  - all systematic uncertainties are assumed to be the same:
    still dominated by statistical uncertainties
  - can reach 95% C.L. upper limits of
    $f_{a3} < 0.13\ (0.04)$

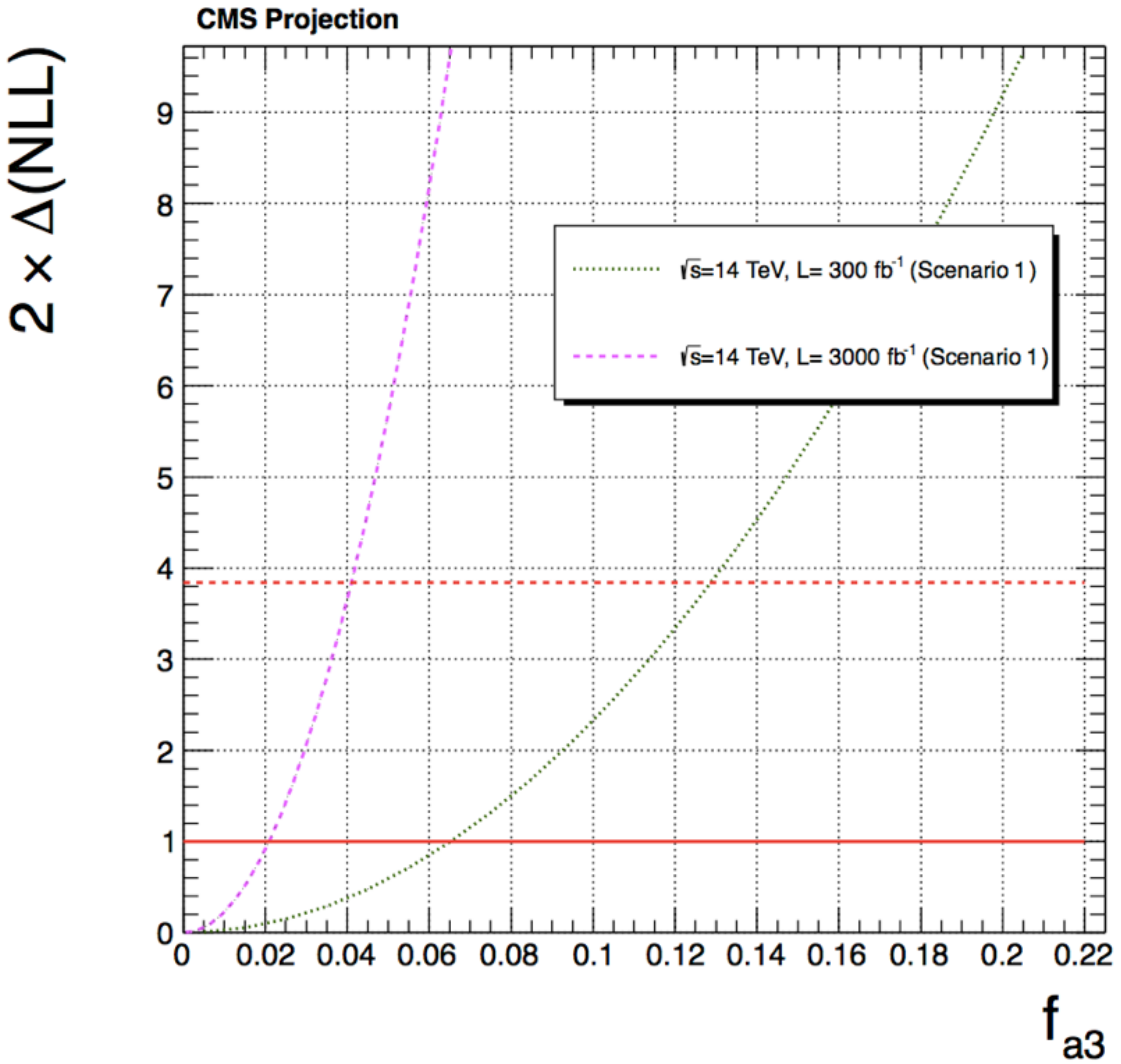

Prospects for the LHC ATLAS

- Exploring sensitivity to couplings @ 300 & 3000/fb
  - background: assuming qq->ZZ background scaled up to account for irreducible background
  - signal: LO MC - reweighing to morph signal hypothesis
- Fitting either
  - templates based on ME-based kinematic discriminants
  - fully correlated 8D likelihood
    (including approx. detector effects)
- Systematics uncertainties approximated to be: *3% luminosity, 5% signal and background yields (lepton reco ε), and 9.4% (7.4%) for 300/fb (3000/fb) for background yield*

ATLAS-PHYS-PUB-2013-013

Observable	Sensitivity
$\ln \frac{\lvert ME(g_1=1,g_2=0,g_4=0)\rvert^2}{\lvert ME(g_1=0,g_2=0,g_4=1)\rvert^2}$	$\lvert g_4\rvert/g_1$
$\ln \frac{\lvert ME(g_1=1,g_2=0,g_4=-2+2i)\rvert^2}{\lvert ME(g_1=1,g_2=0,g_4=2+2i)\rvert^2}$	$\Re(g_4)/g_1$
$\ln \frac{\lvert ME(g_1=1,g_2=0,g_4=2-2i)\rvert^2}{\lvert ME(g_1=1,g_2=0,g_4=2+2i)\rvert^2}$	$\Im(g_4)/g_1$
$\ln \frac{\lvert ME(g_1=1,g_2=0,g_4=0)\rvert^2}{\lvert ME(g_1=1,g_2=1,g_4=0)\rvert^2}$	$\lvert g_2\rvert/g_1$
$\ln \frac{\lvert ME(g_1=1,g_2=-1+i,g_4=0)\rvert^2}{\lvert ME(g_1=1,g_2=1+i,g_4=0)\rvert^2}$	$\Re(g_2)/g_1$
$\ln \frac{\lvert ME(g_1=1,g_2=1-i,g_4=0)\rvert^2}{\lvert ME(g_1=1,g_2=1+i,g_4=0i)\rvert^2}$	$\Im(g_2)/g_1$

$g_1(g_4)$ is effectively the same as (a_1) a_3

Final State	Signal	Background
$4e$	871	474
4μ	1186	641
$2e2\mu$	1035	574
$2\mu 2e$	867	431

Constraints on CP violating interactions

- Likelihood scan in real and imaginary projection of g_4/g_1
  - KD fits show that phase of anomalous couplings can play an important role - *note this can also be parameterized by extending templates' dimensionality a la CMS*
  - 8D - correlation less between the real and imaginary projections - *simultaneously parameterizes kinematics in term of magnitude & phase of anomalous couplings*

ME sensitive fits

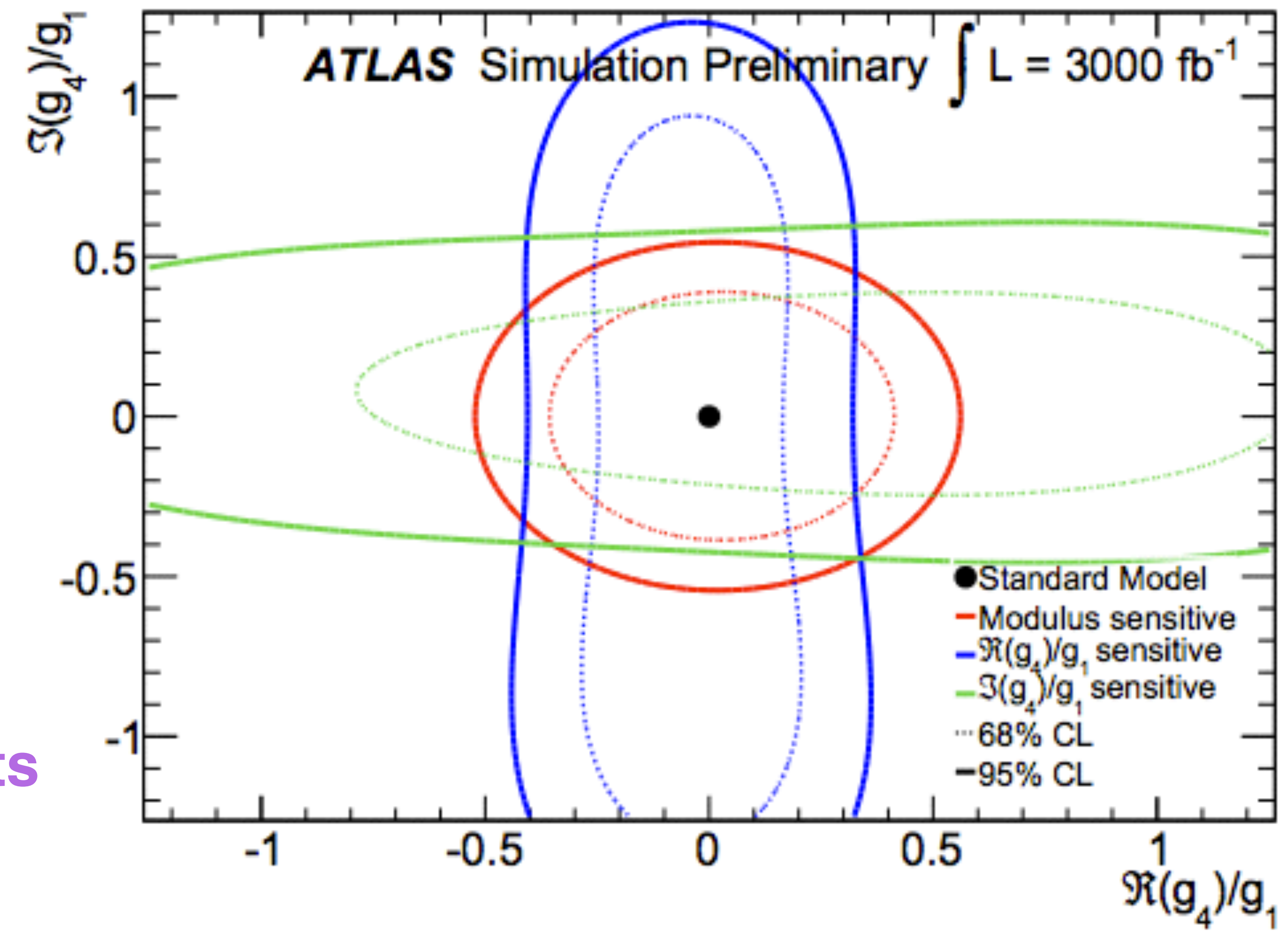

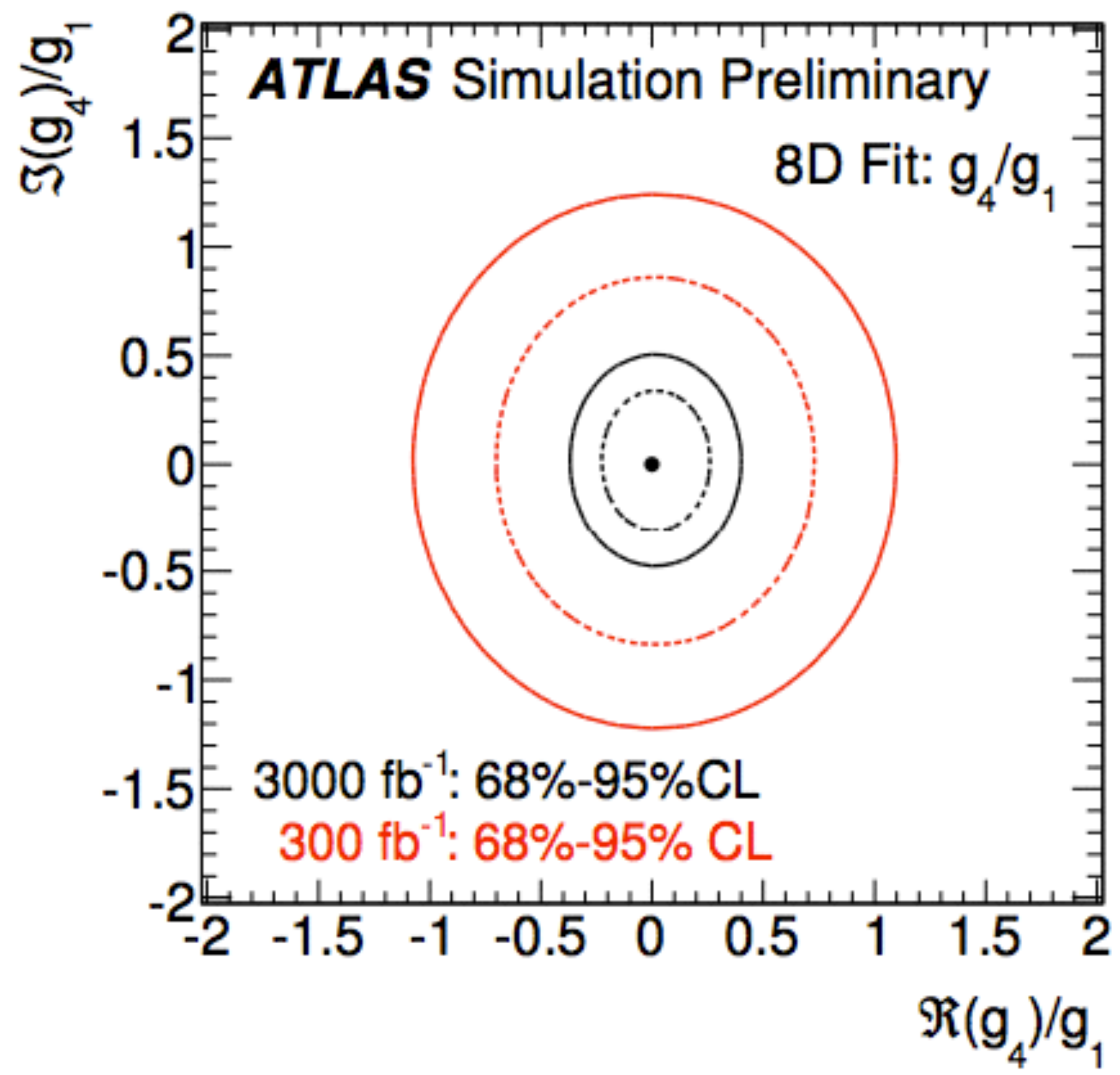

8D fits

ATLAS-PHYS-PUB-2013-013

Luminosity	$\|g_4\|/g_1$	$\Re(g_4)/g_1$	$\Im(g_4)/g_1$	$\|g_2\|/g_1$	$\Re(g_2)/g_1$	$\Im(g_2)/g_1$
300 fb^{-1}	1.03	(-1.01, 1.01)	(-1.02, 1.02)	1.39	(-0.88, 0.38)	(-1.13, 1.13)
3000 fb^{-1}	0.49	(-0.34, 0.26)	(-0.34, 0.48)	0.81	(-0.33, 0.11)	(-0.73, 0.75)

Luminosity	$\|g_4\|/g_1$	$\Re(g_4)/g_1$	$\Im(g_4)/g_1$	$\|g_2\|/g_1$	$\Re(g_2)/g_1$	$\Im(g_2)/g_1$
300	1.20	(-0.88, 0.91)	(-1.02, 1.05)	1.02	(-0.84,0.44)	(-1.19, 1.18)
3000	0.60	(-0.30, 0.33)	(-0.39, 0.42)	0.60	(-0.30,0.11)	(-0.71, 0.68)

Fermilab

Comparison

- ATLAS analysis also produced likelihood scan as a function of f_{ai} & ϕ_i
- $f_{a3} = f_{g4}$ — comparable results between ATLAS and CMS
  (f_{a3} < 0.04 @ 95% C.L.)

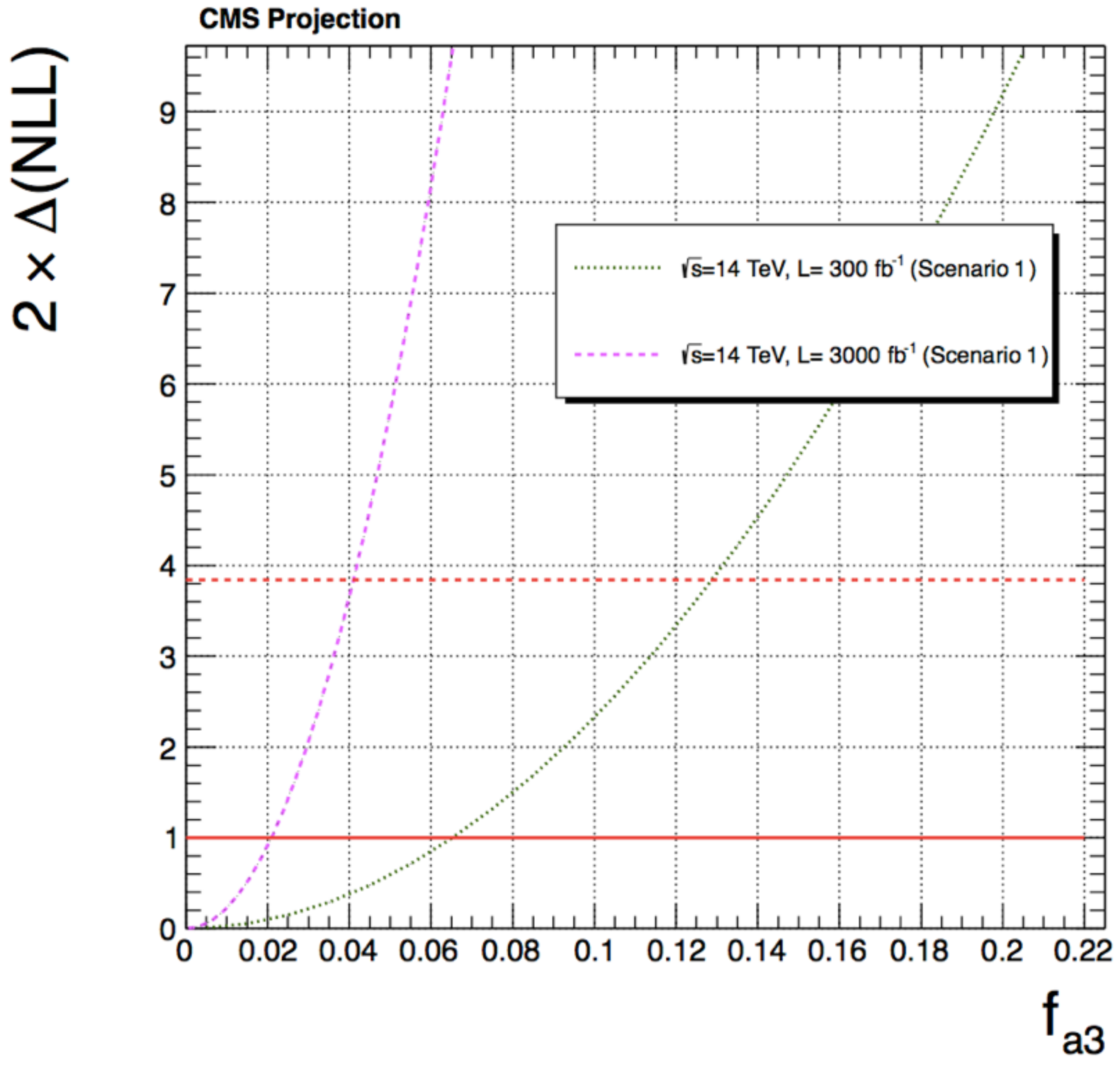

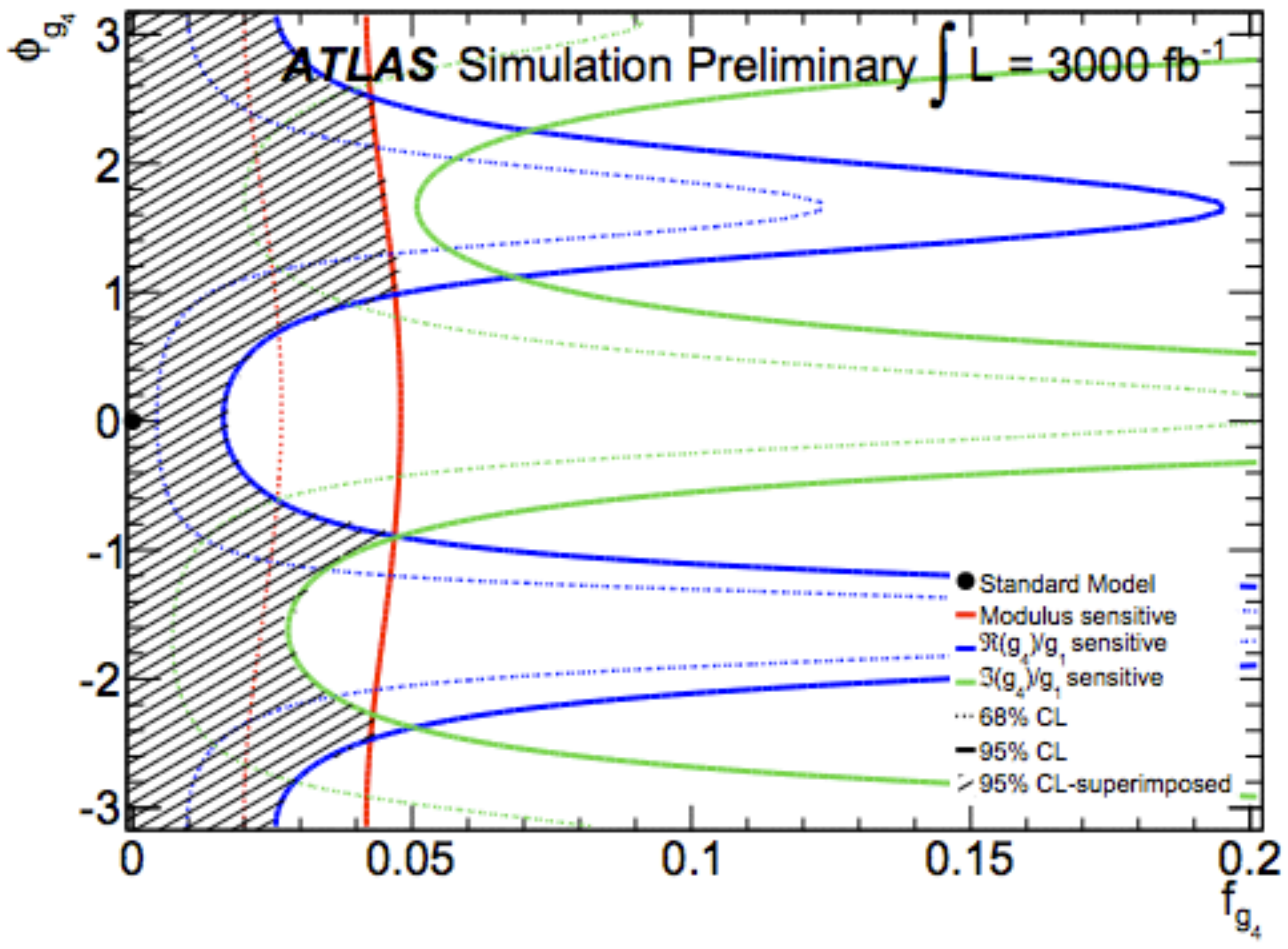

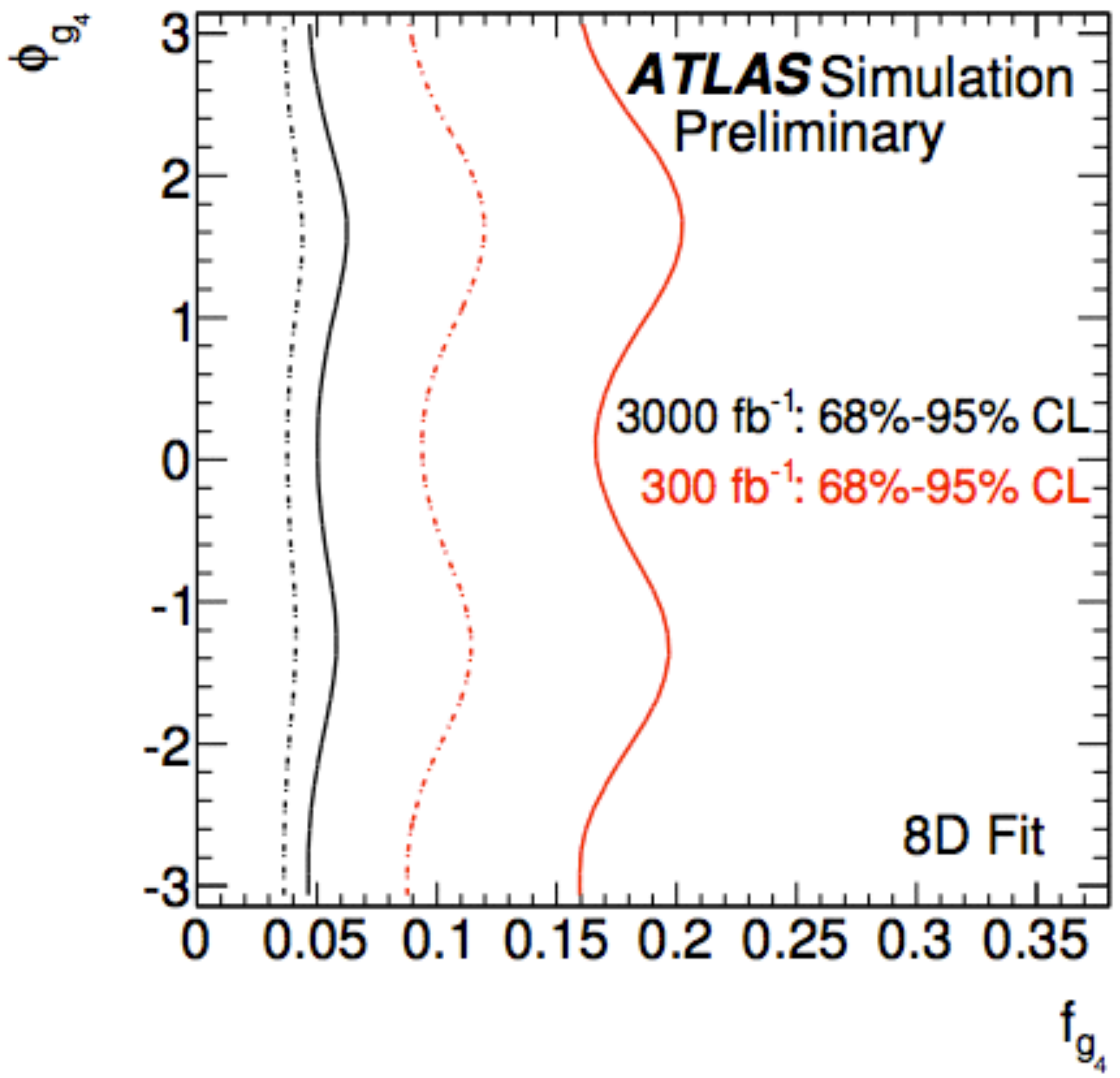

NOTE: the parameterization used in CMS is equivalent to the ATLAS modulus sensitive variable

Fermilab

Summary of results

Parameter	Observed	Expected
H→WW→eνμν		
$f_{a3}^{WW}\cos(\phi_{a3}^{WW})$	$-0.03^{+1.03}_{-0.97}$ $[-1.00, 1.00]$	$0.00^{+1.00}_{-1.00}$ $[-1.00, 1.00]$
H→ZZ→4ℓ		
$f_{a3}\cos(\phi_{a3})$	$0.00^{+0.14}_{-0.11}$ $[-0.40, 0.43]$	$0.00^{+0.33}_{-0.33}$ $[-0.70, 0.70]$
Combined H→ZZ→4ℓ & H→WW→eνμν		
$f_{a3}\cos(\phi_{a3})$	$0.00^{+0.08}_{-0.08}$ $[-0.27, 0.28]$	$0.00^{+0.23}_{-0.23}$ $[-0.53, 0.53]$

Observed 95% C.L Limits

$H \to WW^* \to e\nu\mu\nu$		
$f_{g4} < 0.78$ for $\phi_{g4} = 0$	and	$f_{g4} < 0.84$ for $\phi_{g4} = \pi$
$H \to ZZ^* \to 4\ell$		
$f_{g4} < 0.11$ for $\phi_{g4} = 0$	and	$f_{g4} < 0.54$ for $\phi_{g4} = \pi$
Combination of $H \to ZZ^* \to 4\ell$ and $H \to WW^* \to e\nu\mu\nu$		
$f_{g4} < 0.090$ for $\phi_{g4} = 0$	and	$f_{g4} < 0.41$ for $\phi_{g4} = \pi$

Conclusions

- CMS & ATLAS have mature programs for constraining the tensor structure of HVV interactions (HZZ, HWW, Hγγ, and HZγ)
    - advanced techniques used to exploit all of the decay kinematics of the 4-body final states
    - measurements still limited by statistical uncertainties
    - constraining $a_2^{\gamma\gamma}$ ($a_2^{\gamma\gamma}$) from $a_3^{Z\gamma}$ ($a_3^{Z\gamma}$) couplings with high integrated luminosity is possible
- Projections show that ZZ anomalous couping constraints can be improved by a factor of 10 with the full HL-LHC integrated luminosity

BACKUP

4l analyses CMS

- 2 pairs of opposite-sign same flavor leptons (e or μ)
  (sub)leading lepton pT>20 (10 GeV)
  mll >= 4 GeV (all combinations)
  40 < m1 (closest to Z mass) < 120 GeV
  12 < m2 < 120 GeV

- SM ZZ contributions taken from NLO MC sim.

- Z+X backgrounds estimated from a loose ID control region

105.6< $m_{4\ell}$ < 140.6 GeV

Channel	4e		4μ		2e2μ	
Energy	7 TeV	8 TeV	7 TeV	8 TeV	7 TeV	8 TeV
$q\bar{q} \to ZZ$	0.84 ± 0.10	2.94 ± 0.33	1.80 ± 0.11	7.65 ± 0.49	2.24 ± 0.28	8.86 ± 0.68
$gg \to ZZ$	0.03 ± 0.01	0.20 ± 0.05	0.06 ± 0.02	0.41 ± 0.10	0.07 ± 0.02	0.50 ± 0.13
$Z + X$	0.62 ± 0.14	2.77 ± 0.62	0.22 ± 0.09	1.19 ± 0.48	1.06 ± 0.29	4.29 ± 1.10
Bkg.	1.49 ± 0.17	5.91 ± 0.71	2.08 ± 0.14	9.25 ± 0.69	3.37 ± 0.40	13.65 ± 1.30
Signal	0.70 ± 0.11	3.09 ± 0.47	1.24 ± 0.14	5.95 ± 0.71	1.67 ± 0.26	7.68 ± 0.98
Observed	1	9	3	15	6	16

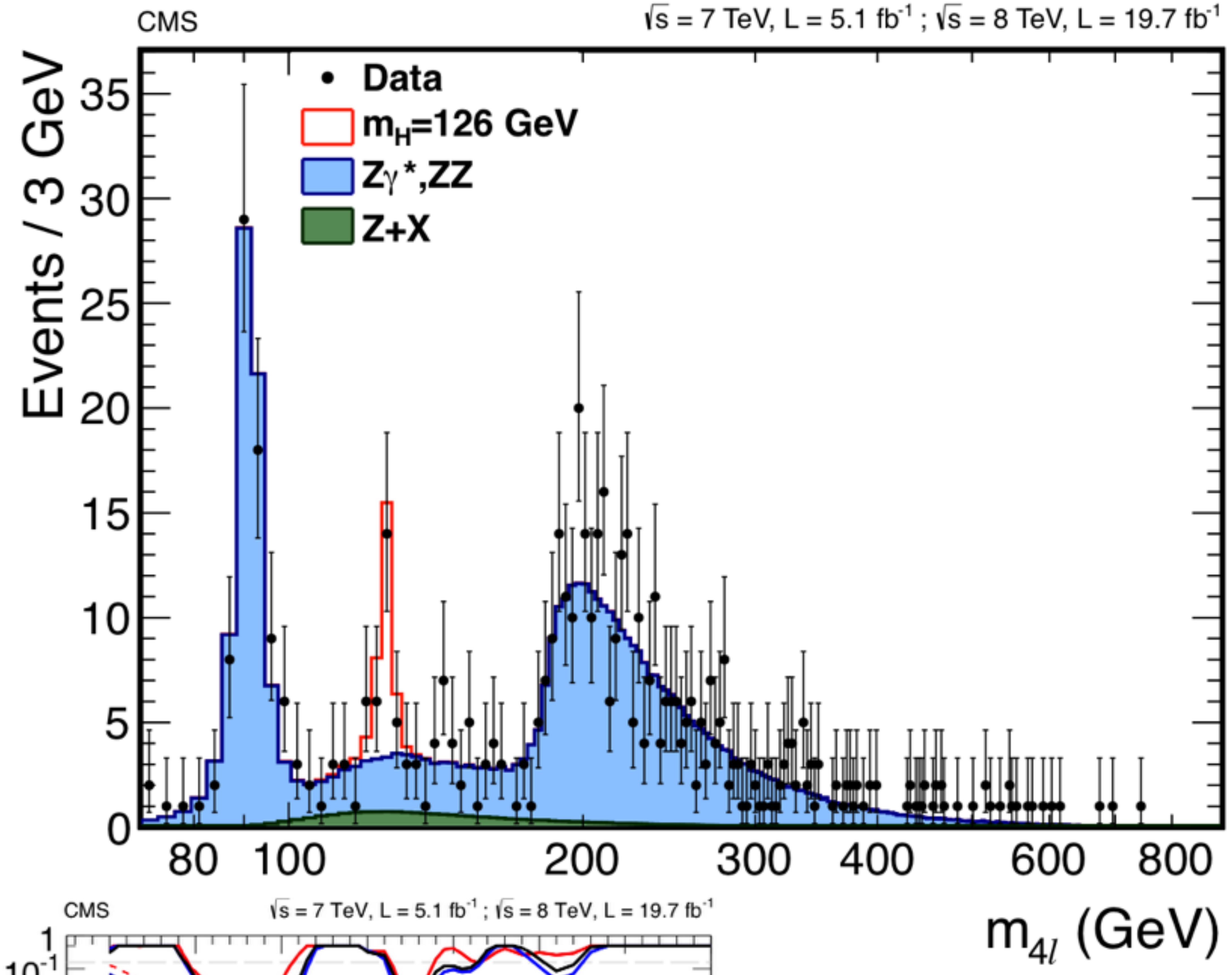

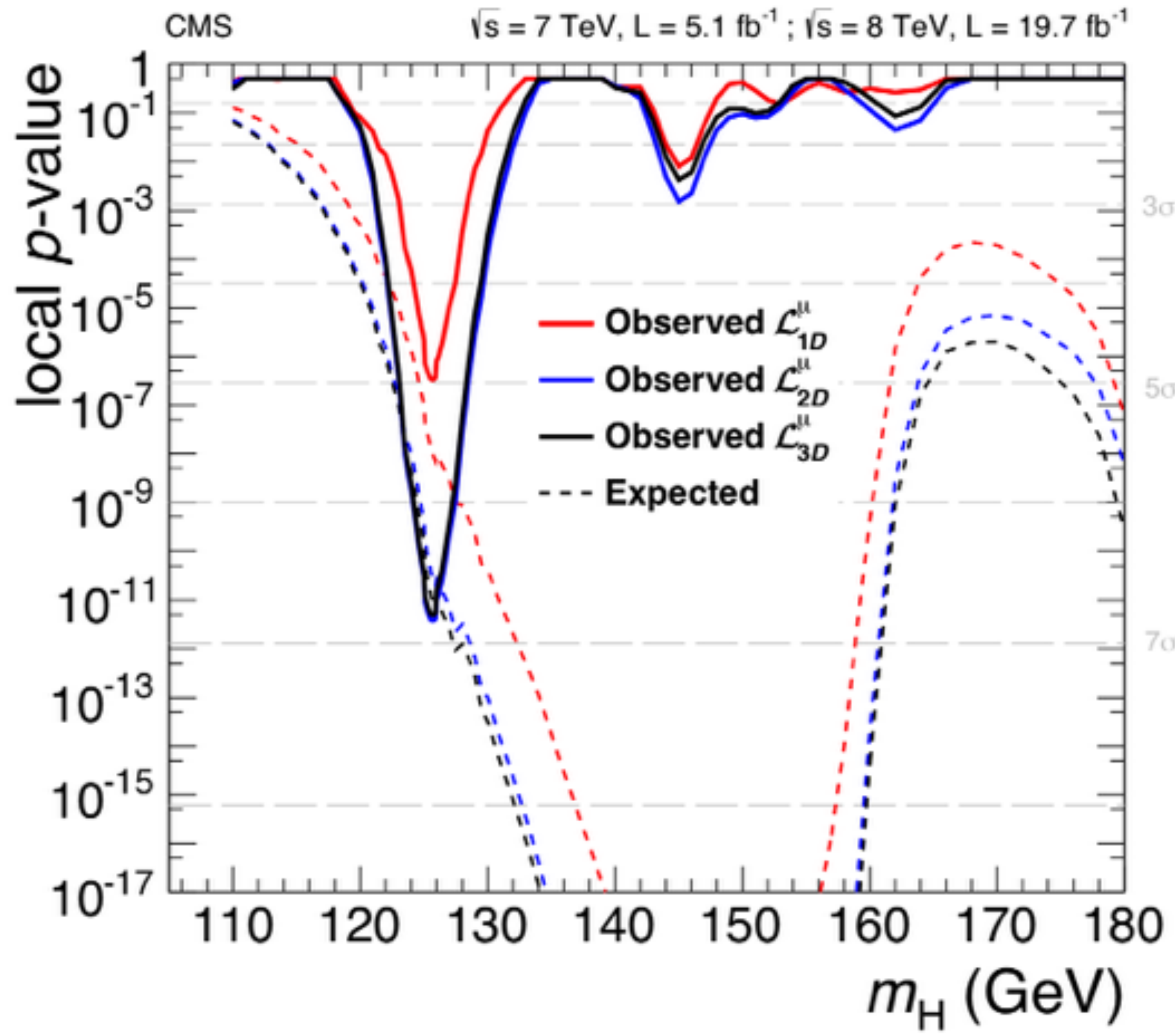

Fermilab

4l analyses ATLAS

- two pairs of opposite-sign same flavor leptons
  three leading leptons pT>20, 15, 10 GeV
  50 < m12 (closest to Z mass) < 106 GeV
  12 < m34 < 115 GeV

- SM ZZ contributions taken from NLO MC sim.

- Z+X backgrounds estimated from a loose ID control region

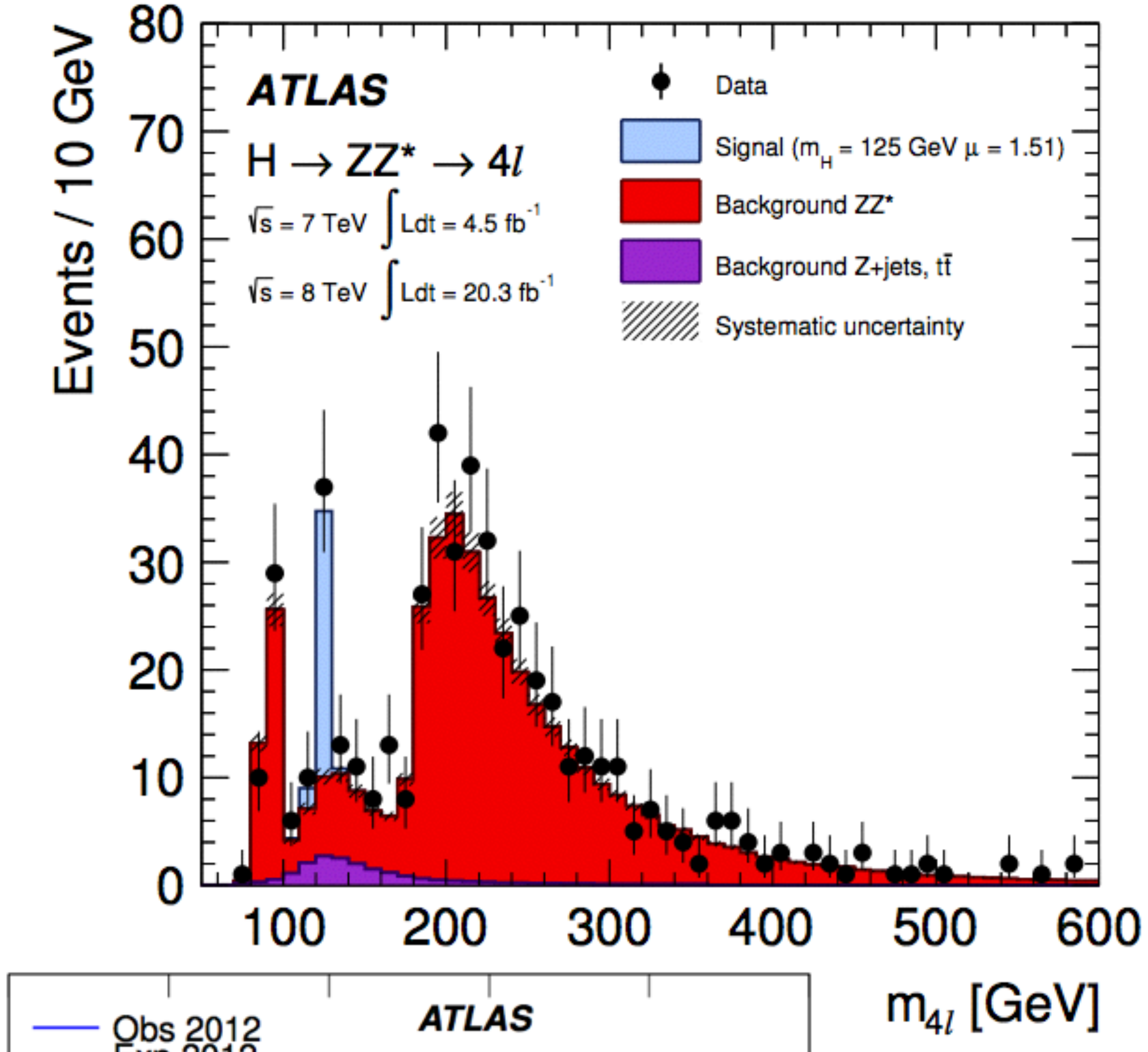

$115 < m_{4\ell} < 130$ GeV

	Signal	ZZ^*	$t\bar{t}$, $Z+$jets	Observed
		$\sqrt{s}$ = 7 TeV		
4μ	1.02±0.10	0.65±0.03	0.14±0.06	3
$2\mu 2e$	0.47±0.05	0.29±0.02	0.53±0.12	1
$2e2\mu$	0.64±0.06	0.45±0.02	0.13±0.05	2
$4e$	0.45±0.04	0.26±0.02	0.59±0.12	2
Total	2.58±0.25	1.65±0.09	1.39±0.26	8
		$\sqrt{s}$ = 8 TeV		
4μ	5.81±0.58	3.36±0.17	0.97±0.18	13
$2\mu 2e$	3.00±0.30	1.59±0.10	0.52±0.12	8
$2e2\mu$	3.72±0.37	2.33±0.11	0.84±0.14	9
$4e$	2.91±0.29	1.44±0.09	0.52±0.11	7
Total	15.4 ±1.5	8.72±0.47	2.85±0.39	37

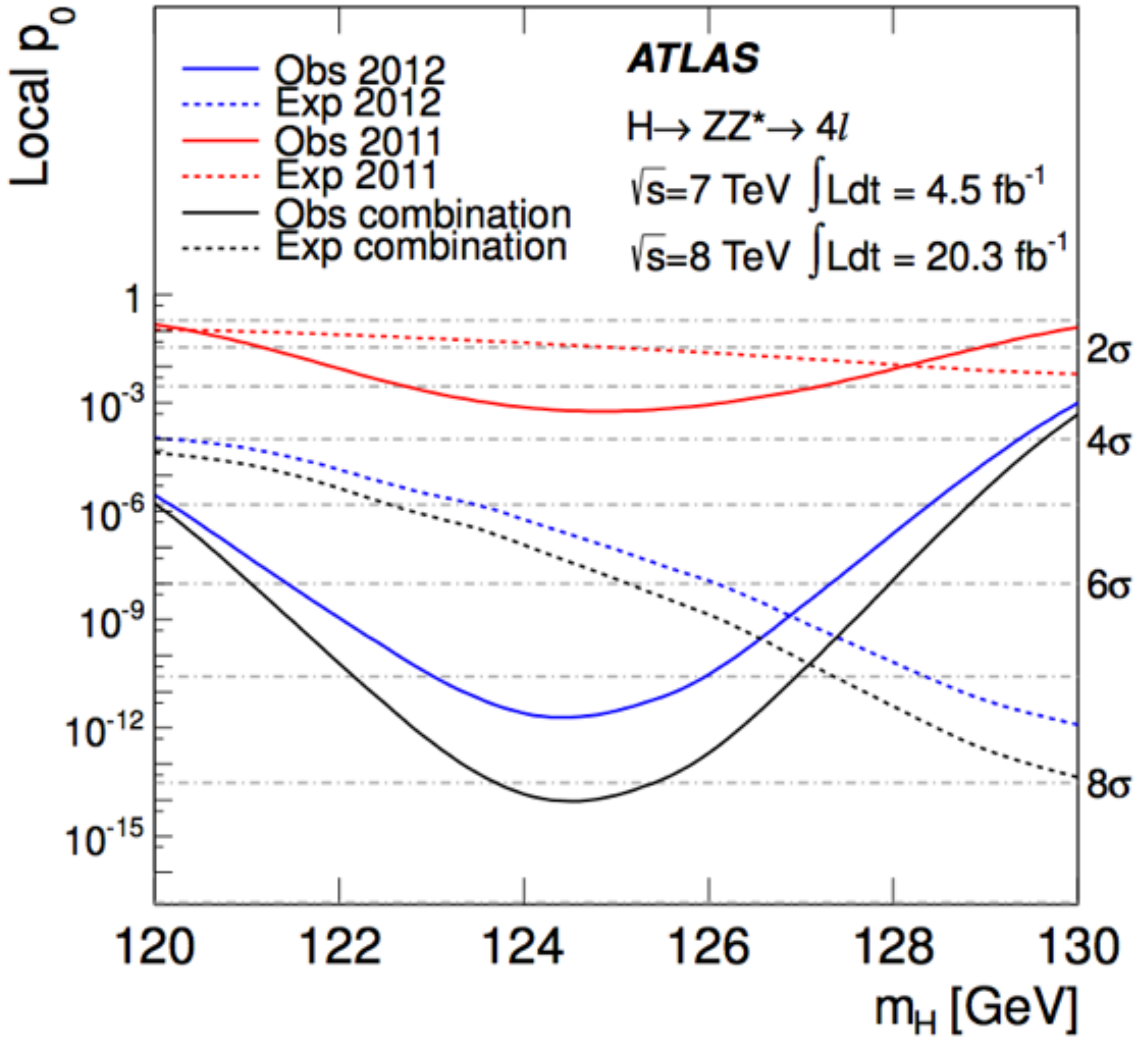

Fermilab

Observables

- An example of a complete set of observables describing the higgs decay kinematics

$$m_{4l} = (q_{11}+q_{12}+q_{21}+q_{22})^2$$
$$m_{z1} = (q_{11}+q_{12})^2$$
$$m_{Z2} = (q_{21}+q_{22})^2$$
$$\cos(\theta^*) = (q11+q12)\cdot z/|q11+q12|$$

$$\Phi = \frac{\boldsymbol{q}_1 \cdot (\hat{\boldsymbol{n}}_1 \times \hat{\boldsymbol{n}}_2)}{|\boldsymbol{q}_1 \cdot (\hat{\boldsymbol{n}}_1 \times \hat{\boldsymbol{n}}_2)|} \times \cos^{-1}(-\hat{\boldsymbol{n}}_1 \cdot \hat{\boldsymbol{n}}_2)$$
$$\Phi_1 = \frac{\boldsymbol{q}_1 \cdot (\hat{\boldsymbol{n}}_1 \times \hat{\boldsymbol{n}}_{\mathrm{sc}})}{|\boldsymbol{q}_1 \cdot (\hat{\boldsymbol{n}}_1 \times \hat{\boldsymbol{n}}_{\mathrm{sc}})|} \times \cos^{-1}(\hat{\boldsymbol{n}}_1 \cdot \hat{\boldsymbol{n}}_{\mathrm{sc}})$$

$$\theta_1 = \cos^{-1}\left(-\frac{\boldsymbol{q}_2 \cdot \boldsymbol{q}_{11}}{|\boldsymbol{q}_2||\boldsymbol{q}_{11}|}\right)$$
$$\theta_2 = \cos^{-1}\left(-\frac{\boldsymbol{q}_1 \cdot \boldsymbol{q}_{21}}{|\boldsymbol{q}_1||\boldsymbol{q}_{21}|}\right)$$

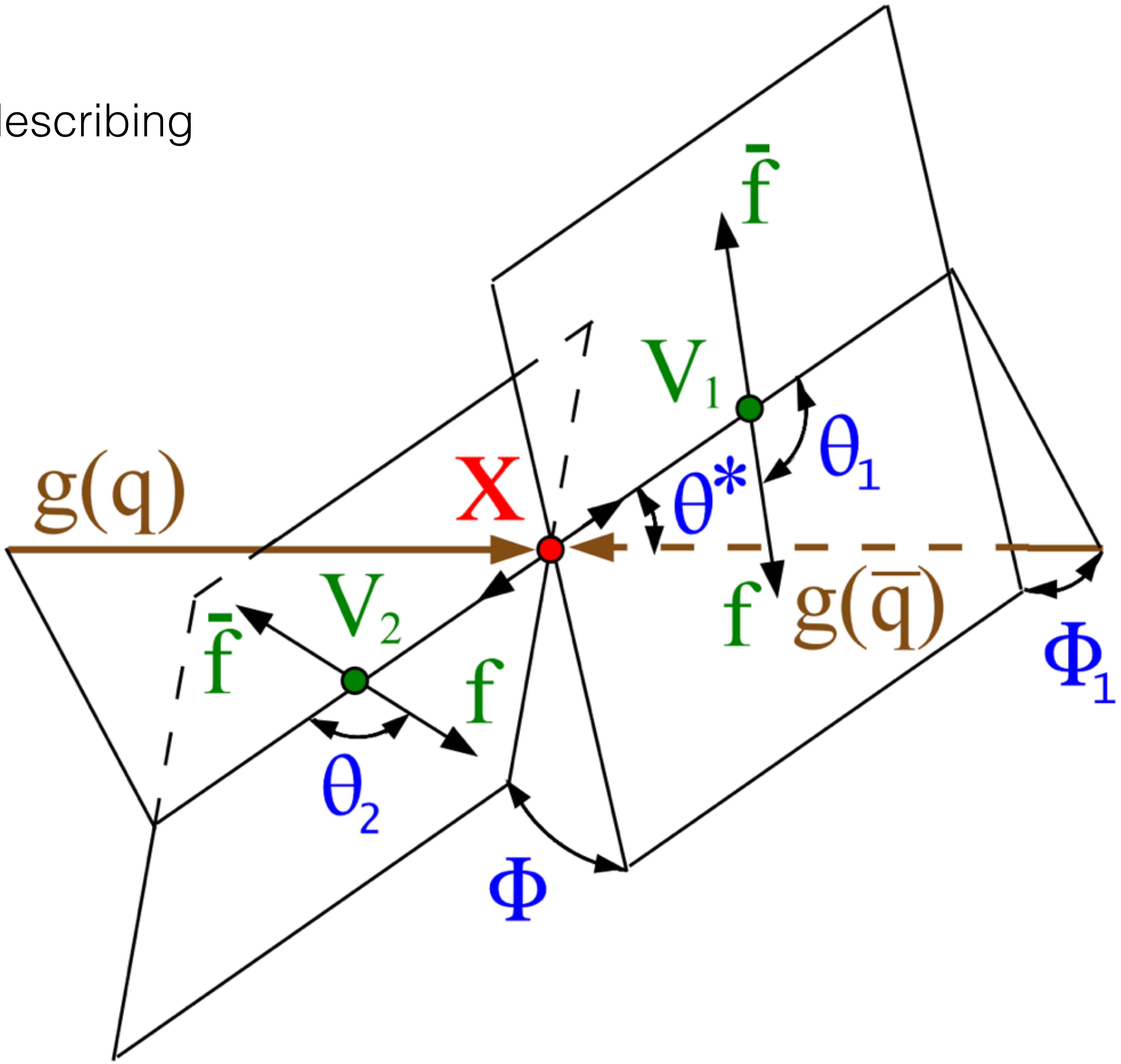

- other variables, pT & η, are sensitive to NLO effects & insensitive to CP

Fermilab

ATLAS distributions

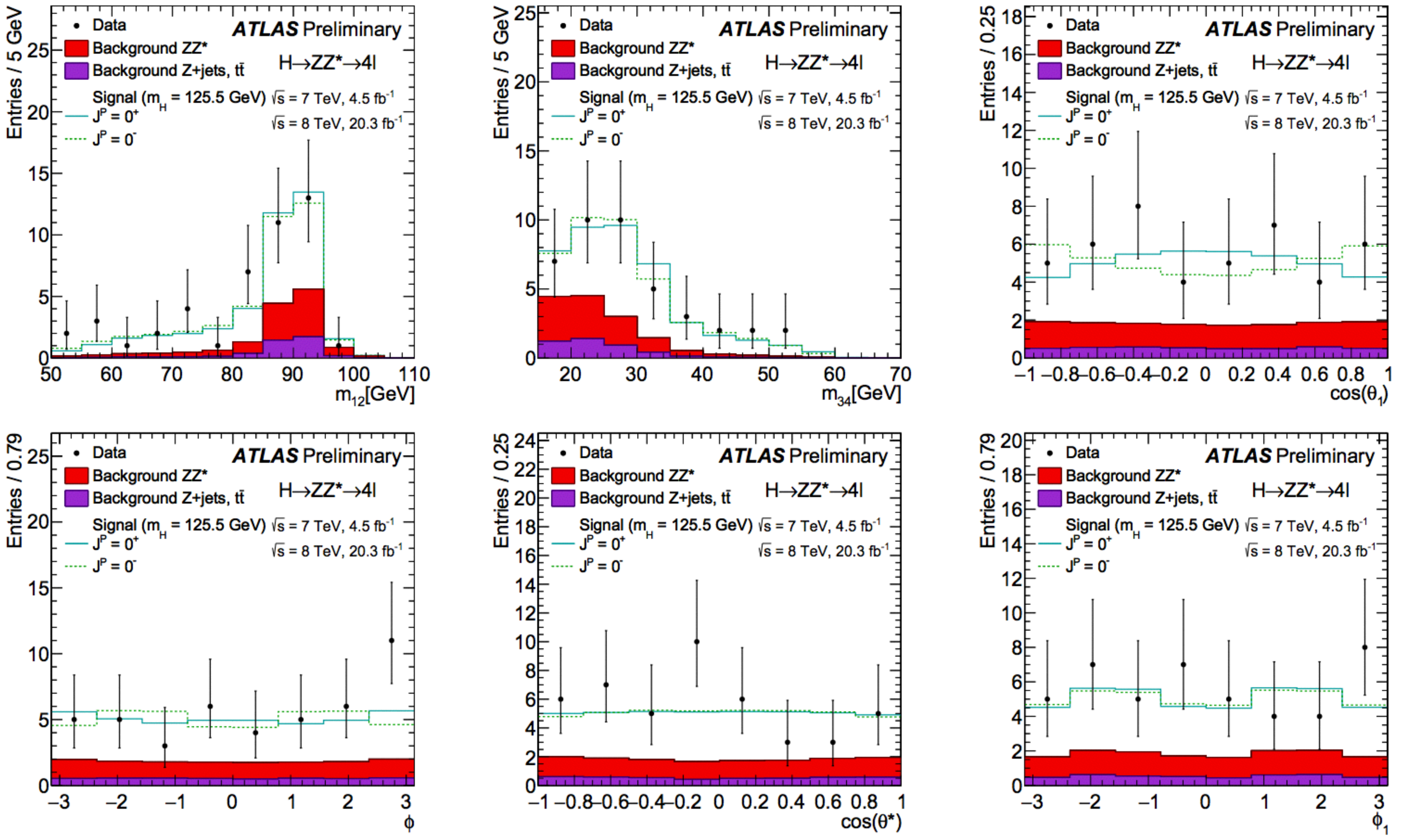

Fermilab

Other production modes

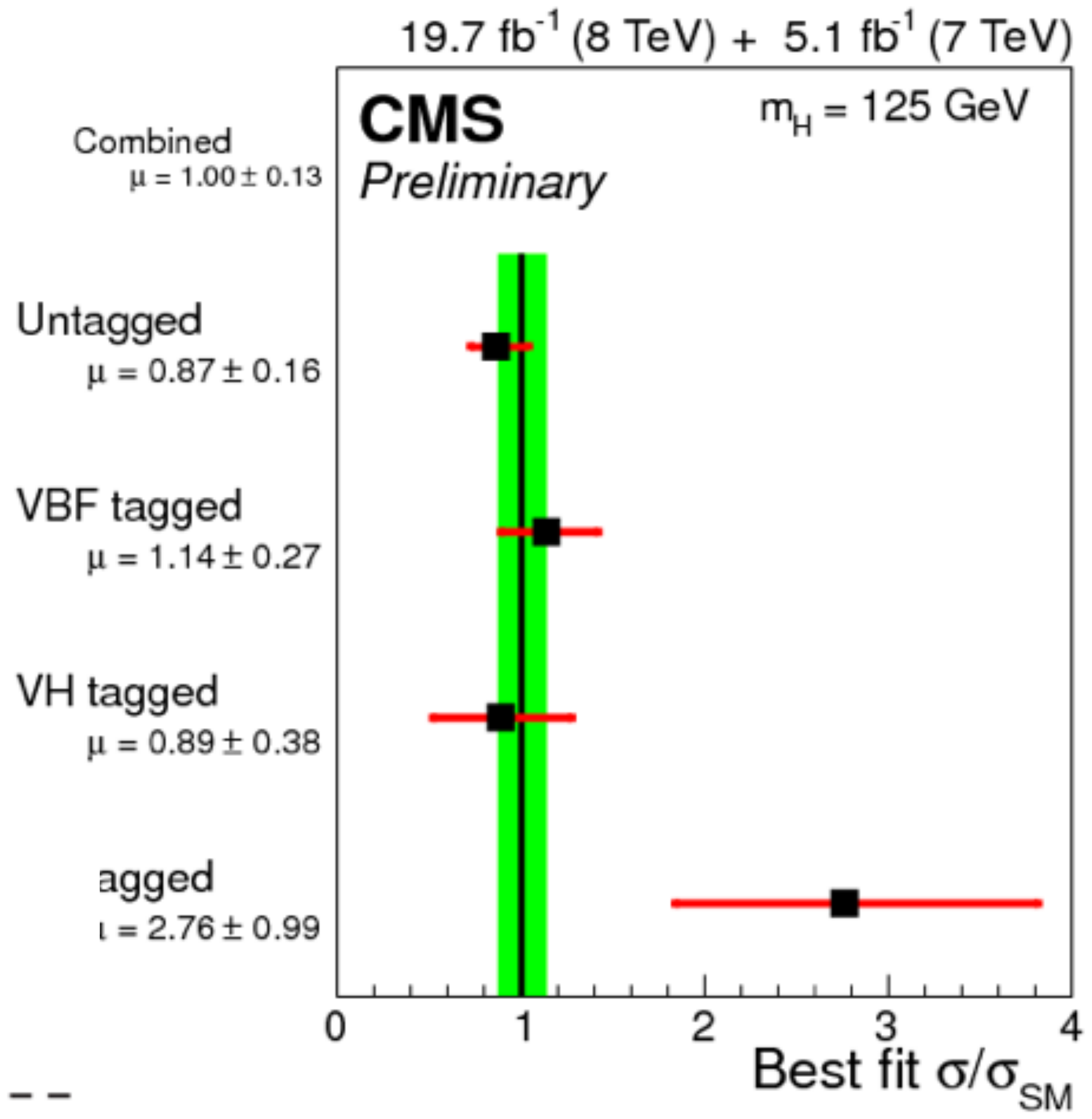

CMS-PAS-HIG-14-009

- As sensitivity to other production mechanisms become sensitive, new opportunities arise
- 0^--like events have an enhancement at large $\sqrt{s}$ - leading to increased sensitivity in associated production and VBF production channels

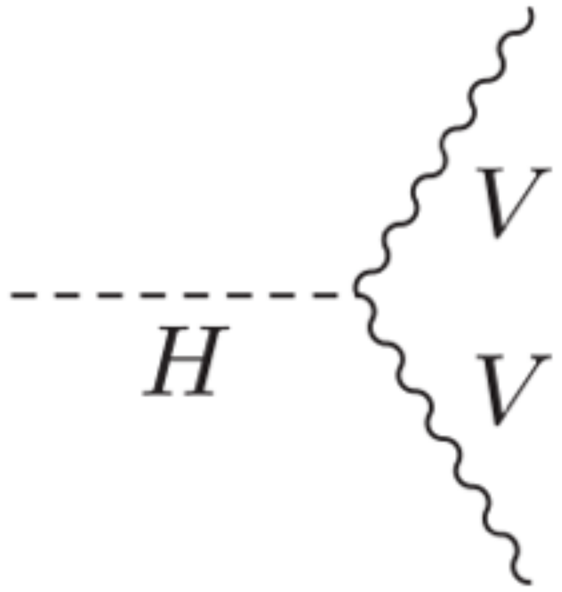

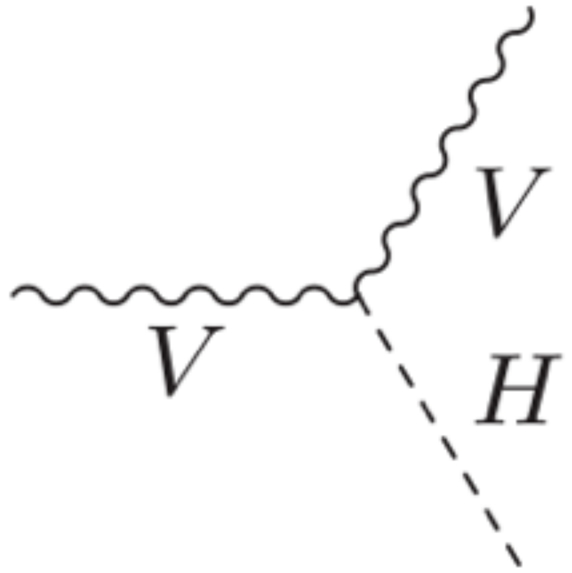

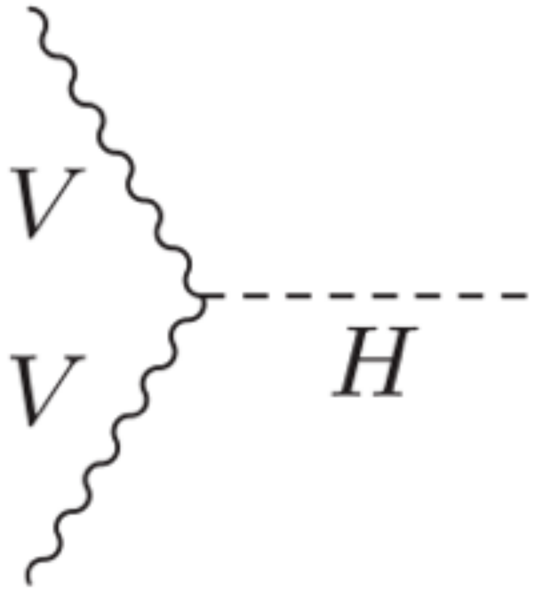

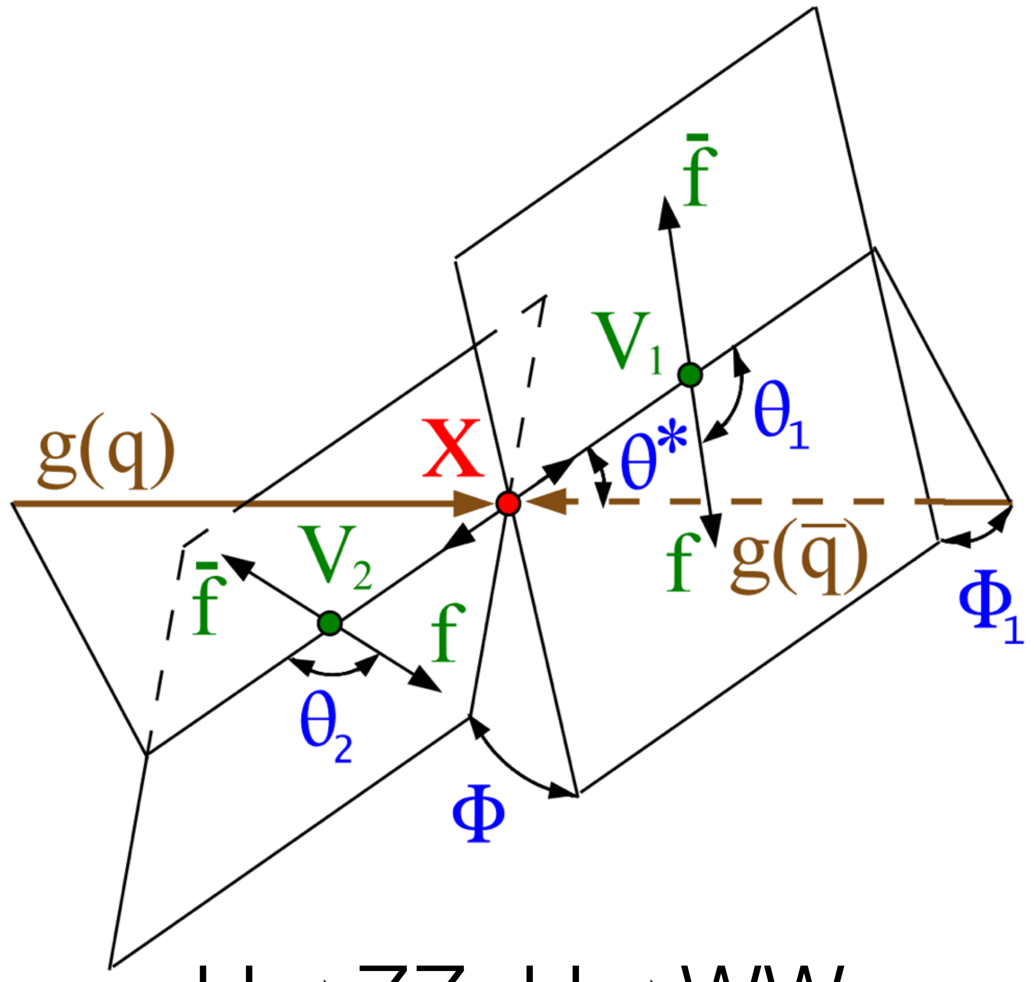

H→ZZ, H→WW

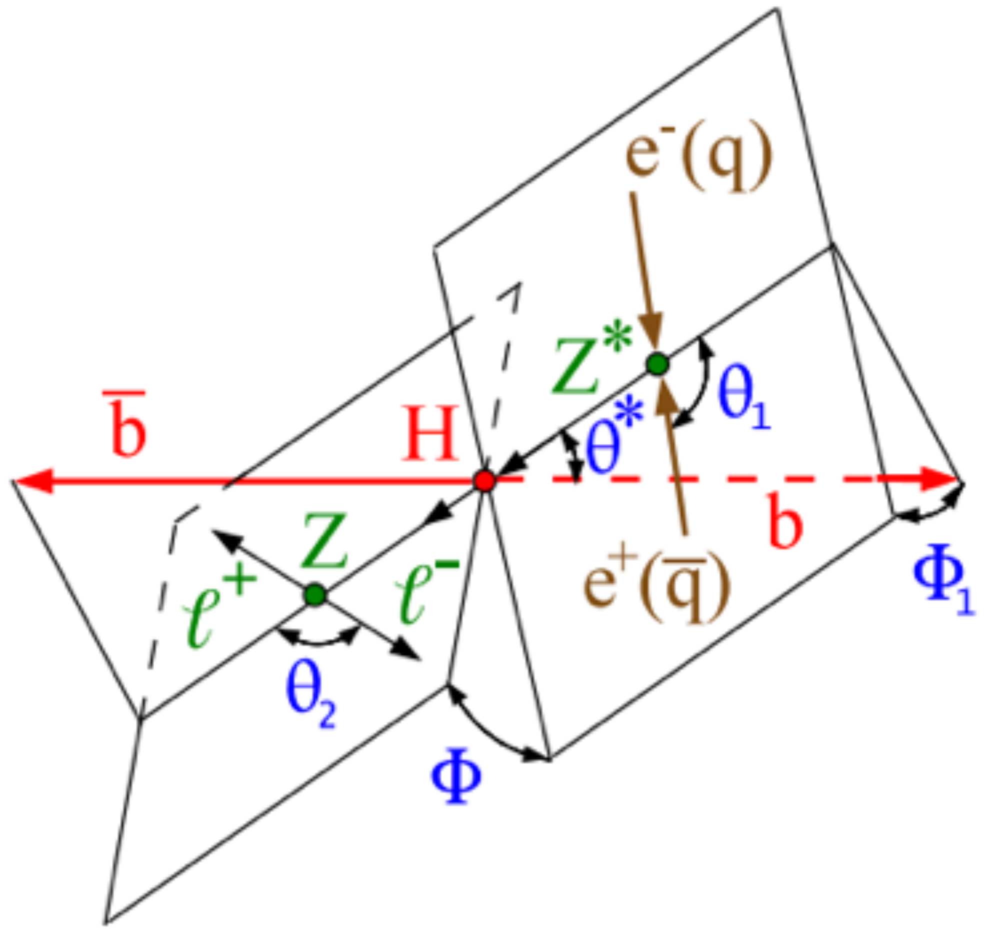

associated prod.

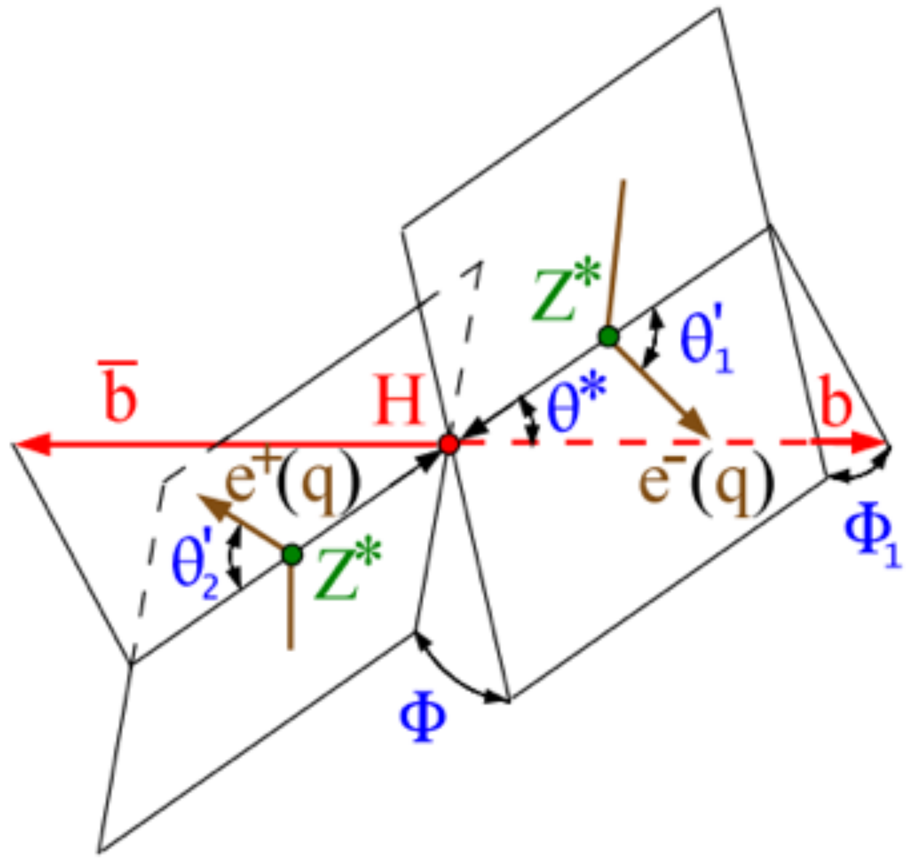

VBF

Fermilab

VH & VBF

- Kinematic distribution for 0+ (red), 0- (blue), 50-50 mixture (green & magenta)

Fermilab

Prospects other production modes

- Projections out to 300/fb & 3000/fb show strong sensitivity to CP-violating HVV interactions
  - Associated production: assuming only Z→Z(ll)H(bb)
  - VBF production: assuming H(γγ) + H(ZZ)

→dominant sensitivity from associated and VBF production mechanisms!

$$f_{CP} = \frac{|a_3|^2 \sigma_3^{H\to ZZ}}{\Sigma |a_i|^2 \sigma_i^{H\to ZZ}}$$

$$e.g. \quad \frac{\sigma_3^{H\to ZZ}}{\sigma_1^{H\to ZZ}} \sim 0.160$$

Summary of projections for discovery potential @ LHC & e+e- collider

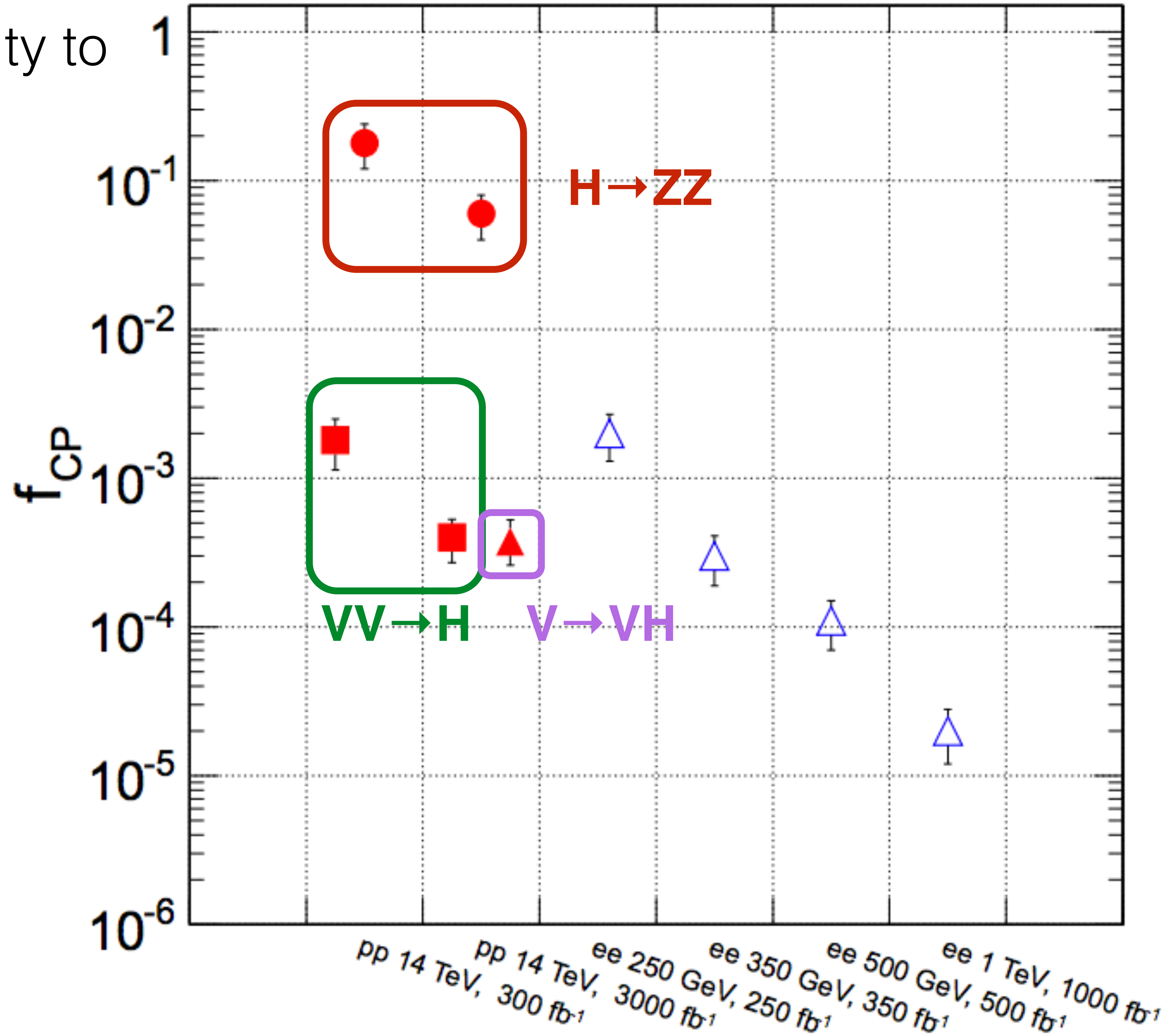

arXiv:1310.8361v2

Fermilab

ATLAS monte carlo

- signals modeled using *Powheg-Box Monte Carlo*
  - includes both ggF and VBF up to NLO in QCD
  - pT spectrum reweighted to NNLO and NNLL predictions

$H \to W(l\nu)W(l\nu)$

Process	MC generator	$\sigma \cdot \mathcal{B}$ (pb)
Signal		
ggF $H \to WW^*$	POWHEG+PYTHIA8	0.435
VBF $H \to WW^*$	POWHEG+PYTHIA8	0.0356
VH $H \to WW^*$	PYTHIA8	0.0253
WW		
$q\bar{q} \to WW$ and $qg \to WW$	POWHEG+PYTHIA6	5.68
$gg \to WW$	GG2VV+HERWIG	0.196
$(q\bar{q} \to W) + (q\bar{q} \to W)$	PYTHIA8	0.480
$q\bar{q} \to WW$	SHERPA	5.68
VBS $WW + 2\,\text{jets}$	SHERPA	0.0397
Top quarks		
$t\bar{t}$	POWHEG+PYTHIA6	26.6
Wt	POWHEG+PYTHIA6	2.35
$tq\bar{b}$	ACERMC+PYTHIA6	28.4
$t\bar{b}$	POWHEG+PYTHIA6	1.82
Other dibosons (VV)		
$W\gamma$ ($p_T^\gamma > 8\,\text{GeV}$)	ALPGEN+HERWIG	369
$W\gamma^*$ ($m_{\ell\ell} \leq 7\,\text{GeV}$)	SHERPA	12.2
WZ ($m_{\ell\ell} > 7\,\text{GeV}$)	POWHEG+PYTHIA8	12.7
VBS $WZ + 2\,\text{jets}$ ($m_{\ell\ell} > 7\,\text{GeV}$)	SHERPA	0.0126
$Z\gamma$ ($p_T^\gamma > 8\,\text{GeV}$)	SHERPA	163
$Z\gamma^*$ (min. $m_{\ell\ell} \leq 4\,\text{GeV}$)	SHERPA	7.31
ZZ ($m_{\ell\ell} > 4\,\text{GeV}$)	POWHEG+PYTHIA8	0.733
$ZZ \to \ell\ell\nu\nu$ ($m_{\ell\ell} > 4\,\text{GeV}$)	POWHEG+PYTHIA8	0.504
Drell-Yan		
Z ($m_{\ell\ell} > 10\,\text{GeV}$)	ALPGEN+HERWIG	16500
VBF $Z + 2\,\text{jets}$ ($m_{\ell\ell} > 7\,\text{GeV}$)	SHERPA	5.36

CMS discriminant details

$$\mathcal{P}_{\rm SM} = \mathcal{P}^{\rm kin}_{\rm SM}(m_1, m_2, \vec{\Omega}|m_{4\ell}) \times \mathcal{P}^{\rm mass}_{\rm sig}(m_{4\ell}|m_{\rm H}),$$
$$\mathcal{P}_{J^P} = \mathcal{P}^{\rm kin}_{J^P}(m_1, m_2, \vec{\Omega}|m_{4\ell}) \times \mathcal{P}^{\rm mass}_{\rm sig}(m_{4\ell}|m_{\rm H}),$$
$$\mathcal{P}^{\rm int}_{J^P} = \left(\mathcal{P}^{\rm kin}_{\rm SM+J^P}(m_1, m_2, \vec{\Omega}|m_{4\ell}) - \mathcal{P}^{\rm kin}_{J^P}(m_1, m_2, \vec{\Omega}|m_{4\ell}) - \mathcal{P}^{\rm kin}_{\rm SM}(m_1, m_2, \vec{\Omega}|m_{4\ell})\right),$$
$$\mathcal{P}^{\rm int\perp}_{J^P} = \left(\mathcal{P}^{\rm kin}_{\rm SM+J^P\perp}(m_1, m_2, \vec{\Omega}|m_{4\ell}) - \mathcal{P}^{\rm kin}_{J^P}(m_1, m_2, \vec{\Omega}|m_{4\ell}) - \mathcal{P}^{\rm kin}_{\rm SM}(m_1, m_2, \vec{\Omega}|m_{4\ell})\right),$$
$$\mathcal{P}_{\rm q\bar{q}ZZ} = \mathcal{P}^{\rm kin}_{\rm q\bar{q}ZZ}(m_1, m_2, \vec{\Omega}|m_{4\ell}) \times \mathcal{P}^{\rm mass}_{\rm q\bar{q}ZZ}(m_{4\ell}),$$
$$\mathcal{P}_{\rm ggZZ} = \mathcal{P}^{\rm kin}_{\rm ggZZ}(m_1, m_2, \vec{\Omega}|m_{4\ell}) \times \mathcal{P}^{\rm mass}_{\rm ggZZ}(m_{4\ell}),$$

$$\mathcal{D}_{\rm bkg} = \frac{\mathcal{P}_{\rm SM}}{\mathcal{P}_{\rm SM} + c \times \mathcal{P}_{\rm q\bar{q}ZZ}} = \left[1 + c(m_{4\ell}) \times \frac{\mathcal{P}^{\rm kin}_{\rm q\bar{q}ZZ}(m_1, m_2, \vec{\Omega}|m_{4\ell}) \times \mathcal{P}^{\rm mass}_{\rm q\bar{q}ZZ}(m_{4\ell})}{\mathcal{P}^{\rm kin}_{\rm SM}(m_1, m_2, \vec{\Omega}|m_{4\ell}) \times \mathcal{P}^{\rm mass}_{\rm sig}(m_{4\ell}|m_{\rm H})}\right]^{-1},$$
$$\mathcal{D}_{J^P} = \frac{\mathcal{P}_{\rm SM}}{\mathcal{P}_{\rm SM} + \mathcal{P}_{J^P}} = \left[1 + \frac{\mathcal{P}^{\rm kin}_{J^P}(m_1, m_2, \vec{\Omega}|m_{4\ell})}{\mathcal{P}^{\rm kin}_{\rm SM}(m_1, m_2, \vec{\Omega}|m_{4\ell})}\right]^{-1},$$
$$\mathcal{D}_{\rm int} = \frac{\mathcal{P}^{\rm int}_{J^P}(m_1, m_2, \vec{\Omega}|m_{4\ell})}{\mathcal{P}^{\rm kin}_{\rm SM} + \mathcal{P}^{\rm kin}_{J^P}}.$$

ATLAS discriminant details

$$O_1(\kappa_{HVV}) = \frac{2\Re(ME(\kappa_{\text{SM}}\neq 0;\, \kappa_{HVV},\kappa_{AVV}=0;\, \alpha=0)^* \cdot ME(\kappa_{HVV}\neq 0;\, \kappa_{\text{SM}},\kappa_{AVV}=0;\, \alpha=0))}{|ME(\kappa_{\text{SM}}\neq 0;\, \kappa_{HVV},\kappa_{AVV}=0;\, \alpha=0)|^2},$$

$$O_2(\kappa_{HVV}) = \frac{|ME(\kappa_{HVV}\neq 0;\, \kappa_{\text{SM}},\kappa_{AVV}=0;\, \alpha=0)|^2}{|ME(\kappa_{\text{SM}}\neq 0;\, \kappa_{HVV},\kappa_{AVV}=0;\, \alpha=0)|^2},$$

$$O_1(\kappa_{AVV},\alpha) = \frac{2\Re(ME(\kappa_{\text{SM}}\neq 0;\, \kappa_{HVV},\kappa_{AVV}=0;\, \alpha=0)^* \cdot ME(\kappa_{AVV}\neq 0;\, \kappa_{\text{SM}},\kappa_{HVV}=0;\, \alpha=\pi/2))}{|ME(\kappa_{\text{SM}}\neq 0;\, \kappa_{HVV},\kappa_{AVV}=0;\, \alpha=0)|^2},$$

$$O_2(\kappa_{AVV},\alpha) = \frac{|ME(\kappa_{AVV}\neq 0;\, \kappa_{\text{SM}},\kappa_{HVV}=0;\, \alpha=\pi/2)|^2}{|ME(\kappa_{\text{SM}}\neq 0;\, \kappa_{HVV},\kappa_{AVV}=0;\, \alpha=0)|^2}.$$

CMS summary

Parameter	Observed	Expected	$f_{ai}^{VV}=1$
$f_{\Lambda1}\cos(\phi_{\Lambda1})$	$0.22^{+0.10}_{-0.16}$ $[-0.25, 0.37]$	$0.00^{+0.16}_{-0.87}$ $[-1.00, 0.27]$ $\cup[0.92, 1.00]$	1.1% (16%)
$f_{a2}\cos(\phi_{a2})$	$0.00^{+0.41}_{-0.06}$ $[-0.66, -0.57]$ $\cup[-0.15, 1.00]$	$0.00^{+0.38}_{-0.08}$ $[-0.18, 1.00]$	5.2% (5.0%)
$f_{a3}\cos(\phi_{a3})$	$0.00^{+0.14}_{-0.11}$ $[-0.40, 0.43]$	$0.00^{+0.33}_{-0.33}$ $[-0.70, 0.70]$	0.02% (0.41%)
$f_{\Lambda1}^{WW}\cos(\phi_{\Lambda1}^{WW})$	$0.21^{+0.18}_{-1.21}$ $[-1.00, 1.00]$	$0.00^{+0.34}_{-1.00}$ $[-1.00, 0.41]$ $\cup[0.49, 1.00]$	78% (67%)
$f_{a2}^{WW}\cos(\phi_{a2}^{WW})$	$-0.02^{+1.02}_{-0.16}$ $[-1.00, -0.54]$ $\cup[-0.29, 1.00]$	$0.00^{+1.00}_{-0.12}$ $[-1.00, -0.58]$ $\cup[-0.22, 1.00]$	42% (46%)
$f_{a3}^{WW}\cos(\phi_{a3}^{WW})$	$-0.03^{+1.03}_{-0.97}$ $[-1.00, 1.00]$	$0.00^{+1.00}_{-1.00}$ $[-1.00, 1.00]$	34% (49%)
$f_{\Lambda1}^{Z\gamma}\cos(\phi_{\Lambda1}^{Z\gamma})$	$-0.27^{+0.34}_{-0.49}$ $[-1.00, 1.00]$	$0.00^{+0.83}_{-0.53}$ $[-1.00, 1.00]$	26% (16%)
$f_{a2}^{Z\gamma}\cos(\phi_{a2}^{Z\gamma})$	$0.00^{+0.14}_{-0.20}$ $[-0.49, 0.46]$	$0.00^{+0.51}_{-0.51}$ $[-0.78, 0.79]$	<0.01% (0.01%)
$f_{a3}^{Z\gamma}\cos(\phi_{a3}^{Z\gamma})$	$0.02^{+0.21}_{-0.13}$ $[-0.40, 0.51]$	$0.00^{+0.51}_{-0.51}$ $[-0.75, 0.75]$	<0.01% (<0.01%)
$f_{a2}^{\gamma\gamma}\cos(\phi_{a2}^{\gamma\gamma})$	$0.12^{+0.20}_{-0.11}$ $[-0.04, +0.51]$	$0.00^{+0.11}_{-0.09}$ $[-0.32, 0.34]$	<0.01% (<0.01%)
$f_{a3}^{\gamma\gamma}\cos(\phi_{a3}^{\gamma\gamma})$	$-0.02^{+0.06}_{-0.13}$ $[-0.35, 0.32]$	$0.00^{+0.15}_{-0.11}$ $[-0.37, 0.40]$	<0.01% (<0.01%)

Cross sections for f_{ai} Conversion

Interaction	Anomalous Coupling	Coupling Phase	Effective Fraction	Translation Constant
HZZ	Λ_1	$\phi_{\Lambda 1}$	$f_{\Lambda 1}$	$\sigma_1/\tilde{\sigma}_{\Lambda 1} = 1.45 \times 10^4\ \mathrm{TeV}^{-4}$
	a_2	ϕ_{a2}	f_{a2}	$\sigma_1/\sigma_2 = 2.68$
	a_3	ϕ_{a3}	f_{a3}	$\sigma_1/\sigma_3 = 6.36$
HWW	Λ_1^{WW}	$\phi_{\Lambda 1}^{\mathrm{WW}}$	$f_{\Lambda 1}^{\mathrm{WW}}$	$\sigma_1^{\mathrm{WW}}/\tilde{\sigma}_{\Lambda 1}^{\mathrm{WW}} = 1.87 \times 10^4\ \mathrm{TeV}^{-4}$
	a_2^{WW}	ϕ_{a2}^{WW}	f_{a2}^{WW}	$\sigma_1^{\mathrm{WW}}/\sigma_2^{\mathrm{WW}} = 1.25$
	a_3^{WW}	ϕ_{a3}^{WW}	f_{a3}^{WW}	$\sigma_1^{\mathrm{WW}}/\sigma_3^{\mathrm{WW}} = 3.01$
	$\Lambda_1^{\mathrm{Z}\gamma}$	$\phi_{\Lambda 1}^{\mathrm{Z}\gamma}$	$f_{\Lambda 1}^{\mathrm{Z}\gamma}$	$\sigma_1'/\tilde{\sigma}_{\Lambda 1}^{\mathrm{Z}\gamma} = 5.76 \times 10^3\ \mathrm{TeV}^{-4}$
HZγ	$a_2^{\mathrm{Z}\gamma}$	$\phi_{a2}^{\mathrm{Z}\gamma}$	$f_{a2}^{\mathrm{Z}\gamma}$	$\sigma_1'/\sigma_2^{\mathrm{Z}\gamma} = 22.4 \times 10^{-4}$
	$a_3^{\mathrm{Z}\gamma}$	$\phi_{a3}^{\mathrm{Z}\gamma}$	$f_{a3}^{\mathrm{Z}\gamma}$	$\sigma_1'/\sigma_3^{\mathrm{Z}\gamma} = 27.2 \times 10^{-4}$
H$\gamma\gamma$	$a_2^{\gamma\gamma}$	$\phi_{a2}^{\gamma\gamma}$	$f_{a2}^{\gamma\gamma}$	$\sigma_1'/\sigma_2^{\gamma\gamma} = 28.2 \times 10^{-4}$
	$a_3^{\gamma\gamma}$	$\phi_{a3}^{\gamma\gamma}$	$f_{a3}^{\gamma\gamma}$	$\sigma_1'/\sigma_3^{\gamma\gamma} = 28.8 \times 10^{-4}$